Paleogeographic Reconstructions in the Western Mediterranean and Implications for Permian Pangea Configurations

Katharina Aubele

München 2015

Paleogeographic Reconstructions in the Western Mediterranean and Implications for Permian Pangea Configurations

Katharina Aubele

Dissertation
zur Erlangung des Doktorgrades
an der Fakultät für Geowissenschaften der
Ludwig–Maximilians–Universität München

vorgelegt von
Katharina Aubele
aus München

München, den 09.02.2015

Erstgutachter: Prof. Valerian Bachtadse
Zweitgutachter: Prof. Giovanni Muttoni
Tag der mündlichen Prüfung: 08.07.2015

Preamble

This work presents the synthesis of the following scientific articles published in or submitted to various peer-reviewed scientific journals. The articles are listed here in order of appearance in the text.

K. Aubele, V. Bachtadse, G. Muttoni, A. Ronchi and M. Durand. A Paleomagnetic Study of Permian and Triassic Rocks from the Toulon-Cuers Basin, SE France: Evidence for intra-Pangea Block Rotations in the Permian, Tectonics, *2012,* ***31*** *(TC3015), doi:10.1029/2011TC003026*

K. Aubele, V. Bachtadse, G. Muttoni and A. Ronchi. Paleomagnetic data from late Paleozoic dykes on Sardinia: evidence for intra-Sardinian block rotations and implications on the Pangea megashear system, Geochemistry, Geophysics, Geosystems, *2014,* ***15****, 1684-1697, doi:10.1002/2014GC005325*

K. Aubele, V. Bachtadse, G. Muttoni, A. Ronchi and D. V. Kent. New Early Permian Paleopoles from Sardinia confirm intra-Pangea Mobility, *submitted to Tectonics*

U. Kirscher, **K. Aubele**, G. Muttoni, A. Ronchi and V. Bachtadse. Paleomagnetism of Jurassic Carbonate Rocks from Sardinia - No Indication of Post Jurassic Internal Block Rotations, Journal of Geophysical Research Solid Earth, *2011,* ***116*** *(B12), 1978-2012, doi:10.1029/2011JB008422*

Zusammenfassung

Bereits zu Beginn des 20. Jahrhunderts entwickelte Alfred Wegener seine allgemein bekannte Rekonstruktion der Kontinente, indem er die Fragmente kontinentaler Kruste durch Schließung der großen Ozeane entlang ihrer heutigen Küstenlinien zusammenfügte, so dass alle Kontinente zu einer Landmasse vereint waren. Den resultierenden Superkontinent nannte er "Pangäa" (Wegener, 1920). In dieser Rekonstruktion liegen sich Nord- und Südamerika gegenüber und Nordwestafrika grenzt an die Südostküste Nordamerikas.

Lange Zeit nahm man an, dass die Paläogeographie dieses Superkontinents sich im Laufe seiner Existenz nicht bedeutend verändert hat, sondern dass die Kontinente sich im Jura im Wesentlichen aus der gleichen Konfiguration heraus voneinander gelöst haben, zu der sie sich ursprünglich im Paläozoikum zusammengefunden hatten. In der Tat gibt es vielfältige geologische, paläontologische und geophysikalische Hinweise dafür, dass Wegeners Pangäa-Konfiguration von der späten Trias bis in den frühen Jura Bestand hatte.
In den späten Fünfzigerjahren des vergangenen Jahrhunderts entwickelte sich mit der Paläomagnetik eine Methode, die es ermöglicht, die Bewegungen der Kontinente über das Alter des ältesten bekannten Ozeanbodens hinaus zu rekonstruieren. Aufgrund des Dipolcharakters des Erdmagnetfeldes gilt das jedoch nur für die Rekonstruktion von paläogeographischen Breitenlagen, die Lage bezüglich der Längengrade kann mit Hilfe des Erdmagnetfeldes nicht eindeutig bestimmt werden. Eine nicht unerhebliche Anzahl paläomagnetischer Studien hat gezeigt, dass Wegeners Pangäarekonstruktion, auch Pangäa A genannt, mit globalen paläomagnetischen Daten in prä-triassischer Zeit nicht kompatibel ist. Zwingt man die Nord- und Südkontinente Pangäas, Laurasia und Gondwana für diese Zeit in die Pangäa A Konfiguration, so ergibt die auf paläomagnetischen Daten basierende paläogeographische Rekonstruktion ein signifikantes Überlappen kontinentaler Krustenanteile (siehe z. B. Van der Voo (1993); Muttoni *et al.* (1996, 2003) und darin zitierte Werke). Ein solches Überlappen lässt sich jedoch mit grundlegenden geologischen

Prinzipien nicht vereinen. Im Lauf der Jahrzehnte wurden vielfältige alternative prä-triassische paläogeographische Pangäarekonstruktionen erstellt, die im Einklang mit den paläomagnetischen Daten sind. Der Hauptunterschied im Vergleich dieser Rekonstruktionen zur klassischen Pangäa A Konfiguration liegt in der Lage der Südkontinente relativ zu den Nordkontinenten. Um den kontinentalen Überlapp zu vermeiden, werden die Südkontinente unter Beibehaltung ihrer Breitenlage um ca. 30 Längengrade relativ zu den Nordkontinenten weiter im Osten platziert, so dass Nordwestafrika gegenüber Europa zu liegen kommt (Pangäa B, Irving (1977)). Da - wie erwähnt - der Dipolcharakter des Erdmagnetfeldes keine Aussagen über die Position der Kontinente bezüglich der Längengrade zulässt, ist dies mit den paläomagnetischen Daten vereinbar. Die alternativen Konfigurationen müssen jedoch alle vor dem Auseinanderbrechen Pangäas im Jura wieder in die für diesen Zeitraum allgemein akzeptierte Wegener-Konfiguration zurückgeführt werden. Dies geschieht - wiederum im Einklang mit den paläomagnetischen Daten - unter Beibehaltung der Breitenlage der Kontinente entlang einer postulierten kontinentalen dextralen Scherzone. Der Versatz von 2000 bis 3000 km fand laut Muttoni *et al.* (2003) in einem Zeitraum von ca. 20 Ma im frühen Perm statt. Dadurch ergibt sich eine entsprechend hohe Versatzrate von 10 bis 15 cm/a.

Diese Arbeit befasst sich im Rahmen mehrerer paläomagnetischer Studien mit der Suche nach dieser großen Scherzone, deren Existenz seit Jahrzehnten umstritten ist. Der große Versatz wurde vermutlich von mehreren Störungssegmenten aufgenommen, die eine mehrere hundert Kilometer breite diffuse und segmentierte Scherzone bildeten. Paläogeographische Rekonstruktionen legen nahe, dass die Scherzone unter Anderem den Bereich des heutigen Mittelmeerraumes umfasst hat (Arthaud and Matte, 1977). Die Tizi-N'-Test-Verwerfung und ihre westliche Fortsetzung, die Süd-Atlas-Störung, sowie Verwerfungen entlang der nördlichen Pyrenäen und innerhalb des Armorikanischen Massivs (Bretagne) bilden demnach die Hauptblattverschiebungssysteme, die die Scherzone begrenzen. Krustenblöcke, die in entsprechend großen Störungssystemen liegen, können um vertikale Achsen rotieren (Nelson and Jones (1987) und darin zitierte Werke). Diese Rotationen können mit Hilfe der Paläomagnetik quantifiziert werden.

Kapitel 1 leitet in die vorstehend beschriebene Problematik ausführlich ein und beleuchtet insbesondere die einzelnen Abschnitte dieser Arbeit. Somit wird deutlich, wie die Ergebnisse der Studien, aus denen sich die vorliegende Arbeit zusammensetzt, aufeinander aufbauen und einen konsistenten Lösungsansatz für die eingangs beschriebene Diskrepanz zwischen den Polwanderkurven Laurasias und

Gondwanas entwickeln.

Kapitel 2 beschreibt eine paläomagnetische Studie, die im Toulon-Cuers Becken, Südfrankreich durchgeführt wurde. Das Toulon-Cuers Becken entstand während einer Phase der Extension im südlichen variszischen Gürtel Europas, und ist sukzessive mit Sedimenten verfüllt worden. Außer mächtigen permo-triassischen Sedimentpaketen finden sich hier auch Laven und Pyroklastika als Produkte eines extensionsgetriggerten Vulkanismus, die ebenfalls Gegenstand der hier durchgeführten Studie sind. Die Ergebnisse der Untersuchungen können sehr gut mit bereits vorhandenen Literaturdaten in Einklang gebracht werden und zeigen, dass es zur fraglichen Zeit durchaus Bewegungen zwischen klar definierten Krustenblöcken gab, die Zeugen einer generellen Mobilität der Kruste in diesem Bereich sind. Es handelt sich hierbei um Blockrotationen um vertikale Achsen, so wie sie im Spannungsfeld einer kontinentalen Transformstörung zu erwarten sind. Dabei werden Rotationen im und gegen den Uhrzeigersinn dokumentiert, woraus eine komplexe Geometrie und Anordnung der Krustenblöcke abgeleitet werden kann. Hieraus wird ein tektonisches Modell entwickelt, welches mit gängigen Modellen (siehe McKenzie and Jackson (1983) in Nelson and Jones (1987)) in Einklang gebracht wird. Die triassischen paläomagnetischen Daten aus dem Gebiet belegen im Gegensatz dazu keine Rotationen und legen daher den Schluss nahe, dass die Krustenmobilität in dem Bereich zu Beginn des Mesozoikums zum Erliegen gekommen war. Somit belegt diese Studie deutlich, dass es im von Muttoni *et al.* (2003) postulierten zeitlichen Rahmen Hinweise für eine generelle Mobilität innerhalb Pangäas gibt.

Unter Berücksichtigung dieser Ergebnisse wurde die folgende Studie an magmatischen Ganggesteinen ("Dykes") in Sardinien (Italien) durchgeführt, um die laterale räumliche Dimension der Scherzone besser abschätzen zu können. Kapitel 3 stellt die Ergebnisse dieser Studie vor. Die Dykes treten schwarmförmig auf und sind in einem Zeitraum zwischen 298 ± 5Ma und 270 ± 10Ma in den Korsika-Sardinien-Batholith intrudiert (Atzori and Traversa, 1986; Vaccaro *et al.*, 1991; Atzori *et al.*, 2000). Zusätzlich zu den Rotationen, die auch hier mittels paläomagnetischer Daten nachgewiesen werden konnten, gibt die Orientierung der einzelnen Dykeschwärme Aufschluss über das tektonische Spannungsfeld, das während der Platznahme der Dykes vorherrschte. Diese kombinierten Ergebnisse bestätigen und ergänzen die Ergebnisse der vorhergehenden Studie in Südfrankreich.

Ergänzend zu den Untersuchungen an den Ganggesteinen Sardiniens werden Daten von permischen Sedimenten und Vulkaniten präsentiert, die in verschiedenen

Regionen Sardiniens beprobt wurden (Kapitel 4). Die paläomagnetischen Daten belegen, dass Sardinien in mindestens zwei Krustensegmente zerlegt war, welche relativ zueinander und auch relativ zur europäischen Polwanderkurve rotiert sind. Auch hier wiederholt sich das Muster von Rotationen im und gegen den Uhrzeigersinn. In dieser Studie werden die Ergebnisse aus den vorangehenden Kapiteln sowie aus der weiterführenden Literatur zusammengefasst, so dass ein zeitlich und räumlich verfeinertes Bild der Krustenblöcke im westlichen Mittelmeerraum zur Zeit des frühen Perm entsteht. Durch die verbesserte Definition der Geometrie der einzelnen Blöcke kann das in Kapitel 2 beschriebene tektonische Modell bestätigt werden.

Kapitel 5 befasst sich abschließend mit dem zeitlichen Rahmen der Aktivität entlang der fraglichen Scherzone. Ausgehend von der Annahme, dass sich die Kontinente im Jura bereits in einer Pangäa A Konfiguration befunden haben, sollten die paläomagnetischen Daten von jurassischen Gesteinen keine Hinweise auf Scherbewegungen geben. Hierzu wird eine Studie an jurassischen Sedimenten Sardiniens vorgestellt. Die paläomagnetischen Daten der untersuchten Krustensegmente belegen, dass es in post-jurassischer Zeit in Sardinien keine Blockrotationen der einzelnen Segmente relativ zueinander gab und Sardinien somit ab jener Zeit als tektonisch einheitlicher Block behandelt werden muss. Des Weiteren zeigen die paläomagnetischen Pole, die aus den paläomagnetischen Richtungen für eine Referenzlokalität berechnet wurden, keine signifikante Abweichung von der Polwanderkurve des europäischen Kontinents nach Besse and Courtillot (2002). Diese Kohärenz der paläomagnetischen Daten bestätigt die weithin akzeptierte Beobachtung, dass sich Pangäa zur Zeit des Jura bereits in der Wegener Konfiguration (Pangäa A) befunden hat und untermauert die Aussagekraft paläomagnetischer Studien in diesem Zusammenhang. Zugleich kann anhand dieser Daten ausgeschlossen werden, dass die alpidische Orogenese die Ursache für bedeutende Krustenblockrotationen in dieser Region gebildet hat.

Die Ergebnisse der oben genannten Studien werden in dieser Arbeit zusammengeführt. Im Verbund mit Daten aus der Literatur untermauern sie, dass es zwischen dem frühen Perm und der frühen Trias entlang eines ausgedehnten Gürtels, der mindestens vom französischen Zentralmassiv über Südfrankreich bis nach Korsika-Sardinien reichte, bedeutende Krustenbewegungen in Form von Blockrotationen innerhalb Pangäas gab. Die vorliegende Synthese schafft somit ein konsistentes Bild der generellen Krustenmobilität zwischen den nördlichen Teilen Pangäas (Laurasia) und den Südkontinenten (Gondwana). Der durch die präsentierten Stu-

dien abgesteckte zeitliche Rahmen korreliert mit den Abschätzungen von Muttoni *et al.* (2003) zur Transformation zwischen verschiedenen Pangäakonfigurationen. Diese Arbeit bestätigt außerdem, dass das mittlere Perm eine Zeit großräumiger Reorganisation der kontinentalen Platten war, die von anhaltender magmatischer Aktivität begleitet war (Deroin and Bonin, 2003; Isozaki, 2009). Anhand der hier vorgestellten neuen Daten in Kombination mit bereits bekannten paläomagnetischen Daten aus der Region ergibt sich ein klares Muster von Rotationen im und gegen den Uhrzeigersinn von einzelnen störungsbegrenzten Krustenblöcken. Diese Arbeit belegt, dass die Paläomagnetik ein hervorragendes Instrument zur Quantifizierung jener Krustenblockrotationen ist, die oftmals die einzigen verbleibenden Indizien für ehemals großräumige Scherzonen bieten, nachdem die Störungen selbst aufgrund vielfältiger Prozesse nicht mehr aufgeschlossen sind (Umhoefer, 2000). Die tektonischen Modelle von McKenzie and Jackson (1983) in der Interpretation nach Nelson and Jones (1987) werden als Erklärungsgrundlage für die beobachteten Rotationen herangezogen und erweitert.

Contents

1 Introduction

Early in the 20^{th} century, Alfred Wegener developed his famous global continental reconstruction of all existing landmasses by joining them along their present day coastlines into one supercontinent which he called "Pangea" (Wegener, 1920). In this reconstruction, South America faces North America and northwest Africa opposes southeast North America.

Outside the realm of paleomagnetic studies, it has been a long held tenet that the continental constituents of Pangea disseminated from essentially Wegener's Pangea fit in the Jurassic and in fact, there is widespread geological, paleontological and geophysical evidence supporting this assumption during the Late Triassic to Early Jurassic. Klitgord and Schouten (1986) demonstrated most convincingly that the paleogeography of Early Jurassic time, just prior to the opening of the central Atlantic, was essentially that of Pangea A by correlating conjugate seafloor magnetic anomalies and marine fracture zones. The validity of this paleogeography, however, was questioned for earlier Mesozoic and late Paleozoic times, from which no in situ seafloor survived (see Irving (1977); Morel and Irving (1981)). Ever since the rise of paleomagnetism as an alternative means to reconstruct the paleolatitudinal positions of the continents, it has been shown repeatedly that global paleomagnetic data are incompatible with the Wegener fit (Pangea A) for pre-Late Triassic times. Pioneering work of Van Bemmelen and colleagues in the 1960s revealed Permian

inclinations that indicated more northerly paleolatitudes for the northern part of the Italian Peninsula than were predicted from the available Permian poles of Stable Europe. Irving (1977) describes a substantial cratonic overlap between Gondwana and Laurasia for the late Paleozoic to early Mesozoic when reconstructed in an A-type Pangea configuration. This, however, cannot be reconciled with fundamental geological concepts. A more recent study by Muttoni *et al.* (1996) confirms the observed crustal overlap for the Early Permian. This discrepancy has become a fundamental enigma of late Paleozoic to early Mesozoic paleogeographic reconstructions based on paleomagnetic data. Various arguments have been invoked in order to explain the large disparity in the apparent polar wander paths (APWPs) of Laurasia and Gondwana, especially in the Early Permian. Tentative explanations are (1) the effects of poor data quality, especially from Gondwana as discussed in Van der Voo (1993) and Rochette and Vandamme (2001), (2) the effects of an unrecognized non-dipole field contribution contaminating the geocentric axial dipole (GAD) which would ultimately lead to a bias in the paleomagnetic data resulting in the observed crustal overlap (Van der Voo and Torsvik, 2001; Torsvik and Van der Voo, 2002), and (3) inclination shallowing in sediments which - if unaccounted for - leads to an enhancement of said data bias (Rochette and Vandamme, 2001). These arguments, however, have been addressed by Muttoni *et al.* (2003). In their paleomagnetic study on well dated volcanic rocks from low latitudes of one hemisphere, they were able to avoid the possible effects of both a non-dipole contribution to the GAD field and inclination shallowing in sedimentary rocks. Additionally, their study shows the coherence of Adria and Africa (as a representative of Gondwana), thus providing once more good quality paleomagnetic data from Gondwana documenting the incoherency of the paleomagnetic record with a Pangea A-type reconstruction for the Early Permian.

A number of alternative Pangea reconstructions have been suggested which are in agreement with the paleomagnetic data from Pangea for the Early Permian. Those reconstructions return to the conceptual ideas of Van Hilten (1964), noting the longitude indeterminacy of paleomagnetic data. To avoid the impossible continental overlap, these alternative Pangea configurations place Gondwana farther to the east with respect to Laurasia in the Early Permian. This essentially results in the Pangea B configuration of Irving (1977) with South America and Africa facing the southern margin of Europe. As mentioned before, it is an undisputed fact that the continental constituents of Pangea disseminated from the classical Wegener fit in Jurassic times. Therefore, the continents need to be transferred from the Pangea B configuration to this configuration before the Jurassic. This crustal reorganization implies the

existence of a large continental dextral shear zone extending approximately along the paleoequator. This shear zone would accommodate the substantial westward shift of Gondwana covering 2000 to 3000 km, essentially maintaining the paleolatitudes of the involved continents. The time-window for the transformation only spans 20 million years from the Early to Middle Permian (Muttoni *et al.*, 2003) and therefore requires high rates of shearing of about 10 to 15 cm/a. Presumably, the large offset was accommodated by several segments of transform faults defining a wide and diffuse shearzone.

The continental-scale events of dextral shearing related to late Paleozoic Pangea instability should have left a fingerprint in the crustal structure and geological record of portions of southern Europe formerly located between Laurasia and Gondwana. Cassinis *et al.* (2012) outline in their extensive study on the Permian continental basins in the southern Alps of Italy the existence of two distinct tectono-sedimentary cycles that can be observed in the late Paleozoic and early Mesozoic continental successions of southern Europe. The sedimentary record clearly testifies to two major geodynamic events in the aftermath of the Variscan orogenesis. (1) the Late Carboniferous to Early Permian evolution of the Gondwana-Eurasia collisional margin into a diffuse dextral transform margin and (2) the Middle to Late Permian opening of the Neotethys ocean and the associated extensional tectonic regime. Although Cassinis *et al.* (2012) do not associate their observations in the sedimentary record of southern Europe with the Pangea transformation *sensu* Muttoni *et al.* (2003), the record is indicative of the general intra-Pangea mobility and reorganization of tectonic plates during the Permian.

In addition to the above described sedimentary record documenting the evolution of the Gondwana-Laurasia boundary into a diffuse dextral transform margin, in an earlier study, Arthaud and Matte (1977) outline the tectonic setting for large-scale shearing within Pangea. They identify the High Atlas fault, the Biscay-North Pyrenean fault, and the South Armorican shears in Britanny as first-order wrench faults. Following the geological and structural evidence, we conclude that the outlines of the putative Pangea transform zone include parts of the present day Mediterranean realm. Based on previous observations of large-scale rotations of crustal segments trapped in continental-scale shear zones, which could be quantified via paleomagnetic methods (e. g. Nelson and Jones (1987)), several paleomagnetic studies were conducted systematically in the southwestern part of Europe in order to find evidence for the existence of the highly-debated continental-scale shearzone and intra-Pangea mobility within the temporal and spatial frames given by Muttoni

et al. (2003) and Arthaud and Matte (1977), respectively. The studies are outlined shortly hereafter.

Chapter 2 presents paleomagnetic data from Permo-Triassic sedimentary and volcanic rocks from the Toulon-Cuers basin in southeast France. Here, a total of 150 samples from 14 sites were collected; 108 samples yielded reliable paleomagnetic component directions based on stepwise thermal demagnetization. After removal of an initial viscous magnetic component from room temperature up to 200°C, a second component of reverse polarity was identified in almost all samples of Permian age and construed as being of primary character. The Triassic samples behave in essence similarly, with the notable difference that here, two polarities of magnetization are present. Positive field tests suggest the primary character of this characteristic magnetization. The latitudes of the resulting Early to Mid Permian paleopoles agree well with the corresponding segment of the APWP for Europe (Smethurst *et al.*, 1998), whereas the longitudes are distributed along a small circle segment, indicating clockwise and counterclockwise rotations of the sampled regions relative to stable Europe which is indicative for a complex geometry and interaction pattern of the crustal segments. This finding is compatible with well-received general tectonic models (e. g. McKenzie and Jackson (1983) as in Nelson and Jones (1987)) dealing with crustal block rotations related to shearing. Based on these models, a simple ball bearing model was developed to accomodate the observed rotations of both, clockwise and counter-clockwise sense. The Triassic poles, instead, plot close to the Triassic segment of the European APWP, indicating coherence of the sampled crustal segments with cratonic stable Europe. This result provides a robust upper time constraint for the rotations observed in the Permian rocks, i. e. rotations of these blocks seem to have ceased in the Triassic. The results suggest a wrench faulting event associated with intra-Pangea crustal instability and transformation during the Permian, thus confirming the timeframe initially set by Muttoni *et al.* (2003).

After having established an improved time constraint for intra-Pangea mobility, the next study focusses on the spatial extent of the identified mobile zone (chapter 3). To this end, 13 late Variscan dykes (233 samples) from Sardinia ranging in age from 298 ± 5Ma to 270 ± 10Ma (Atzori and Traversa, 1986; Vaccaro *et al.*, 1991; Atzori *et al.*, 2000) were sampled for paleomagnetic analysis. Magnetic component directions have been retrieved using thermal and alternating field demagnetization techniques, which gave reproducible results. The paleomagnetic mean declinations differ significantly between northern Sardinia and south-eastern and central-eastern

Sardinia with consistently low inclinations, the latter two regions yielding statistically similar paleomagnetic mean directions. These results indicate that Sardinia fragmented into two, arguably three, crustal blocks after dyke emplacement. In addition to the differences in paleomagnetic declinations, it was found that the original geometry of the dyke swarm is essentially restored after correction with respect to the expected paleomagnetic declinations for reference localities in the different parts of Sardinia. The block rotations documented in this study are reminiscent of the block rotations previously observed in Permian sediments and volcanic rocks from the Toulon-Cuers basin of SE France (Aubele *et al.* (2012), chapter 2), which was located along the European margin immediately to the west of Sardinia in Permian times. After restoration to European coordinates, the latitudes of the Early Permian paleopoles from the Sardinian dykes agree well with the corresponding segment of the APWP of Baltica (Europe) (Torsvik *et al.*, 2012), whereas the longitudes are distributed along a small circle segment, indicating relative rotations of the sampled regions with respect to stable Europe.

Complementary paleomagnetic data from Permian sedimentary rocks and pyroclastic deposits from northern and southern Sardinia are presented in chapter 4. New paleomagnetic poles for the Early Permian from 18 sites (167 samples) from northern and southern Sardinia are presented. Reproducible paleomagnetic component directions have been retrieved using thermal demagnetization. The new paleomagnetic poles - transferred into European coordinates to account for the opening of the Ligurian Sea and the Bay of Biscay in the Cenozoic - are compared with data from stable Europe. Whereas the Early Permian pole for northern Sardinia is rotated clockwise (cw) to the west of the coeval segment of the APWP of stable Europe, the coeval paleomagnetic pole for central-southern Sardinia is rotated counterclockwise (ccw) away to the east of the APWP, thus suggesting post-Early Permian differential vertical axis rotations between central-southern and northern parts of the island, which is in agreement with earlier paleomagnetic data from Sardinia and the greater Mediterranean realm as presented in the previous chapters.
In addition, chapter 4 combines the previously discussed results and literature data. This allows a substantial refinement of the outlines of the Early Permian crustal blocks in the western Mediterranean and confirms the ball bearing model of differential crustal block rotations presented in chapter 2.

Chapter 5 presents a paleomagnetic study on Jurassic marine sedimentary rocks on Sardinia which provides evidence for the crustal coherence of Sardinia ever since

the Jurassic. A total of 280 oriented drill cores were taken from 44 sites of Middle and Late Jurassic age in the Nurra, Baronie-Supramonte, Barbagia-Sarcidano and Sulcis regions. Despite generally weak remanent magnetization intensities, in the order of less than 1 mA/m, thermal and alternating field demagnetization was successfully applied to extract a characteristic remanent magnetization component in about 60% of the samples. The results from this study indicate only insignificant amounts ($\pm 10^{\circ}$) of post-Jurassic rotations within the island of Sardinia. In addition, the paleomagnetic poles for the Early and Late Jurassic time period from this study coincide with the apparent polar wander path (APWP) after Besse and Courtillot (2002) for stable Europe at the time. The documented absence of crustal block rotations within the Sardinia block indicates that intra-Pangea mobility had ceased by the time the Jurassic sediments acquired their magnetic remanence which is in agreement with the generally accepted Jurassic Pangea A. These findings are indicative for the general suitability of the adopted paleomagnetic approach and allow to preclude deformation processes related to the alpine orogeny to be the cause for eventual rotations in older rocks from the area.

The synthesis of paleomagnetic studies presented here provides evidence for a belt of mobile crustal blocks straddling at least from southern France, the Massif Central, the Maures-Estérel block and Corsica-Sardinia during late Early Permian to Early Triassic times. The observed substantial vertical axis block rotations are in agreement with well-received tectonic models (McKenzie and Jackson, 1983; Nelson and Jones, 1987) and confirm the reorganization of continental plates during the Permian, associated with continuous magmatic activity at the time (Deroin and Bonin, 2003). Paleomagnetism on well dated rocks once again proves to be a powerful tool to quantify vertical axis rotations as sole remainders of large-scale faulting after direct evidence for the faults has long vanished due to manifold reasons (Umhoefer, 2000). The timing of intra-Pangea mobility that could be established by the presented studies coincides with the timing of the Pangea B to A transformation as postulated by several authors (Irving, 1977; Muttoni *et al.*, 2003).

2

A Paleomagnetic Study of Permian and Triassic Rocks from the Toulon-Cuers Basin, SE France: Evidence for intra-Pangea Block Rotations in the Permian

By ***K. Aubele, V. Bachtadse, G. Muttoni, A. Ronchi and M. Durand***
published in Tectonics, *2012,* ***31*** *(TC3015), doi:10.1029/2011TC003026.*

Abstract

The identification of a massive shear zone, separating Gondwana from Laurasia during late Palaeozoic times is one of the prerequisites for the controversial Pangea B to A transition. Here we present new paleomagnetic data from Permian and Triassic sediments and volcanic rocks from the Toulon-Cuers basin, SE France, likely to be situated within this intra Pangea shear zone. A total of 150 samples from 14 sites were collected in the field; 108 samples yielded reliable paleomagnetic component directions based on stepwise thermal demagnetization up to maximum temperatures of 690°C. After removal of an initial viscous magnetic component from room temperature up to 200°C, a second component of reverse polarity, oriented to the south-and-up, was identified in almost all samples of Permian age. The Triassic samples behave similarly, with the notable difference that here, two polarities of magnetization are present. Positive field tests suggest the primary character of this characteristic magnetization. The latitudes of the resulting Early to Mid Permian paleopoles agree well with the corresponding segment of the apparent polar wander path (APWP) for Europe, whereas the longitudes are strung out along a small circle segment, indicating relative rotations between the sampled regions and stable Europe. The Triassic poles, instead, plot close to the Triassic segment of the European APWP, and provide an upper time limit for the observed rotations. These results suggest a wrench faulting event associated with intra-Pangea crustal instability and transformation during the Permian.

2.1 Introduction

The Variscan amalgamation of Laurasia and Gondwana was followed by a late Paleozoic period of Pangea instability and reconfiguration. In their classic study on strike-slip faulting in Europe and northern Africa, Arthaud and Matte (1977) point out the existence of a Late Carboniferous - Early Permian right lateral shear system connecting the Appalachians to the Urals, with the central part of this intra-Pangea shear system being presumably located between the Iberian Peninsula and the Bohemian massif (Fig. 2.1).

Within this tectonic setting, the High Atlas fault, the Biscay-North Pyrenean fault, and the South Armorican shears in Britanny (see also Bard (1997)) acted as first-order wrench faults. Based on the original observations made by Arthaud and Matte (1977), Muttoni *et al.* (1996, 2003) suggested that this episode of intra-Pangea wrench faulting was followed by the transformation of Pangea from an Early Per-

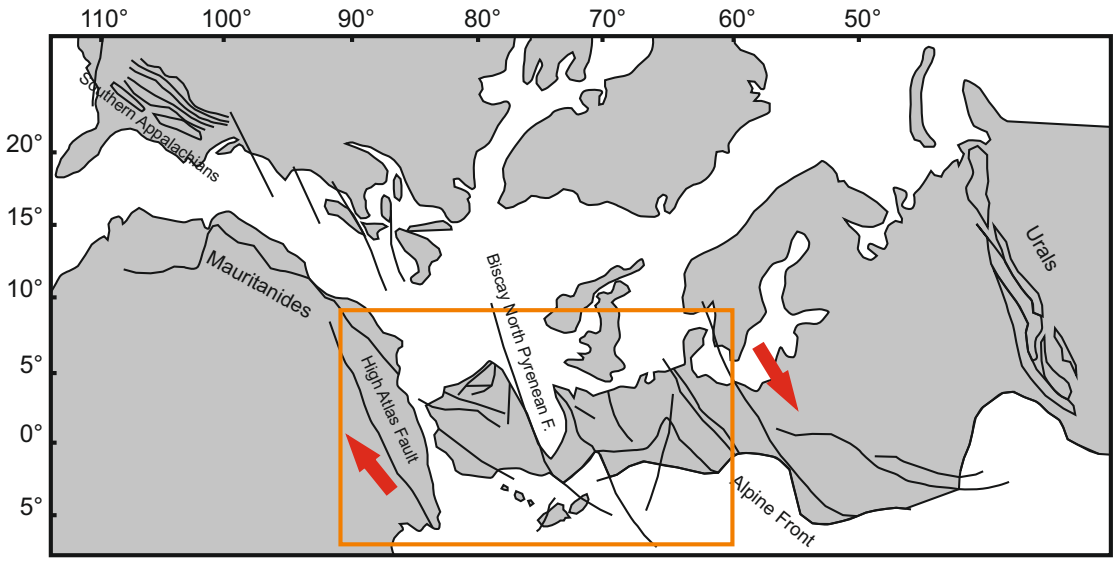

Figure 2.1: Location and outlines of the Pangea Transform Zone after Arthaud and Matte (1977).

mian configuration termed B after Irving (1977), characterized by South America and Africa located to the south of Europe and Asia, respectively, to a Late Permian Wegenerian A-type configuration by way of 3000km of dextral displacement of Laurasia relative to Gondwana occurring essentially during the middle part of the Permian (Fig. 2.2) (see Muttoni *et al.* (2003)).

However, the necessity to arrange Laurasia and Gondwana in a Pangea B configuration as opposed to the classic Wegenerian geometry has been challenged by several authors who questioned the quality of the palaeomagnetic data set for the Carboniferous and Permian and therefore the derived magnitude of the continental overlap between the two supercontinents at the basis of the Pangea B concept (see Muttoni *et al.* (2003); Irving (2005) and Domeier *et al.* (2012) for different views on the Pangea controversy).

The continental-scale events of dextral shearing related to late Paleozoic Pangea instability should have left a fingerprint in the crustal structure of portions of southern Europe formerly located between Laurasia and Gondwana (Figs. 2.1, 2.2). For example, tectonic block rotations have been observed in Early Permian rocks from the French Massif Central, while Late Permian rocks from the same area are unrotated (Chen *et al.* (2006) and references therein); large rotations have also been documented in Late Carboniferous - Permian rocks from Maures-Estérel in southern

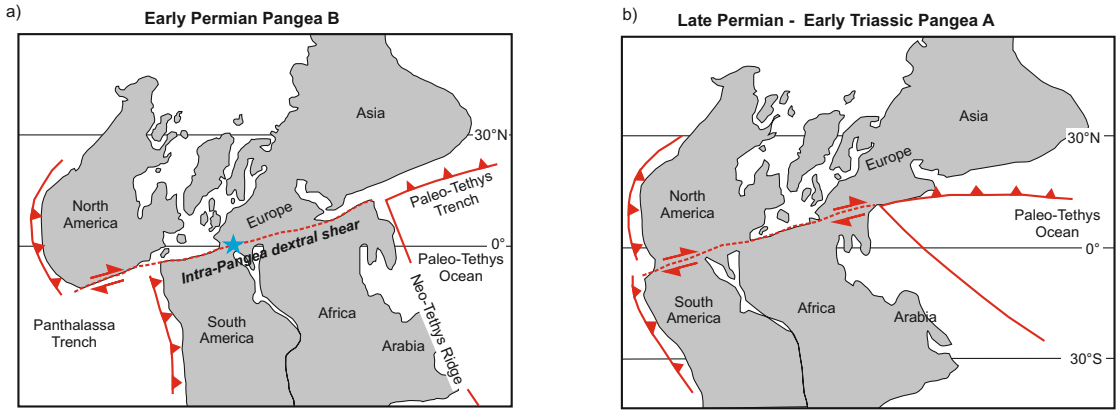

Figure 2.2: a) Pangea B configuration after Irving (1977) in the Early Permian. b) Wegenarian Pangea A configuration after Muttoni *et al.* (2003, 2004) in the Late Permian to Early Triassic. The blue star marks the study location in SW Europe. Modified after Muttoni *et al.* (2009).

France and from Corsica-Sardinia (Edel, 2000; Emmer *et al.*, 2005); in Sardinia, recent paleomagnetic results indicate that these rotations should have occurred before Jurassic times (Aubele, 2010; Kirscher *et al.*, 2011).
Despite this growing body of knowledge, it is fair to say that the precise timing, geographic distribution, and triggering mechanism(s) of these block rotations are still poorly constrained. In order to enhance our knowledge on Permian deformation and block rotations in the Mediterranean, we carried out a paleomagnetic study on Permian - Triassic sediments and Permian volcanic rocks from the Toulon-Cuers region of southern France (see Figs. 2.3 and 2.4).

2.2 Geological setting

In the course of the late Paleozoic period of crustal instability and re-equilibration of the European and African lithosphere, the Toulon-Cuers basin in SE Provence opened as a result of NE - SW directed crustal extension (McCann *et al.*, 2006).
In the following paragraphs, the stratigraphic units of the Toulon-Cuers basin and the associated age estimates taken from the literature are described (Durand, 2001) [1]. Figure 2.4 (modified after Durand (2008)) summarizes the stratigraphic and numer-

[1]for detailed stratigraphic information, the reader is referred to the supplemental material provided online

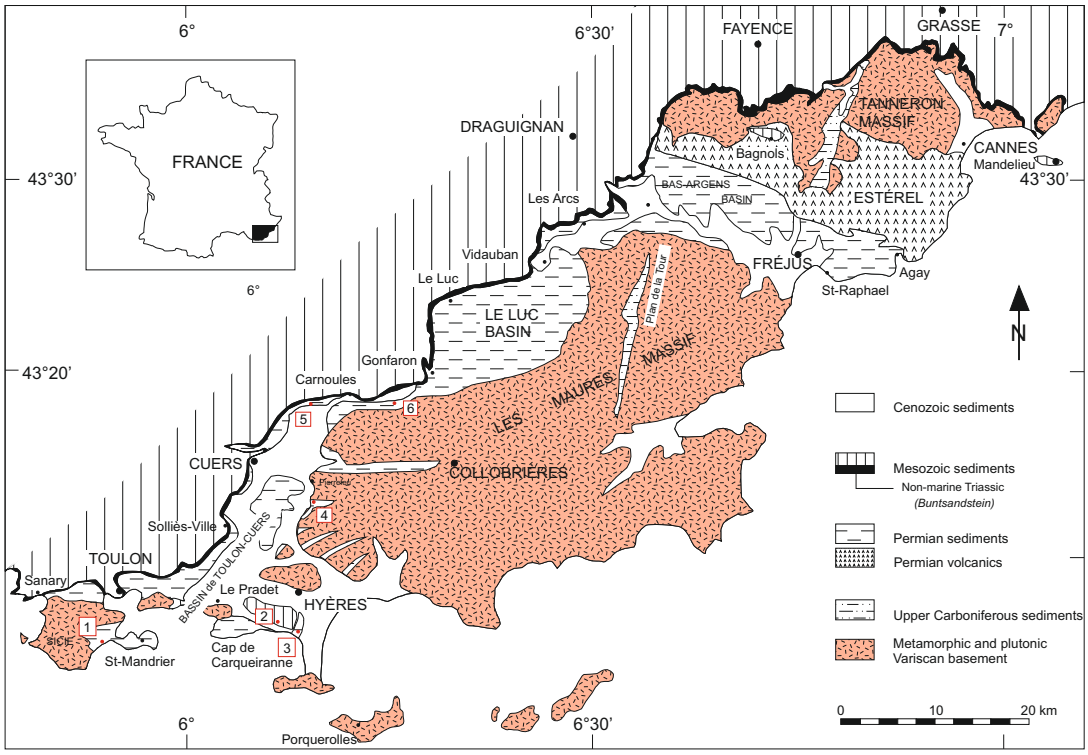

Figure 2.3: Geological outline of Provence, SE France including sample locations (1: five sites within the Saint-Mandrier Fm., 2: three sites within the Grès de Gonfaron (sandstone), 3: three sites within the Les Salettes Fm., 4: sites within the Les Pellegrins Fm. (rejected from the dataset), 5: one site within the Bron Fm. near Carnoules, 6: two sites within the Bron Fm. near Saint Barthélémy). From Cassinis *et al.* (2003), modified and redrawn.

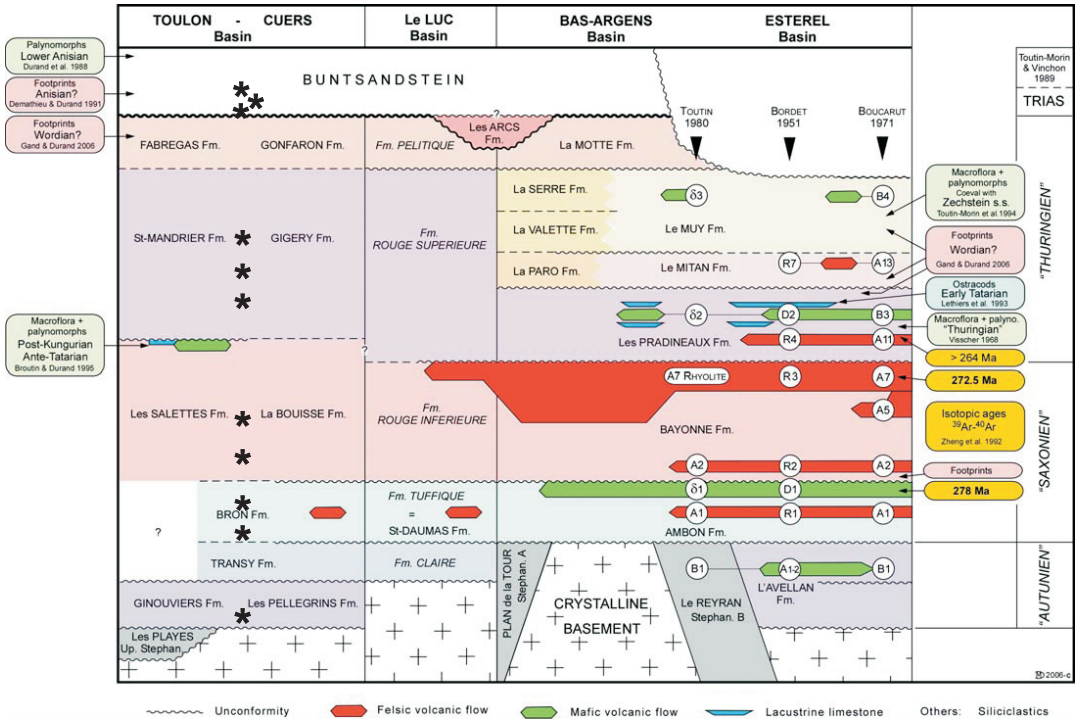

Figure 2.4: Lithostratigraphic correlations through the Permian basins of Provence with location of the dating elements. Asterisks indicate the position of the sampled horizons. After Durand (2008) and references therein.

ical ages of the studied units after Visscher (1968); Durand *et al.* (1988); Demathieu and Durand (1991); Zheng *et al.* (1992); Lethiers *et al.* (1993); Broutin and Durand (1995) and Gand and Durand (2006).

2.2.1 Permian stratigraphy

Les Pellegrins Formation

The oldest unit, the 50 to 80m-thick Les Pellegrins Formation unconformably overlies the metamorphic basement throughout the Toulon-Cuers basin. It starts with a conglomerate/breccia unit containing mainly basement-derived phyllitic clasts, followed by an alternation of thick grey to yellow sandstone lenses representing fluvial channel-fills and thinner dark-grey silt and clay layers pertaining to floodplain deposits. Red hues are very localized and siderite nodules and lenses are frequent.

The age of the Les Pellegrins Formation is broadly constrained between the Stephanian and the middle-late Autunian ($\sim 299 - 282$Ma) (Parent, 1932; Bouillet and Lutaud, 1958; Bassot, 1987; Ronchi *et al.*, 1998).
The transition to the overlying unit, the Transy Formation (not sampled for paleomagnetic investigation), is marked by an angular unconformity reaching up to 15°. The lower part of the Transy Formation consists of pale conglomeratic sandstones with high mineralogical maturity whereby most clasts are made of quartz.

Bron Formation

The Bron Formation, located stratigraphically above the Transy Formation and exposed near Carnoules and Pignans (St. Barthélémy) is characterized by a variably thick sequence of alternating arkosic sandstones, siltstones and red to greenish clays. Tuff deposits associated with rhyolitic lava flows are also present. According to its stratigraphic position, the Bron Formation can be dated to post-Stephanian to pre-Kungurian ($\sim 299 - 275$Ma).

Les Salettes Formation

The Les Salettes Formation is highly heterogeneous in composition; the lower member comprises tuffs associated with more than 7 basaltic lava flows that reach local thicknesses between 10 and 40m. These flows, outcropping in the Carqueiranne area, pertain to the second Permian magmatic (alkaline) cycle of the Western Mediterranean (Leroy and Cabanis, 1993). The remainder of the lower member consists of coarse- to medium-grained sandstones and conglomerates with volcanic clasts arranged in low-angle, cross-stratified tabular sets pertaining to braided river settings. The upper member of the Les Salettes Formation, the Bau Rouge Limestone, crops out along the cliffs of Cap Garonne. It was defined by Durand (1993) as a 25m-thick unit consisting of limestone beds of mainly lacustrine environment with domal stromatolites and black chert nodules. Macroscopic plant remains and palynomorphs led Broutin and Durand (1995) to suggest a post-Kungurian to pre-Tatarian age for the Bau Rouge member.

Saint-Mandrier Formation

The Permian Saint-Mandrier Formation reaches a total thickness of about 700m (see Durand (2008) p. 706). The upper part of the section contains 7 rhyolitic tuff beds that present the last phase of Permian volcanic activity in Provence. Sediments

of meandering-channel settings are also present (Durand, 1993); according to sedimentological evidence, these sediments were deposited by bed-load, medium-scale streams under mild to semi-arid climate conditions (Durand, 1993).

Gonfaron Formation

The 40m-thick Gonfaron Formation represents the uppermost part of the Permian sequence within the Toulon-Cuers basin (coeval to the Fabregas Formation as shown in Figure 2.4). It consists of a rather monotonous succession of red claystones and siltstones interlayered with green, thinly-bedded and fine-grained sandstones with sedimentary structures like current and wave ripples, desiccation cracks, and small load casts. Trace fossils were described by Demathieu *et al.* (1992).

2.2.2 Triassic stratigraphy

Buntsandstein Group

Two formations have been defined within the Buntsandstein Group of Provence: the basal Poudingue de Port-Issol Formation and the Grès de Gonfaron Formation (Glinzboeckel and Durand, 1984; Durand *et al.*, 1988). The 8m-thick Poudingue de Port-Issol is a grain supported oligomictic conglomerate consisting mainly of quartzpebbles and small cobbles derived from quartz veins with silicious matrix. It is well exposed to the south of Port-Issol Point, Fabregas and Carqueiranne Point. Its high mineralogical and textural maturity speak in favour of protracted, maybe even polycyclic, fluvial transport. Many pebbles also display secondary edges due to abrasion by wind-blown sand and thus testify to arid climates, recognized also in other parts of Europe around the middle part of the Scythian (Early Triassic) (Durand *et al.*, 1989).
The 12m-thick Grès de Gonfaron Formation (not to be confused with the Permian Gonfaron Formation) is mainly comprised of coarse- to medium-grained grey-greenish to red sandstones, locally alternating with claystones (e.g. near Plage de la Garonne), pertaining to floodplain to playa settings. The presence of frequent carbonate concretions of pedogenic origin and, in the upper part, of paleosols (dolocretes, silicretes) indicate arid to semi-arid climates (Durand *et al.*, 1989). The Grès de Gonfaron Formation is dated to the early Anisian ($\sim$ 245Ma) based on palynomorphs (Durand *et al.* (1988) and references therein).
In the study area, the Grès de Gonfaron strata are tilted up to 80° as a consequence of tectonic activity related to the Pyrenean-Provençal orogeny (mainly Paleocene to

Early Eocene in age) that lead to N-S shortening in the Toulon region (M. Durand, pers. communication).

Muschelkalk Group

Along the Triassic belt of Provence, the Grès de Gonfaron Formation is overlain by the Grès en plaquettes de Solliès Formation attributed to the Muschelkalk Group (Durand, 2001). It consists of yellowish grey sandstones containing halite pseudomorphs that are considered as the first evidence of post-Variscan marine influence in the area (Durand, 2001).

2.3 Field and Laboratory Methods

A total of 150 oriented core samples were taken from 14 sites at six locations (Fig. 2.3); 108 samples yielded reliable paleomagnetic component directions, described hereafter. In stratigraphic order, the sampled rock units are: (1) Les Pellegrins Fm., (2) Bron Fm., (3) Les Salettes Fm., (4) Saint-Mandrier Fm., (5) Poudingue de Port-Issol Fm. and (6) Grès de Gonfaron Fm. Within each formation, several sites were drilled in the field with a gasoline-powered, water-cooled rock-drill and oriented using a standard magnetic compass; samples were then labelled with an univocal code containing the formation name acronym, e.g. MAN for the Saint-Mandrier Fm., followed by the site number (1, 2, ...). Individual samples taken at each site are again numbered, such that sample 1 from site 1 from the St. Mandrier Formation is labelled MAN1-1.
Subsequently all samples were in the laboratory cut into $\sim$ 10cc cylindrical specimens. Multiple specimens cut from one sample were used to provide checks on the consistency of the natural remanent magnetization (NRM) and on additional rock-magnetic measurements.
All samples were studied in the paleomagnetic laboratory of the University of Munich. The specimens were stepwise thermally demagnetized using a Schoenstedt oven. The magnetization was measured with a 2G Enterprises DC-SQUID (Superconducting QUantum Interference Device) cryogenic magnetometer in a magnetically shielded room. Hysteresis parameters were determined using a Variable Field Translation Balance (VFTB, Krása *et al.* (2007)). Pilot studies demonstrated that thermal demagnetization is more efficient than alternating field demagnetization, and thus the vast majority of the specimens was thermally demagnetized using increments of $20 - 30$°C up to maximum temperatures of 690°C. Demagnetization results were plotted on orthogonal vector diagrams (Zijderveld, 1967) and analyzed using the

least square method (Kirschvink, 1980) on linear portions of the demagnetization paths defined by at least four consecutive demagnetization steps. The linear fits were anchored to the origin of the demagnetization axes where appropriate. Only occasionally the combined use of remagnetization circles and endpoint data (McFadden and McElhinny, 1988) was applied to retrieve component directions with overlapping coercivity spectra. Subsequently, site mean directions were calculated from the paleomagnetic directions of the individual samples. Thus, it was possible to calculate a virtual geomagnetic pole for each site.

2.4 Rock-magnetic data

Rock-magnetic measurements were performed on selected samples representative of the main studied lithologies (Fig. 2.5).
All tuff samples from the Les Salettes Formation show very similar rock-magnetic behaviours (Fig. 2.5a). Key features of the heating portion of the thermomagnetic experiments are (a) a drop in intensity at $\sim 150 - 180$°C, followed by (b) an increase in intensity at $\sim 230 - 250$°C and (c) a final decrease in intensity observed at ~ 575°C. The cooling portion of the thermomagnetic experiments does not follow the heating curve below ~ 575°C whereby it reveals much lower intensities. The hysteresis measurements suggest the presence of a single magnetic phase that tends to saturate at fields of around 600mT (Fig. 2.5a).
The wasp-waisted shape of the hysteresis curves of the Saint-Mandrier tuff samples (Fig. 2.5b) implies the coexistence of two phases with contrasting coercivity spectra (Jackson *et al.*, 1990; Tauxe *et al.*, 1996).
Based on the thermomagnetic curves, these two magnetic phases are interpreted as magnetite and heamatite with Curie temperatures (Moskowitz, 1981) of ~ 570°C and ~ 660°C, respectively.
The thermomagnetic curves of sandstone and redbed samples from the Saint-Mandrier Formation (Fig. 2.5c) commonly display intensity drops at ~ 575°C, close to the Curie temperature of magnetite. Minor amounts of a higher coercivity phase are also inferred from the hysteresis loops that display a slightly wasp-waisted shape (Fig. 2.5c).

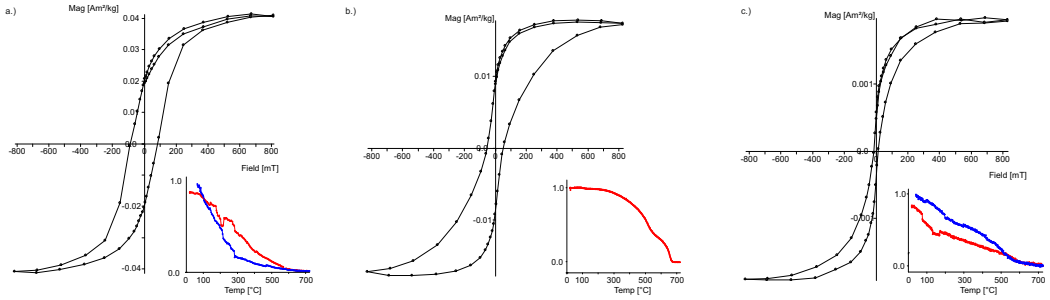

Figure 2.5: Hysteresis curve for a.) one of the Les Salettes tuff samples, b.) one of the Saint-Mandrier tuff samples and c.) one of the Saint-Mandrier redbed samples. The thermomagnetic curves are plotted with normalized intensities.

2.5 Paleomagnetic data

Characteristic component (ChRM) directions retrieved from the investigated stratigraphic units are discussed hereafter; site mean directions and the associated VGPs are summerized in Table 2.1.

2.5.1 Bron Formation

The Permian Bron Formation was sampled at three sites (BAR1, BAR2, BRO; Tab. 2.1) from two localities (#5 and #6 in Fig. 2.3) near the town of Carnoules and near Pignans (St. Barthélémy). The orthogonal projection diagrams (Fig. 2.6a) clearly show the presence of two components; a lower temperature viscous component successfully isolated up to $\sim 200°C$ is usually followed by a higher temperature component oriented to the south-and-up and trending toward the origin of the orthogonal projection at up to 690°C. The high temperature ChRM component is used to calculate site mean directions listed in Table 2.1 and plotted on Figure 2.8 before and after bedding tilt correction. The ChRM site mean direction from site BAR2 at St. Barthélémy (Table 2.1) is characterized by a very high α_{95} of 37.9° and was therefore excluded from further analysis.

2.5.2 Les Salettes Formation

The Permian Les Salettes Formation was sampled at three sites (SAL1, SAL2, SAL3; Tab. 2.1) to the east of the town of Toulon (#3 in Fig. 2.3). Here, samples from a conglomerate horizon, from igneous extrusives, and from tuff deposits were taken.

Table 2.1: Site characteristics, paleomagnetic data, site mean directions and virtual geomagnetic pole positions from this study.

Site characteristics						In situ			Bedding corrected			VGP location	
Name	Age (Ma)[1]	Formation[2]	GLat	GLon	N/N'	D°	I°	α_{95}	D°	I°	α_{95}	PLat	PLon
BAR1	285 ± 10	tuff	43.49	6.36	6/9	188.6	-23.0	3.9	180.1	-18.1	3.9	-56.3	5.8
BAR2	285 ± 10	tuff	43.49	6.36	6/7	50.4	5.1	37.9	49.3	11.3	37.9	-32.8	302.1
BRO	285 ± 10	red sdst	43.30	6.19	13/14	208.2	-10.5	6.4	199.1	-16.3	6.4	-51.5	334.7
SAL1[3]	273 ± 2.6	cgl	43.09	6.07	4/7	–	–	–	–	–	–	–	–
SAL2	273 ± 2.6	ext ig	43.09	6.07	13/19	236.6	-49.4	9.4	232.4	-24.6	9.4	-36.0	293.4
SAL3	273 ± 2.6	tuff	43.09	6.07	3/4	239.0	-54.8	7.8	220.5	-9.3	7.8	-37.6	311.2
MAN1	260 ± 10	tuff	43.08	5.9	4/6	183.4	-33.9	5.1	181.1	-21.7	5.1	-58.2	4.0
MAN2	260 ± 10	tuff	43.08	5.9	7/11	179.1	-29.1	4.0	176.8	-19.3	4.1	-56.8	11.8
MAN3	260 ± 10	tuff	43.08	5.9	5/7	179.4	-29.4	2.6	175.4	-20.8	2.6	-57.5	14.4
MAN4	260 ± 10	red sdst	43.08	5.9	7/8	178.5	-21.4	3.9	170.2	-21.1	4.0	-56.8	23.8
MAN5	260 ± 10	red sdst	43.08	5.9	4/6	180.6	-20.6	41.3	172.4	-24.7	41.6	-59.2	20.6
GAR1	243 ± 2.9	grey and red sdst	43.09	6.03	6/8	50.6	-70.5	13.3	184.8	-28.9	13.3	-62.1	356.1
GAR2	243 ± 2.9	grey and red sdst	43.09	6.03	6/12	171.9	81.1	30.7	10.6	15.3	23.8	-53.4	346.8
GAR3	243 ± 2.9	grey and red sdst	43.09	6.03	10/16	212.3	75.6	10.9	17.9	24.1	10.9	-55.9	333.7

GLat/GLon: Geographic latitude/longitude of sampling site; N/N': number of analysed samples/total amount of samples; D°/I°: Paleomagnetic declination/inclination; α_{95}: Circle of 95% confidence; PLat/PLon: Latitude/Longitude of virtual geomagnetic pole. All VGP's are mirrored to the southern hemisphere for better visualization. Stratigraphic age estimates come from Durand (2006, 2008) and references therein. [1]) The stratigraphic ages were transformed into numerical ages using the International Stratigraphic Chart with listed numerical ages from Gradstein *et al.* (2005) and Ogg *et al.* (2008). [2]) Abbreviations: sdst – sandstone, cgl – conglomerate, ext ig – extrusive igneous rocks. [3]) conglomerate test, no mean direction.

The conglomerate samples were used to perform a conglomerate test (Fig. 2.7). The detailed thermal demagnetization experiments performed on the samples from the Les Salettes Formation show at least two components with overlapping unblocking spectra, indicated by the curved shape of the orthogonal vector end point projections (Fig. 2.6b). As can be seen from the normalized intensity decay plot, the low temperature component carries more than 80% of the magnetization intensity and was successfully removed by heating up to $\sim 300°C$ (Fig. 2.6b, inset). The high temperature ChRM direction points towards the southwest with negative inclinations (Fig. 2.6b); the associated site mean directions (Tab. 2.1) are plotted on Figure 2.8 before and after bedding tilt correction. Because of the homogeneous bedding attitude at these sites, and because the rocks only display reverse polarity, it was not possible to perform a fold or reversal test. However, paleomagnetic results based on four samples from the polymictic conglomerate at site SAL1 show widely dispersed paleomagnetic directions which are taken as evidence for a primary age of magnetization (Fig. 2.7).

2.5.3 Saint-Mandrier Formation

Five sites were drilled within the Permian Saint-Mandrier Formation (sites MAN1, MAN2, MAN3, MAN4, MAN5; Tab. 2.1) near the harbour of St. Mandrier (#1 in Fig. 2.3). The demagnetization behaviour of the samples is characterized by an initial NRM intensity increase up to $\sim 200°C$ due to the removal of a low temperature component, followed by a gradual intensity decrease up to $\sim 660°C$ (Fig. 2.6c). The high temperature ChRM component is consistently oriented toward the south with negative inclinations (Fig. 2.6c). The resulting ChRM site mean directions (Tab. 2.1), characterized by low α_{95} values ($\leq 5.1°$, saved for site MAN5), are plotted on Figure 2.8 before and after bedding tilt correction.

2.5.4 Grès de Gonfaron Formation

Three sites from the Triassic grey to red sandstones of the Grès de Gonfaron Formation (sites GAR1, GAR2, GAR3; Tab. 2.1) sampled at the Cap de la Garonne (#2 in Fig. 2.3) showed during thermal demagnetization the presence of two distinct magnetic component directions. A slight increase in NRM intensity upon removal of a low temperature viscous overprint up to $\sim 100°C$ is followed by a continuous intensity decrease up to $\sim 660°C$ associated with a dual polarity ChRM component direction oriented either to the north-and-down or to the south-and-up after correction for bedding tilt (Fig. 2.6d). The ChRM site mean directions (Tab. 2.1) are

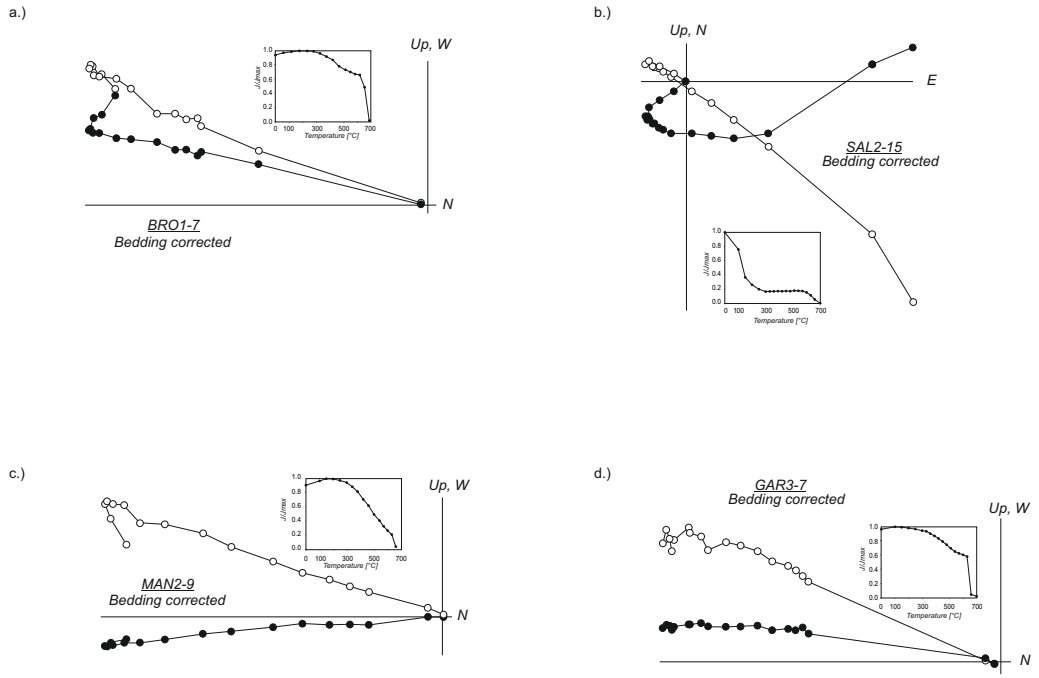

Figure 2.6: Results of thermal demagnetization experiments plotted as orthogonal vector diagrams (Zijderveld, 1967) in stratigraphic coordinates together with normalized diagrams of intensity decay. Full (open) dots represent vector endpoints projected onto the horizontal (vertical) plane. For clarity NRM values are not plotted.

plotted in Figure 2.9 before and after bedding tilt correction. A reversal test performed on the ChRM directions from the N= 22 samples of the three sites resulted positive and classified as 'C' after McFadden and McElhinny (1990), confirming the primary character of the isolated ChRM component (Fig. 2.9).

2.5.5 Data Summary

Permian and Triassic site mean directions are shown in Figures 2.8 and 2.9, respectively.
The Permian site mean directions show consistently negative inclinations, pointing toward the S-SW after bedding tilt correction; a conglomerate test performed in the Les Sallettes Formation revealed randomly distributed paleomagnetic directions indicating that the isolated ChRM is primary in origin. High temperature char-

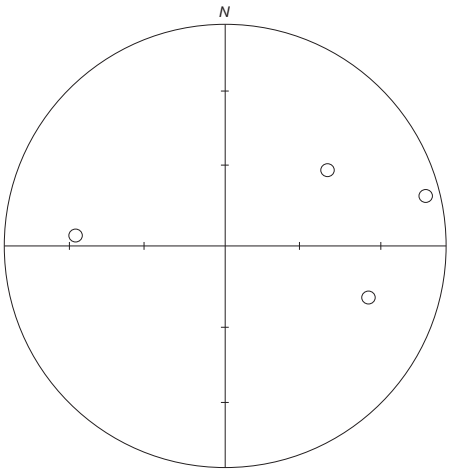

Figure 2.7: Paleomagnetic results based on four samples from a polymictic conglomerate from the Les Salettes Formation show a widely distributed directional data set which might be taken as evidence for a primary age of magnetization. Open symbols indicate negative inclinations.

acteristic palaeomagnetic directions of dual polarity were identified in the Triassic samples. The primary character of the ChRM of these rocks was confirmed by a positive reversal test.

2.6 Interpretation

The following main observations and interpretations can be drawn from the paleomagnetic data outlined above.

1. The Early Permian paleopoles derived from our data show a clear distribution along a small circle that was calculated using the least square method (standard deviation of 4.1°) (Fig. 2.10). This distribution indicates similar paleolatitudes for the studied rocks at the time of their formation. Published poles from the Corso-Sardinian block (Table 2.2; Edel (2000) and references therein) were rotated to European coordinates using the rotation parameters of Van der Voo (1969) and Gattacceca *et al.* (2007). These rotated poles (Table 2.3) as well as the poles from the Maures-Estérel region (Table 2.2; Edel (2000)) also plot on this small circle (Fig. 2.10).

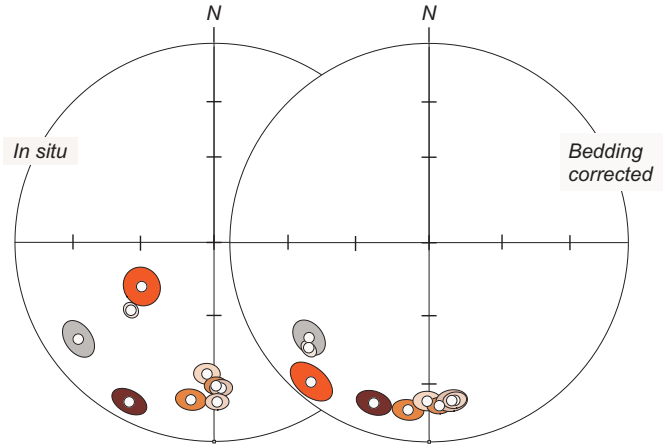

Figure 2.8: Stereographic projections of all Permian site mean directions in in situ and bedding corrected coordinates. Open symbols indicate negative inclinations.

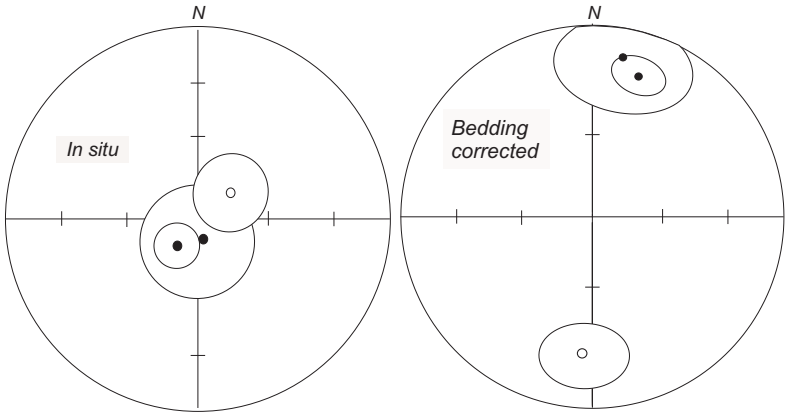

Figure 2.9: Stereographic projections of all Triassic site mean directions in in situ and bedding corrected coordinates. Open (closed) symbols indicate negative (positive) inclinations.

2. The inclinations measured in samples from different sites do not show any statistically significant scatter. This is in clear contrast with the wide range of observed declinations, indicating true relative rotations between the individual blocks.

3. The small circle that fits the distribution of paleopoles intersects the APWP of Baltica (Smethurst *et al.*, 1998) in the Early Permian ($\sim 290 - 260$Ma), in good agreement with the stratigraphic ages of the sampled units.

4. The Early Permian paleopoles from this study plot on either side of the Baltica APWP, indicating clockwise and counterclockwise relative rotations of the studied crustal blocks with respect to stable Europe.

5. The observed block rotations of the crustal blocks can be accounted for by a single, mean Euler pole located in Western Europe (Fig. 2.10). This indicates that these block rotations occurred largely about vertical axes and broadly within the shear zones *sensu* Arthaud and Matte (1977) or Muttoni *et al.* (1996, 2003).

6. The Triassic poles from this study (GAR) of Scythian to early Anisian age ($\sim 250-245$Ma), plot close to one another and close to the $250-240$Ma portion of the Baltica APWP (Fig. 2.10). A main implication of this observation is that the observed block rotations were largely terminated before the Early Triassic rocks acquired their remanence.

Table 2.2: Paleomagnetic results and VGP's for the Late Carboniferous – Permian formations of the Maures-Estérel-Corsica-Sardinia block (Edel, 2000).

Region	Formations	Age (Ref.)	N	D/I	Dc/Ic	α_{95}	Age mag.	VGP (°N/°E)	Ref.
Maures	Pelitic rocks	255 ± 5 Ma (1)	10	206/-31	196/-14	4	255	51/161	1
	Rhyolites	305 ± 5 Ma (2)	2	241/4	239/-16	–	–	–	3
	Rhyolites	305 ± 5 Ma (2)	7	240/-20	255/-5	6	290-280	14/105	4
	–	305 ± 5 Ma (2)	5	254/-7	247/3	9	290-280	14/105	4
	Rhyolite + Congl.	305 ± 5 Ma (2)	3	192/2	203/-22	15	280-260	44/170	4
	Arcose	300 Ma (3)	1	198/-18	205/0	–	280-260	41/153	3
Estérel	Basalts + Rhyolites	278 – 264 Ma (5)	12	207/-9	207/-23	6	250-220	51/142	3
	Sediments	–	3	204/3	203/-12	5	250	47/150	3
N. Corsica	Ignimbrites (1^{st} cycle)	–	5	–	165/4	7	280-260	44/209	6
	Ignimbrites (2^{nd} cycle)	–	5	–	180/-29	16	250-220	64/189	7
	Dykes	–	16	177/-20	–	10	250-220	58/194	7
	Dolerites	–	–	167/-16	–	10	250-220	54/211	7

	Gabbro	290 ± 10 Ma (8)	–	189/-13	–	5	250-220	54/174	7
NW Sard.	Ignimbrites	303 ± 9 Ma (8)	2	124/24	126/-1	–	280-260	2/253	8
	Sdst.	Permo-Trias (8)	5	128/-7	120/-12	13	250-240	26/262	9
S. Corsica - N. Sardinia	Dykes	–	11	135/-11	–	7	280-260	36/250	10
	Dykes	–	11	133/-2	–	7	280-260	31/249	10
	Ignimbrites	288 ± 11 Ma (11)	6	142/3	142/-2	11	280-260	38/239	12
S. Corsica - N. Sardinia	Ignimbrites	288 ± 11 Ma (11)	4	147/3	–	7	280-260	37/238	7

Age: age of the formation followed by the corresponding reference; N: number of sites; D/I: in situ declination/inclination; Dc/Ic: dip-corrected declination/inclination; Age mag.: assumed magnetization age; Reference: reference of the paleomagnetic study. 1: Merabet and Daly (1986), 2: Begassat (1985), 3: Zijderveld (1975), 4: Edel (2000), 5: (Zheng *et al.*, 1992), 6: Westphal *et al.* (1976a), 7: Westphal (1976), 8: (Edel *et al.*, 1981), 9: Edel (1980), 10: Vigliotti *et al.* (1990), 11: (Del Moro *et al.*, 1975), 12: Zijderveld *et al.* (1970). This table shows unrotated poles.

In summary, on the basis of our data, we suggest the existence in the Toulon-Cuers Basin of various tectonic blocks that rotated by different amounts and sense during a relatively narrow and well-defined time window straddling from sometime after the Early Permian (age of rotated rocks) and before the Early Triassic (age of non rotated rocks).

2.7 Discussion and Conclusions

These findings are discussed in conjunction with data from the literature in quest for possible triggering mechanisms associated with Pangea instability and transformation during the late Paleozoic.
To the west of the study area, a very similar timing of block rotations was observed in the Brive and Saint-Affrique basins of the French Massif Central where Early Permian rocks show rotated paleomagnetic vectors while Late Permian rocks have not been affected by rotations (Chen *et al.* (2006); see also Cogné *et al.* (1990, 1993); Diego-Orozco and Henry (1998); Henry *et al.* (1999); Diego-Orozco *et al.* (2002)). Paleomagnetic data from the Maures-Estérel massif located immediately to the east of our study area suggest a large clockwise block rotation during the Early to Middle Permian (Edel, 2000). A recent palaeomagnetic study on Permo-Carboniferous dykes of Sardinia (Emmer *et al.*, 2005) revealed significant counterclockwise rotations of up to 64° between individual parts of the island that have been demonstrated to predate the Jurassic (Kirscher *et al.*, 2011).
Summarizing the above, paleomagnetic data seem to indicate the existence of an intra-Pangea belt of tectonic blocks straddling from the Massif Central to southern France and Corsica-Sardinia (and speculatively extending eastward to the north of Adria) characterized by complex and differential block rotations that - based on data from Toulon-Cuers - may have largely occurred in post-Early Permian and pre-Early Triassic times. Taken at face value, this timing seems to preclude an origin of the postulated block belt as consequence of dextral wrench tectonics *sensu* Arthaud and Matte (1977), which occurred in the Late Carboniferous - Early Permian and therefore seemingly predated block belt activity in the Middle Permian, as we speculate here. We notice instead that the timing of the Pangea B (Irving, 1977) to Pangea A transformation broadly agrees with the timing of block rotation documented in this study. The transformation occurred essentially during the Middle Permian from an Early Permian Pangea B to a Late Permian Pangea A (Muttoni *et al.*, 1996, 2003, 2009).
Pangea B remains however a strongly debated issue that received considerable at-

Table 2.3: Paleopoles for Corsica-Sardinia from the literature rotated to European coordinates, using rotation parameters of Gattacceca *et al.* (2007); Van der Voo (1969) and projected to the southern hemisphere as plotted in Fig. 2.10.

Region	**Age mag. (Ma)**	α_{95}	**VGP (°N/°E)**	**Reference**[1]
S. Corsica – N. Sardinia	280-260	7	-36/310	Vigliotti *et al.* (1990)
	280-260	7	-38/311	Vigliotti *et al.* (1990)
	280-260	11	-33/302	Zijderveld *et al.* (1970)
	280-260	7	-30/298	Westphal (1976)
N Corsica	280-260	7	-16/285	Westphal *et al.* (1976a)
	250-220	16	-14/264	Westphal (1976)
	250-220	10	-12/270	Westphal (1976)
	250-220	10	-19/278	Westphal (1976)
	250-220	5	-2/264	Westphal (1976)
NW Sardinia	280-260	7	-41/319	Edel *et al.* (1981)
	250-240	13	-48/323	Edel (1980)

Age mag.: assumed magnetization age; Reference: reference of the paleomagnetic study. [1] References always refer to the unrotated and unprocessed poles.

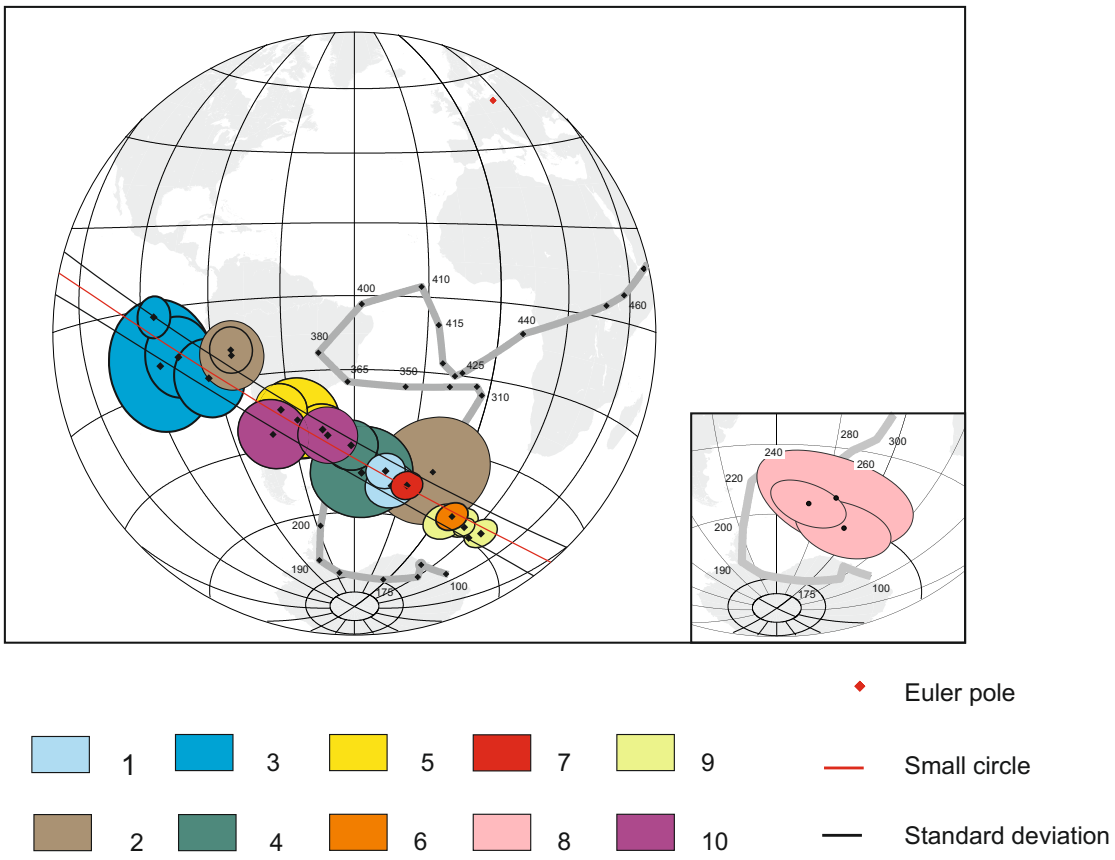

Figure 2.10: 1 – 5: Virtual geomagnetic poles from previous studies (Tables 2.2 and 2.3) and 6 – 10: Virtual geomagnetic poles from this study (Table 2.1) with respect to the apparent polar wander path of Baltica (Smethurst *et al.*, 1998). The poles plot on a small circle about a Euler pole in present day northwest Europe. Legend: 1) Estérel, 2) Maures, 3) N Corsica, 4) NW Sardinia, 5) S. Corsica – N. Sardinia, 6) BAR, 7) BRO, 8) GAR, 9) MAN, 10) SAL. Inset: the inset shows the three Triassic virtual geomagnetic poles from this study (calculated from paleomagnetic mean directions from sites GAR1, GAR2 and GAR3).

tention in the recent years, as briefly (and probably incompletely) summarized hereafter. Domeier *et al.* (2011b) argued against an intra-Pangea transform zone in the Late Permian - Early Triassic but admitted that Pangea B could not be ruled out in the Late Carboniferous - Early Permian, thus confirming previous findings (Muttoni *et al.*, 1996, 2003; Angiolini *et al.*, 2007). More recently, Domeier *et al.* (2011c) reprised Rochette and Vandamme (2001) in stressing that significant inclination shallowing in sediments would result in inaccurate reconstruction of paleolatitudes, therefore artificially generating the crustal overlap between Laurasia and Gondwana on which the Pangea B concept is based, which was however found by Muttoni *et al.* (2003) in igneous rocks that are usually not affected by inclination shallowing. Recent paleomagnetic data from Argentina and Norway re-confirmed Pangea A in the Late Permian - Triassic (Domeier *et al.*, 2011a,b; Dominguez *et al.*, 2011), while Yuan *et al.* (2011) in their study on Permian and Triassic paleolatitudes of the Ukrainian shield concluded that both Pangea B and A are allowed in the Early Permian depending on data selection. More recently, Domeier *et al.* (2012) showed in their comprehensive review that selected paleomagnetic data from the literature can be reconciled with Pangea A also in the Early Permian without invoking non-dipole field contributions (as previously done by Van der Voo and Torsvik (2001) and Torsvik and Van der Voo (2002), see also Muttoni *et al.* (2003) for a discussion); however, we notice that this conclusion (no Pangea B in the Early Permian) was reached (Domeier *et al.*, 2012) by excluding - with little circumstantial explanation - Early Permian data from Adria retrieved (Muttoni *et al.*, 1996, 2003) from rocks that (i) are igneous and therefore not affected by sedimentary inclination shallowing, (ii) pertain to well known stratigraphic and geologic contexts characterized by low tectonic deformation, (iii) have been carefully dated with modern radiometric techniques, (iv) yielded well illustrated and good quality paleomagnetic directions from sites confined to one hemisphere (greatly reducing the possible effects of zonal non-dipole field contaminations on Pangea geometry as previously suggested; see above), and, finally, (v) yielded paleomagnetic poles that agree with available poles from Africa of arguably same age, testifying for substantial tectonic coherence of Adria and Africa, which was incidentally observed also for the Triassic, Jurassic, Cretaceous, and Cenozoic (Muttoni *et al.*, 1996, 2003). Forty years of work on selected rocks from stable parts of Adria that frequently yielded paleomagnetic data of high Van der Voo's Q quality and showed $\sim$ 280Myr of history of substantial tectonic coherence with Africa (e.g. Channel (1996); Muttoni *et al.* (1996, 2003) have been largely excluded from the road of reconciliation to Pangea (Domeier *et al.*, 2012).
Finally, a reconstruction of the Early Permian stress field of Iberia from the analysis of the curved Cantabria-Asturias arc was used to question the likeliness of dextral

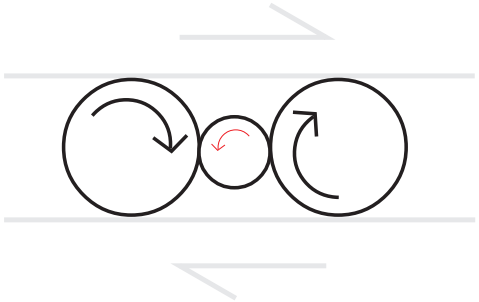

Figure 2.11: Simple ball bearing model to explain the observed differential rotations.

shearing associated with the Pangea B to A transformation in the Early Permian (Weil *et al.*, 2001), but we recall that subsequent analysis placed the transformation largely in the middle part of the Permian (Muttoni *et al.*, 2003), a period for which no stress field reconstruction is available to our knowledge.
While the issue of Pangea B will probably be resolved paleomagnetically by retrieving new and reliable Early Permian data (Yuan *et al.*, 2011), we stress that the 'critically lacking' (Domeier *et al.*, 2012) geological evidence for the major dextral shear between Laurasia and Gondwana required for the Pangea B to A transformation may in fact be represented by the belt of rotated blocks described in this study. The presence within this block belt of counterclockwise rotations (e.g. in Sardinia) as well as of opposite-sense rotations (e.g. in the Toulon-Cuers basin) may seem counterintuitive in a dextral megashear regime, which would predict essentially clockwise rotations. However, Lamb (1987) convincingly demonstrated that the sense of rotation of crustal blocks trapped in a major shear zone very much depends on strain rate, aspect ratio, interaction of blocks, and boundary conditions along the shear zone. Additional examples from the literature show that different amounts of clockwise and counterclockwise rotations of blocks can co-exist under common strike-slip regimes (e.g. Ron *et al.* (1984)). We use a simple configuration of two larger blocks with a smaller block caught in between to illustrate the concept (Fig. 2.11).

In such an assemblage, small clockwise rotations of the larger blocks would cause large counterclockwise rotations of the intervening small block. As our paleomagnetic data indicate that blocks rotated by different amounts, and because the size of the blocks is considerably smaller than that of the transform zone, we adopted as more realistic the model developed by McKenzie and Jackson (1983), which would result in a block arrangement similar to that illustrated in Figure 2.12. Acknowledging the lack of fundamental information about block outlines, aspect ratio of blocks, and interaction among blocks, the adopted model (Fig. 2.12) well illustrates that the

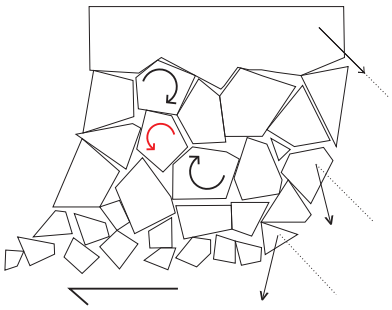

Figure 2.12: The small block model as proposed by McKenzie and Jackson (1983). The brittle upper crust is broken into small blocks which rotate in response to the continuous, ductile deformation at greater depth. Notice the interaction between single blocks. Redrawn and modified after Nelson and Jones (1987). Small black arrows on the right represent the direction of an ancient magnetization direction.

dextral motion of Laurasia relative to Gondwana could have been largely taken up by and distributed among differential rotations of several fault-bounded crustal blocks rather than by a set of discrete, continental-scale shear zones. To our knowledge, there is no theoretical upper limit to the amount of (dextral) displacement that can be taken up by the postulated block belt, which could range from the $\sim$ 600km proposed by Arthaud and Matte (1977) to the $\sim$ 3000km associated with the Pangea B to A transformation.

2.8 Acknowledgments

Paleomagnetic sampling in the Toulon-Cuers basin was carried out by Barbara Emmer and Alexandra Abalmassava. Thanks to Manuela Weiss for support during rock- and paleomagnetic measurements. Financial support to VB by the German Research Foundation (DFG grant Ba1210/8-1) is gratefully acknowledged.
We thank Rob van der Voo for useful comments and for sharing with us his views and opinions while allowing us to maintain ours; further thanks goes to an anonymous reviewer for detailed and constructive comments on the manuscript.

3

Paleomagnetic data from late Paleozoic dykes on Sardinia: evidence for intra-Sardinian block rotations and implications on the Pangea megashear system

By ***K. Aubele, V. Bachtadse, G. Muttoni and A. Ronchi*** *published in* Geochemistry, Geophysics, Geosystems, *2014,* ***15****, 1684-1697, doi:10.1002/2014GC005325.*

3 PALEOMAGNETIC DATA FROM LATE PALEOZOIC DYKES ON SARDINIA: EVIDENCE FOR INTRA-SARDINIAN BLOCK ROTATIONS AND IMPLICATIONS ON THE PANGEA MEGASHEAR SYSTEM

Abstract

Paleomagnetic studies on dyke swarms from the Variscan belt of Europe can be used to reconstruct the debated paleogeography of Pangea during the Permian. Here, we present paleomagnetic data from 13 late Variscan dykes (233 samples) from Sardinia ranging in age from 298 ± 5Ma to 270 ± 10Ma. Magnetic component directions have been retrieved using thermal and alternating field demagnetization techniques, which gave reproducible results. The paleomagnetic mean directions differ significantly between northern Sardinia and south-eastern and central-eastern Sardinia, the latter two regions yielding statistically similar paleomagnetic mean directions. These results indicate that Sardinia fragmented into two, arguably three, crustal blocks after dykes emplacement. We argue that the observed block rotations occurred during the Permian as the result of post-Variscan intra-Pangea mobility.

3.1 Introduction

It has been previously observed that if paleomagnetic data are used to reconstruct Pangea A (Wegenerian Pangea) in the Early Permian, a significant continental overlap of Laurasia and Gondwana would result. One of the options to overcome this problem is to choose an alternative configuration known as Pangea B, characterized by the southern continents of Gondwana located further to the East with respect to Laurasia than in a Pangea A configuration (Irving (1977); Morel and Irving (1981); Muttoni *et al.* (2003); see Aubele *et al.* (2012); Domeier *et al.* (2012) for a discussion of the Pangea controversy). However, since there is no reason to doubt that the opening of the Atlantic Ocean and the dispersal of Pangea started from a Pangea A configuration, a large dextral megashear zone between Laurasia and Gondwana becomes a necessary feature for the transformation from a postulated Pangea B to a widely accepted Pangea A configuration (Fig. 3.1). Based on a variety of geological evidences (e. g. Arthaud and Matte (1977); Burg *et al.* (1994); Stampfli (2001); Cassinis *et al.* (2012)), this tectonic zone is expected to lie within the Mediterranean realm in southern Europe and/or northern Africa.
Recently, we postulated that the tectonic inventory of relatively small crustal blocks including SE France, Corsica, and Sardinia could represent the remnants of a diffuse dextral plate boundary between Laurasia and Gondwana (Aubele *et al.*, 2012). Crustal blocks caught within shear zones may exhibit differential vertical–axis rotations, which can be detected using paleomagnetic techniques as applied in this study.

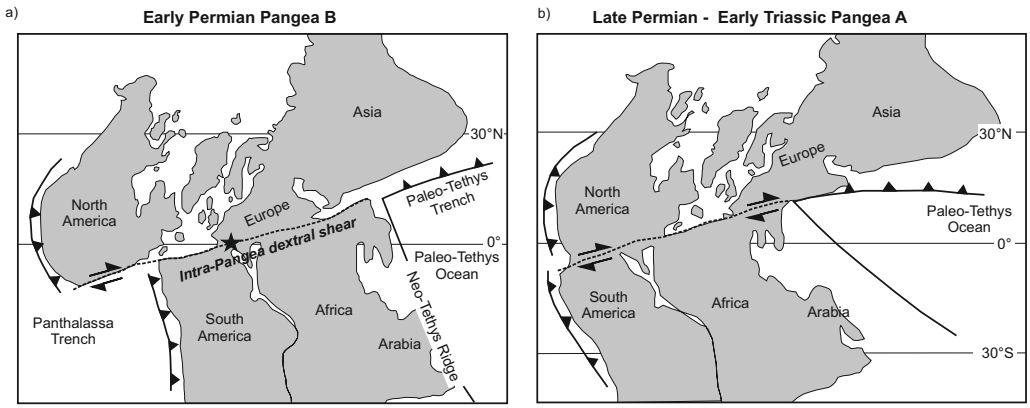

Figure 3.1: Pangea B configuration after Irving (1977) in the early Permian (a). Star: approximate location of the study area. Wegenarian Pangea A configuration in the Late Permian to Early Triassic (b). Modified after Muttoni *et al.* (2009).

The late Variscan Corsica–Sardinia Batholith is crossed from north to south by an impressive dyke swarm; several dykes also cut the Variscan metamorphic basement as well as non–metamorphic Permian volcanic rocks (e. g. Traversa *et al.* (2003)). Two - arguably three - dyke provinces can be identified based on strike directions. If these strike differences are of tectonic origin, the crustal coherence of Sardinia as a single block, which has been proven valid since the Jurassic (Kirscher *et al.*, 2011), can no longer be maintained for pre-Jurassic times. This opens the possibility - explored in this paper - that these dykes were variably rotated shortly after emplacement and could represent evidence of Permian shearing between Laurasia and Gondwana.
The aim of this study is therefore to investigate whether the different strike directions of Sardinian dykes are of primary or secondary origin in order to quantify internal rotations within Sardinia and their implications for the inferred Pangea megashear system.

3.2 Geological Setting and Geochronological Data

Until the opening of the Gulf of Lyon during the Oligocene, the Corsica–Sardinia microplate was part of the southern margin of the European Variscides comprised of metamorphic rocks of Early Cambrian to Early Carboniferous age that were deformed during the collision between Gondwana and Laurasia, as well as a late orogenic magmatic complex emplaced during a Late Carboniferous–Permian

extensional phase (Cortesogno *et al.*, 1998; Funedda and Oggiano, 2009).
According to Carmignani *et al.* (1978, 1994b), the Variscan belt of Sardinia is arranged in three tectono–metamorphic zones: (i) an Inner Zone in the NE, highly deformed with medium- to high-grade metamorphism, (ii) a tectonic Nappe Zone in SE and central Sardinia characterized by greenschist metamorphism, and (iii) a Foreland Zone in the SW, characterized by very-low-grade metamorphism.
Collisional deformation and crustal thickening in the shortened orogenic wedge was succeeded by tectonic inversion and extension associated with plutonism, high temperature/low pressure (HT/LP) metamorphism, exhumation of deep tectonic units, and the development of Late Carboniferous–Permian basins (Funedda and Oggiano, 2009). The emplacement of the Corsica-Sardinia Batholith was associated with this late orogenic tectono-metamorphic evolution (Poli *et al.*, 1989; Carmignani *et al.*, 1994b; Paquette *et al.*, 2003; Cocherie *et al.*, 2005; Casini *et al.*, 2012).
Different mechanisms responsible for the observed post-collisional extension and tectonic unroofing have been discussed by Conti *et al.* (1999). These include: (i) gravitational adjustment of an unstable orogenic wedge (Platt, 1986), (ii) slab breakoff (Davies and von Blanckenburg, 1995), and (iii) convective removal of mantle lithosphere (Platt and England, 1994). All these models maintain high surface level elevation during extension and should be accompanied by the formation of thick molasse basins, which, however, are lacking in the sedimentary record of Sardinia (Conti *et al.*, 1999). In any case, the progressive development of an extensional-transtensional regime is likely to have favored magma ascent and the subsequent intrusion of the Late Paleozoic dyke complexes (Gaggero *et al.*, 2007).
Dyke ages have been reported to vary from Late Carboniferous in the south to Early Triassic in the north (Baldelli *et al.*, 1987; Vaccaro *et al.*, 1991; Traversa and Vaccaro, 1992; Traversa *et al.*, 2003; Atzori *et al.*, 2000; Gaggero *et al.*, 2007). These age data were obtained with different radiometric methods, each with inherent uncertainties. In any case, we stress that magmatic activity in post-Variscan Europe, to which Sardinia belonged, started in the Late Carboniferous and peaked in the Early Permian (Cisuralian). To our account, there is no clear evidence of Late Permian or Early to Middle Triassic magmatism in central-southern Europe, and we therefore speculate that the radiometric ages of Sardinian dykes younger than Early Permian are due to reopening of the radiometric systems and/or analytical uncertainties.
After an overall evaluation of the available geochronological ages, we follow Vaccaro *et al.* (1991) who showed the existence of two main age windows of dykes intrusion based on Rb/Sr analyses of 14 whole-rock samples and nine micas as well as Ar/Ar analyses on four hornblende, one muscovite, and one K-feldspar crystals. The

resulting uncertainty of the Rb/Sr ratio is 1.5%, as determined from reproducibility tests. These analyses show that (i) in south-eastern and central-eastern Sardinia, peraluminous and high initial Sr (Sr_i) calcalkaline dykes intruded from 298 ± 5Ma to 289 ± 4Ma, while (ii) further to the north (Gallura), dyke evolution ranged from peraluminous between 282 ± 4 and 268 ± 4Ma, to low Sr_i calcalkaline at 270 ± 10Ma. Atzori and Traversa (1986) and Atzori *et al.* (2000) presented complementary geochronological data of dykes from central and eastern Sardinia. Their Rb/Sr ages obtained on biotite whole-rock pairs span from 291 ± 3Ma to 271 ± 3Ma, in broad agreement with Vaccaro *et al.* (1991).
Structurally, we identified three different dyke provinces based on predominant strike directions. These are: (i) the northern part of Sardinia, where most of the dykes strike NE-SW, (ii) the central-eastern part of Sardinia, where dykes strike preferentially NW–SE, and (iii) the south-eastern part of Sardinia, which is dominated by NNW-SSE striking dykes (Fig. 3.2).

We sampled 13 dykes within these regions (Table 3.1). Four dykes were sampled in south-eastern Sardinia (CAG, CAS, MUR and VIL; Table 3.1). These dykes belong to the older peraluminous suite dated from 298 ± 5Ma to 289 ± 4Ma (Vaccaro *et al.*, 1991). Six dykes were sampled in the central-eastern part of Sardinia along the Gulf of Orosei (ARB, GAI, ILB, LOC, LAN and BLA; Table 3.1). These dykes as well as the three dykes sampled at sites LUR, LAR and BER in northern Sardinia (Table 3.1) consist of calc-alkaline, high-K low-Si andesites and peraluminous ultra-acid rhyolites dated by Atzori *et al.* (2000) from 291 ± 3Ma to 271 ± 3Ma.

3.3 Field and Laboratory Methods

All samples were taken using a gasoline-powered, water-cooled drill and oriented using a standard magnetic compass. Subsequently, samples were cut into standard 11cc cylindrical specimens. All samples were studied in the paleomagnetic laboratory of the University of Munich. The majority of the specimens was thermally demagnetized using a Schoenstedt furnace adopting increments of $30°C$ up to maximum temperatures of $690°C$. Demagnetization measurements using alternating field (AF) demagnetization were also carried out using steps of 5mT up to a maximum field of 90mT. The results of the AF experiments support the data obtained by thermal demagnetization (Fig. 3.3). After each heating step or increase in alternating field strength, the natural remanent magnetization

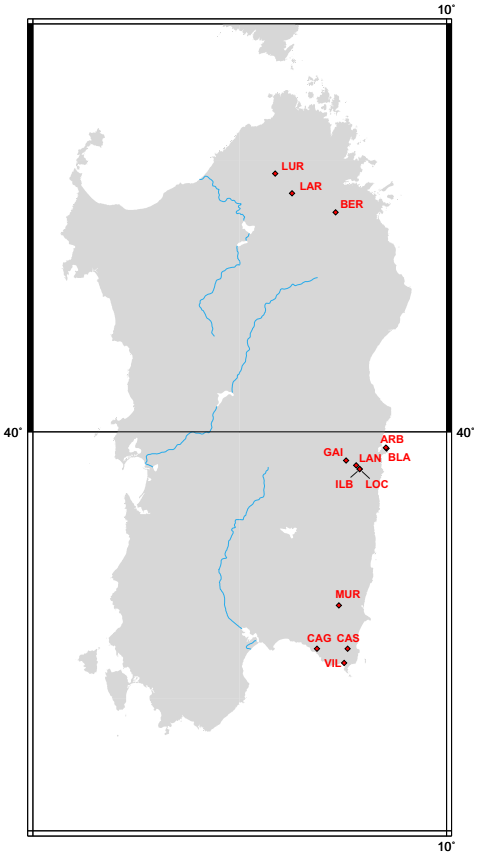

Figure 3.2: Location of the sampling sites of this study.

Table 3.1: Geographic coordinates and paleomagnetic data of sites (=dykes) of this study from Sardinia.

Site[a]	GLat GLon	Strike (°N)	Age (Ma)	D°	I°	k	α_{95}	N/N'	PLat	PLon
LUR	N40°57.2' E9°10.3'	10-30		141.2	-5.9	37.2	5.6	19/24		
BER	N40°48.7' E9°27.8'	10		124.6	4.4	16.3	15.4	7/14		
LAR	N40°52.9' E9°15.2'	60		133.5	-2.0	39.3	8.3	9/14		
Northern Sardinia		NE-SW - NNE-SSW	282±4 to 268±4	133.1	-1.2	68.7	15.0	3/3	31.5	247.9
									−43.3*	321.3*
ARB	N39°56.3' E9°42.6'	345		90.6	-7.4	39.3	7.8	10/17		
GAI	N39°53.6' E9°30.9'	??		104.8	-18.4	38.9	8.4	9/9		
ILB	N39°51.7' E9°34.8'	320		80.6	12.2	41.5	7.6	10/14		
LOC	N39°51.7' E9°34.8'	330		92.9	-16.2	293.2	3.9	6/9		
LAN	N39°52.5' E9°33.8'	280		91.9	14.0	10.9	17.5	8/14		
BLA	N39°56.5' E9°42.4'	330 - 340		91.2	-12.3	45.5	5.5	16/16		
Central-eastern Sardinia		NW - SE	298±5 to 289±4	91.9	-4.8	25.3	13.6	6/6	3.0	280.1
									−52.7*	24.0*
CAG	N39°11.3' E9°22.4'	350 - 360		80.1	–16.6	37.2	6.3	15/23		
CAS	N39°11.3' E9°31.3'	330		77.1	-41.8	31.6	7.5	13/13		
MUR	N39°21.1' E9°28.8'	345-350		85.3	6.1	34.1	6.6	15/24		
VIL	N39°08.1' E9°30.3'	0 - 10		76.5	-29.5	121.0	2.3	32/42		
South-eastern Sardinia		NW-SE - N-S	298±5 to 289±4	80.0	-20.6	15.4	24.2	4/4	-0.9	294.0
									−54.9*	48.2*

[a] GLat/GLon: Geographic latitude/longitude of sampling site; Strike: refers to the strike of the dykes measured in ° clockwise from North; D°/I°: Paleomagnetic declination/inclination; α_{95}: Circle of 95% confidence; N/N': number of analysed samples/total amount of samples; PLat/PLon: Latitude/Longitude of virtual geomagnetic pole. *Paleomagnetic South poles after rotation to European coordinates using rotation parameters after Gattacceca *et al.* (2007) (rotation pole coordinates $\lambda = 43.50^\circ$, $\varphi = 9.50^\circ$, angle 45.00° cw) in order to close the Ligurian ocean and Gong *et al.* (2008) (rotation pole coordinates $\lambda = 43.00^\circ$, $\varphi = -2.00^\circ$, angle 35.00° cw) to account for the opening of the Bay of Biscay.

was measured with a 2G Enterprises cryogenic magnetometer mounting SQUID (Superconducting Quantum Interference Device) sensors located in a magnetically shielded room. Rock-magnetic parameters were determined using a Variable Field Translation Balance (Krása *et al.*, 2007) (Fig. 3.4). Demagnetization results were plotted on orthogonal vector diagrams (Zijderveld, 1967) and analyzed using the least square method (Kirschvink, 1980) on linear portions of the demagnetization paths defined by at least four consecutive demagnetization steps. The linear fits were anchored to the origin of the demagnetization axes where appropriate.

Each dyke yielded one sampling site comprising between a minimum of 9 and a maximum of 42 samples per site, for a total of 13 sites (dykes) and 233 samples (Table 3.1). Site mean directions were calculated using the paleomagnetic software of Bachtadse and Maier (1994), and were used to calculate regional mean directions according to geographic distribution. This resulted in three regional mean directions for northern, central-eastern, and south-eastern Sardinia, based on three, six, and four site mean directions, respectively (Table 3.1).

3.4 Rockmagnetic Data

Rock magnetic analyses include hysteresis measurements, isothermal remanent magnetization (IRM) acquisition in fields up to 700mT, backfield magnetization for the definition of the coercivity of remanence, and, finally, in-field heating (up to $700°C$) and cooling cycles (hereafter referred to as thermomagnetic measurements) in order to estimate the Curie temperature(s) of the magnetic mineral(s) (either using the method described by Moskowitz (1981) or the second derivative of the heating curves as displayed in Fig. 3.4 (d)), as well as to identify possible mineralogical transformations that occurred during heating. The hysteresis loops and the thermomagnetic curves were corrected for diamagnetic and/or paramagnetic contributions (Leonhardt, 2006).
The rock-magnetic analyses on samples from site LAR in the northeastern dyke province indicate the presence of magnetite as the main carrier of the magnetic remanence: the hysteresis curves and the IRM acquisition curve display saturation below 200mT (Fig. 3.4a, b), and the thermomagnetic heating curve (Fig. 3.4c) shows a Curie temperature of $584°C$ (calculated after Moskowitz (1981)). Magnetite with an estimated Curie temperature of $588°C$ is also present in samples from site ARB from the central-eastern dyke province (Fig. 3.4g). Samples from site MUR located in the south-eastern dyke province show IRM acquisition curves that saturate

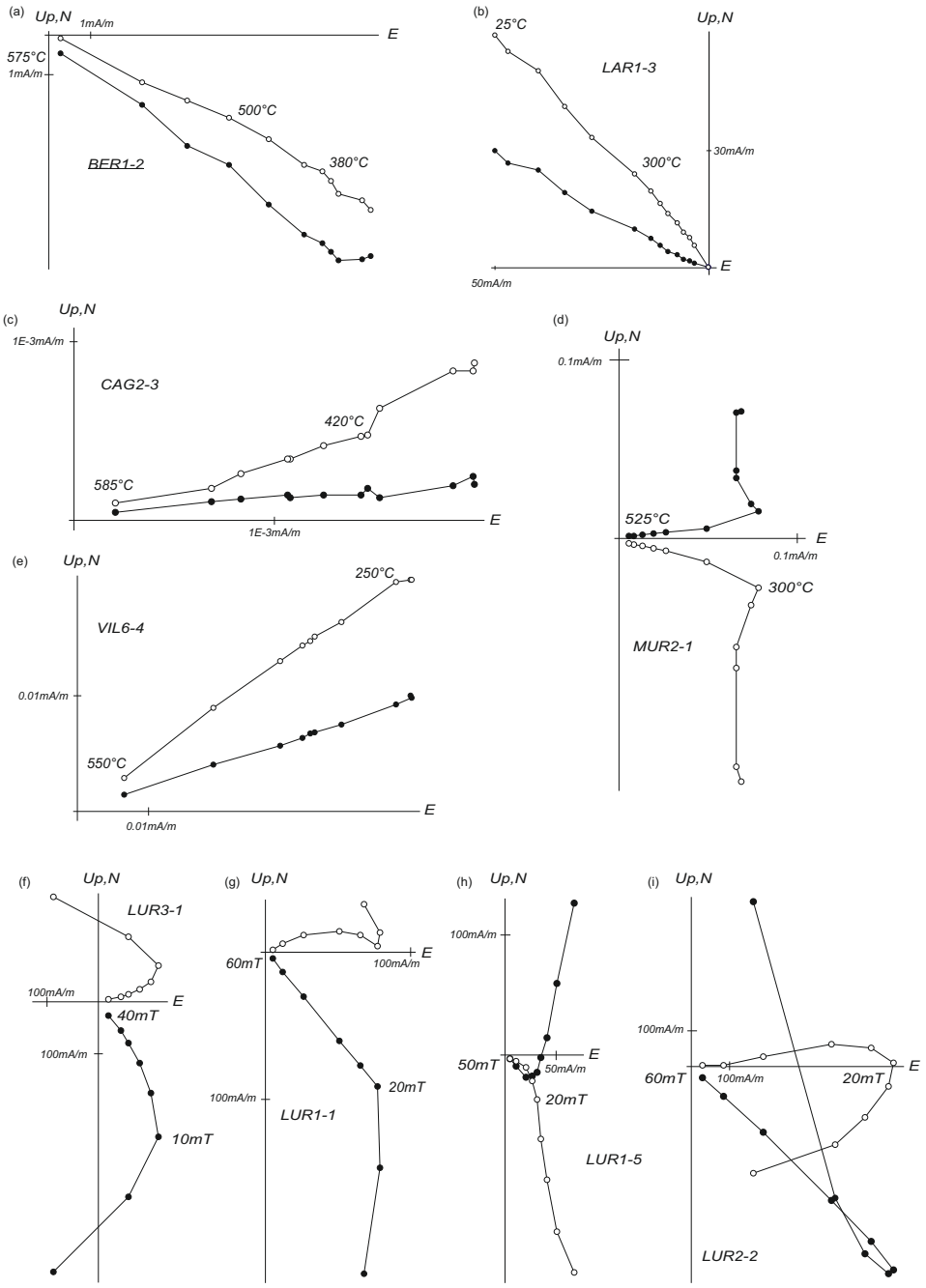

Figure 3.3: Results of thermal (a-e) and alternating field (f-i) demagnetization experiments plotted as orthogonal vector diagrams in geographic (*in situ*, IS) coordinates. Solid and open dots represent vector endpoints projected onto the horizontal and vertical planes, respectively.

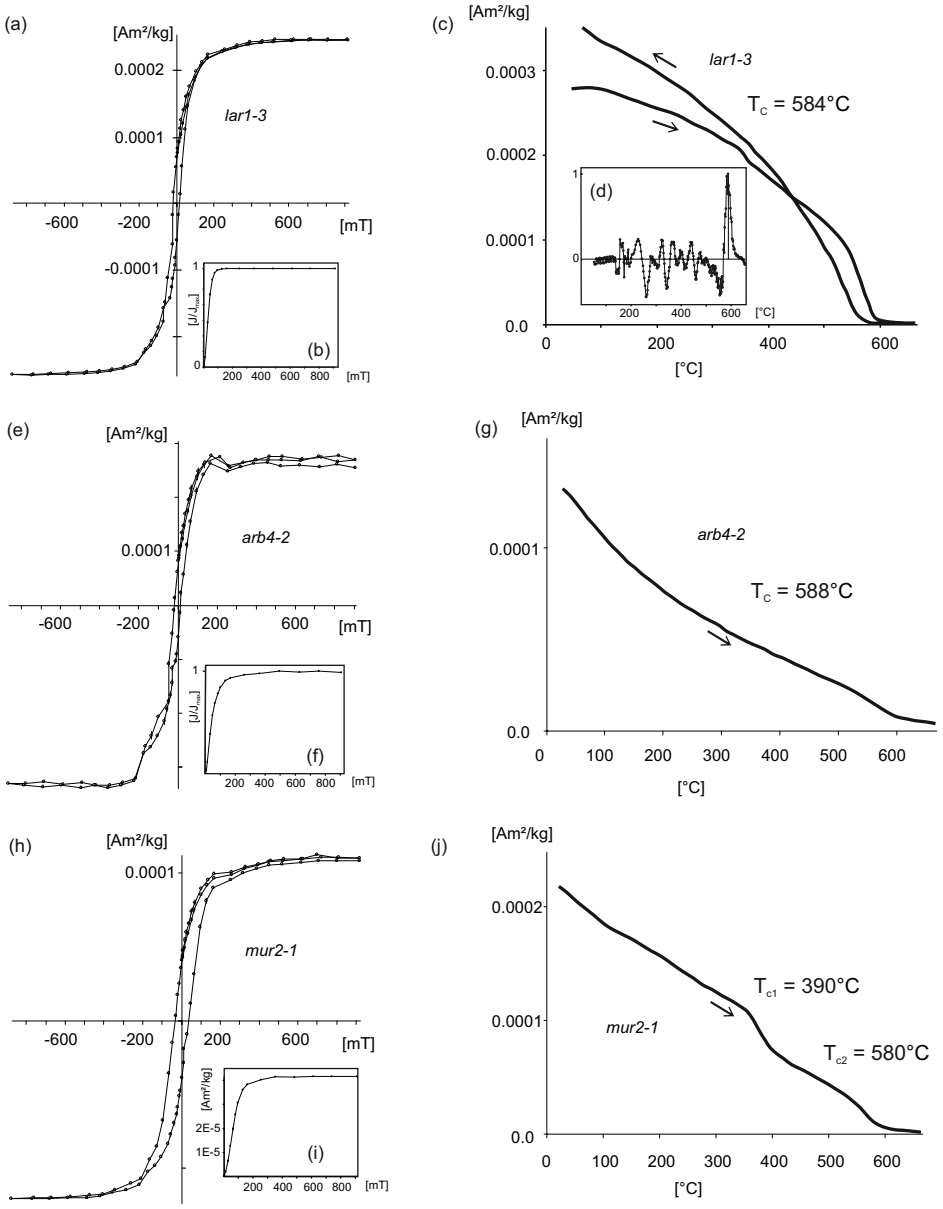

Figure 3.4: Rock–magnetic experiments on representative samples. LAR1–3 from northern Sardinia (a–d), ARB4–2 from central-eastern Sardinia (e–g), and MUR2–1 from south-eastern Sardinia (h–j): hysteresis loops (a, e, h), IRM acquisition curves (b, f, i), thermomagnetic curves (c, g, j) and the second derivative of the heating portion of the thermomagnetic curve (d). [J/J_{max}]: normalized magnetization intensities, [Am^2/kg]: absolute magnetization intensities.

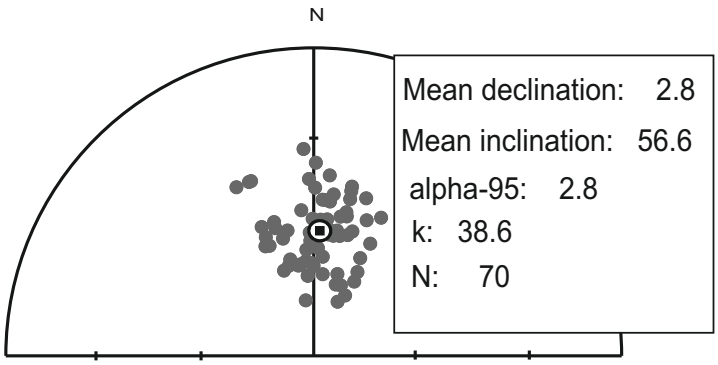

Figure 3.5: Stereographic projection in geographic (*in situ*, IS) coordinates of the low temperature magnetic component directions of samples from this study. The solid rectangle indicates the mean direction with associated 95% confidence circle (α_{95}).

at around 375 mT, while the thermomagnetic curves show a two-step decrease in magnetization intensity at $\sim 390°C$, which could be due to titanomagnetite unmixing, and at $\sim 580°C$, indicating that magnetite is the main carrier of the magnetic remanence in these samples (Fig. 3.4j).

3.5 Paleomagnetic Data

After removal of a viscous overprint at $\sim 50°C$, low temperature (LT) component directions have been observed up to $200 - 250°C$ in about one third of the samples. These LT components, plotted on a stereographic projection (Fig. 3.5), display a mean value of Dec = 2.8°E, Inc = 56.6° (N = 70, k = 38.6, α_{95}=2.8°), in broad agreement with the time averaged geomagnetic field for a nominal point in central Sardinia (Inc = 59.2°).

These LT overprint components are followed at higher temperatures by characteristic remanent magnetization (ChRM) component directions, as illustrated hereafter for the various sampled regions.

3.5.1 Northern Sardinia

The three sites (= dykes) sampled in northern Sardinia (LUR, LAR, BER; Fig. 3.2) yielded a total of 52 samples, 35 of which gave useful paleomagnetic results. After

removal of the low temperature present-day field overprint at $\sim 200°C$ (see above and Fig. 3.5), high temperature ChRM directions were identified (Fig. 3.3) and used to calculate site (dyke) mean directions, which were then averaged to calculate a regional mean direction for northern Sardinia of Dec = 133.1°E, Inc = −1.2° (N = 3, α_{95} = 15.0°; Fig. 3.6, Table 3.1).

3.5.2 Central-Eastern Sardinia

The six sites (= dykes) sampled in central-eastern Sardinia (ARB, GAI, ILB, LOC, LAN and BLA; Fig. 3.2) yielded a total of 79 samples, 59 of which gave useful results. As for the northern Sardinia samples, a low temperature present-day field overprint was removed up to $200-250°C$ (Fig. 3.5). At higher temperatures, ChRM directions have been identified up to $625°C$ and used to calculate site mean directions, which were then averaged to calculate a regional mean direction for central Sardinia of Dec = 91.9°E, Inc = −4.8° (N = 6, α_{95} = 13.6°; Fig. 3.6, Table 3.1).

3.5.3 South-Eastern Sardinia

The four sites sampled in south-eastern Sardinia (CAG, CAS, MUR, VIL; Fig. 3.2) yielded of a total of 102 samples, 75 of which gave useful results. After removal of the present-day field overprint at $\sim 200°C$ (Fig. 3.5), ChRM component directions were isolated up to $575°C$ (Fig. 3.3) and again averaged to calculate site mean directions and a regional mean direction for south-eastern Sardinia of Dec = 80.0°E, Inc = −20.6° (N = 4, α_{95} = 24.2°; Fig. 3.6, Table 3.1).

3.5.4 Data Summary and Comparison with Data from the Literature

The ChRM components found in the sampled dykes show shallow (negative or positive) inclinations and easterly or south-easterly declinations (Fig. 3.6). We note that two sites in south-eastern Sardinia give rather high inclinations of −41.8° (CAS) and −29.5° (VIL). However, data from these sites have been retained because rock-magnetic and paleomagnetic measurements provide no reason to discard them. Consequently, the regional mean direction for the south-eastern sites displays a large limit of 95% confidence (24.2°) compared to the regional means of sites from northern, and central-eastern Sardinia.

Our data from northern Sardinia (mean Dec = 133.1°E, Inc = −1.2°) are similar

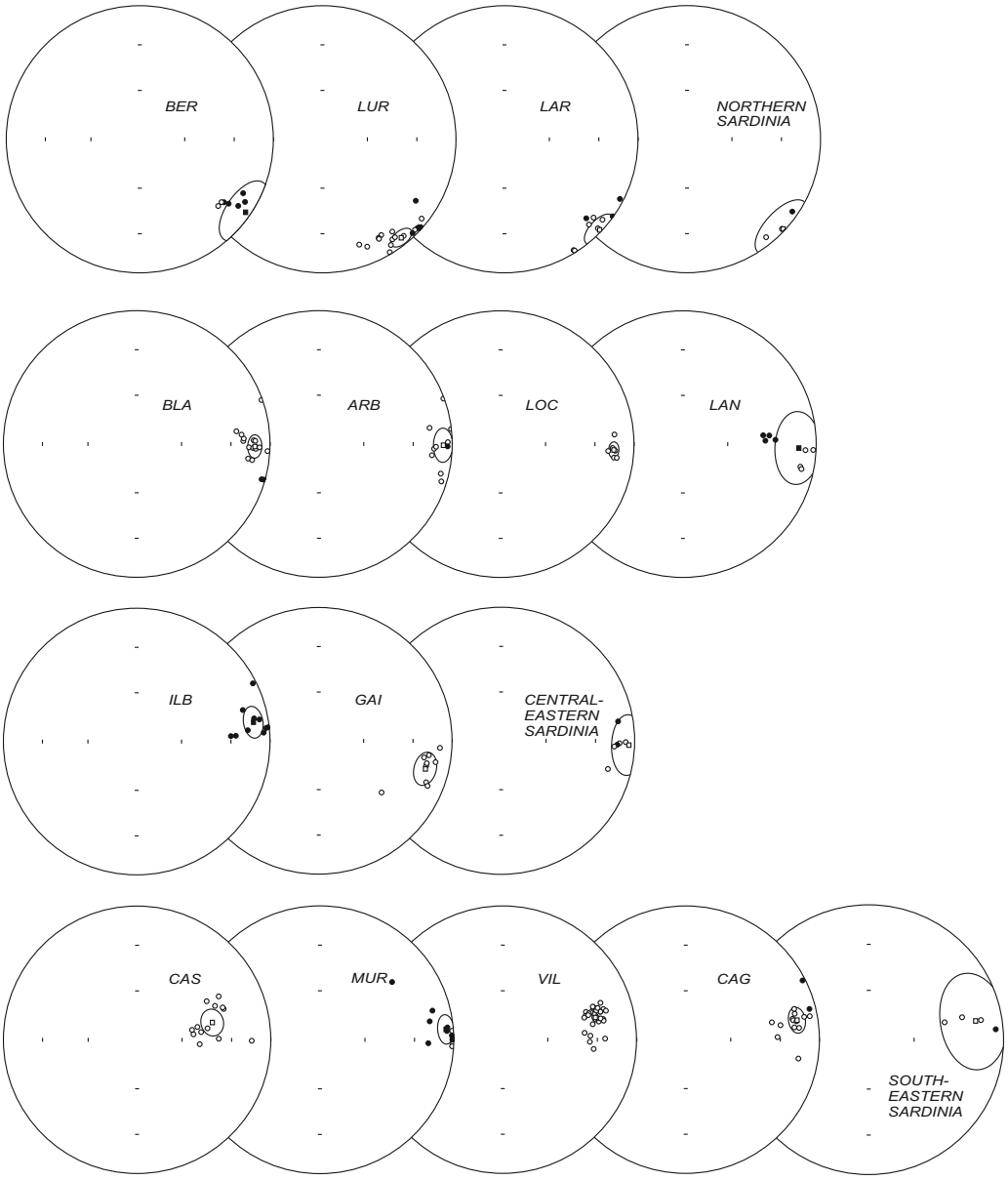

Figure 3.6: Stereographic projection in geographic (*in situ*, IS) coordinates of the high temperature magnetic component directions of samples from this study. Solid and open dots represent projections on the upper and lower hemispheres, respectively. Solid and open rectangles indicate site mean directions with 95% confidence circles (α_{95}). From the site mean directions, regional mean directions were calculated for northern, central–eastern and south–eastern Sardinia, which are also plotted with 95% confidence circles.

to the mean direction of Dec = 132.7°E, Inc = −1.6° obtained by Vigliotti *et al.* (1990) from Upper Paleozoic dykes outcropping in northern Sardinia, as well as to data obtained by Edel *et al.* (1981) from ignimbrites outcropping in NW Sardinia (Nurra) (mean Dec = 126.0°E, Inc = −1.0°), and dated to 296 ± 9Ma using K-Ar dating on biotite crystals. Our data from northern Sardinia are also consistent with data of Vigliotti *et al.* (1990), who conducted paleomagnetic analyses on Upper Paleozoic dykes in southern Corsica, and concluded that southern Corsica and northern Sardinia behaved as a single crustal block with a mean paleomagnetic direction of Dec = 133.7°E, Inc = −6.5°.
Our regional mean directions for central-eastern and south-eastern Sardinia of Dec = 91.9°E, Inc = −4.8° and Dec = 80.0°E, Inc = −20.6°, respectively, are broadly similar to the mean direction of Dec = 85.0°E, Inc = −7.0° obtained by Edel *et al.* (1981) on 28 sites of ignimbrites and andesites from southeastern Sardinia dated to 310–280Ma using different K-Ar clocks (Edel *et al.*, 1981).
From the analysis illustrated above, it appears that significant relative rotations occurred between northern Sardinia-southern Corsica and central-estern Sardinia, while minor rotations occurred between central-estern Sardinia and south-eastern Sardinia. These relative rotations of crustal blocks may represent the results of tectonic stress acting within a large-scale shear zone, as illustrated below.

3.6 Data Interpretation

A paleomagnetic pole was calculated for each of the three investigated dyke provinces using the regional mean directions (Table 3.1). These poles were then restored to European coordinates using rotation parameters of Gattacceca *et al.* (2007) ($\lambda = 43.50°$, $\varphi = 9.50°$, angle 45.00° clockwise) in order to account for the opening of the Ligurian-Provençal Basin, and of Gong *et al.* (2008) ($\lambda = 43.00°$, $\varphi = -2.00°$, angle 35.00° clockwise) to account for the opening of the Bay of Biscay, giving a total (cumulative) rotation pole of $\lambda = 41.93°$, $\varphi = 4.61°$, angle 79.78° clockwise (Table 3.1).
To assess the relative amount of rotational displacement of crustal blocks, the restored poles have been compared to the apparent polar wander path (APWP) of Baltica (Torsvik *et al.*, 2012). Inspection of Figure 3.7 reveals that the poles from this study as well as those of Edel *et al.* (1981) and Vigliotti *et al.* (1990) are strung out along a small circle cutting the 250-280Ma segment of the APWP of Baltica, in broad agreement with the mean ages of dykes emplacement (Vaccaro *et al.*, 1991; Atzori *et al.*, 2000; Gaggero *et al.*, 2007) (taking into account the

inherent uncertainties associated with radiometric dating as well as potential errors in the Baltica APWP arising from the time-averaging of paleopoles that are not always sufficiently well dated). Alternatively, the apparent discrepancy between the (older) dyke poles and the (younger) APWP segment onto which they seem to converge could be due to (undetected) block tilting after dykes emplacement. In any case, we believe that our analysis supports the successful isolation of primary magnetic directions in the studied dykes, and also the assumption that the number of sites/samples used to calculate the mean paleomagnetic poles is sufficient to average out secular variations of the Earth's field at the time of dykes cooling. Furthermore, a single Euler pole of rotation, calculated as the pole to the small circle best fitting the paleomagnetic poles, can account for the differential block rotations observed; this Euler pole lies in Sardinia at Latitude = 40.3°N, Longitude = 8.9°E (Fig. 3.7, small polygon).

In order to estimate the rotations of northern, central-eastern, and south-eastern Sardinia relative to the 270Ma paleopole of Baltica of Torsvik *et al.* (2012), we restored these regions to European coordinates using the rotation parameters of Gattacceca *et al.* (2007) and Gong *et al.* (2008) (see also above), obtaining a position for a nominal point in the central part of northern Sardinia of Lat = 38.28°N, Long = 4.24°E, for a nominal point in the central part of central-eastern Sardinia of Lat = 37.81°N, Long = 3.08°E and for a nominal point in the central part of south-eastern Sardinia of Lat = 37.74°N, Long = 2.32°E. These restored coordinates were then used to calculate the declinations and inclinations expected from the paleomagnetic poles of this study, again rotated to European coordinates. The resulting directions are: Dec = 209.7°E, Inc = −0.8° for northern Sardinia, Dec = 167.5°E, Inc = −4.6° for central-eastern Sardinia, and Dec = 155.2°E, Inc = −20.5° for south-eastern Sardinia. The expected directions for the different parts of Sardinia (restored to Europe) calculated from the 270Ma paleopole of Baltica (Torsvik *et al.*, 2012) are Dec = 195.7°E, Inc = −5.1° for the north, Dec = 195.0°E, Inc = −3.7° for the central-eastern part and Dec = 194.6°E, Inc = −3.3° for the southeast, which implies differences in declinations of 14° counterclockwise for northern Sardinia, 27.5° clockwise for central-eastern Sardinia, and 39.4° clockwise for south-eastern Sardinia. After rotation, the declinations coincide and the dyke provinces show better alignment (Fig. 3.8).

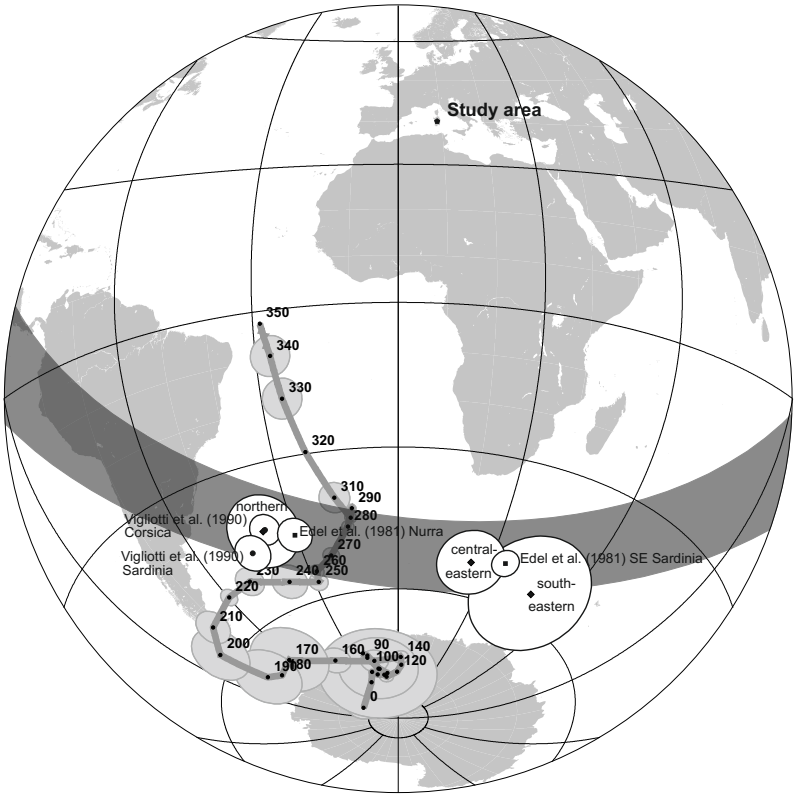

Figure 3.7: Paleomagnetic poles from this study for south–eastern, northern and central–eastern Sardinia (solid diamonds) compared to poles from Edel *et al.* (1981) for southeast Sardinia and Nurra (solid squares) and from Vigliotti *et al.* (1990) for Sardinia and Corsica (circles). All poles are shown in European coordinates, i. e. they have been corrected for the opening of the Ligurian Ocean and the Bay of Biscay (see text for explanation). These poles plot within a small circle band centered on the 250-280Ma time window of the Baltica apparent polar wander path of Torsvik *et al.* (2012) (solid circles with ages attached). The pole of rotation to the small circles (solid polygon) lies within Sardinia (study area), indicating true vertical axis rotations between northern and central–southern Sardinia.

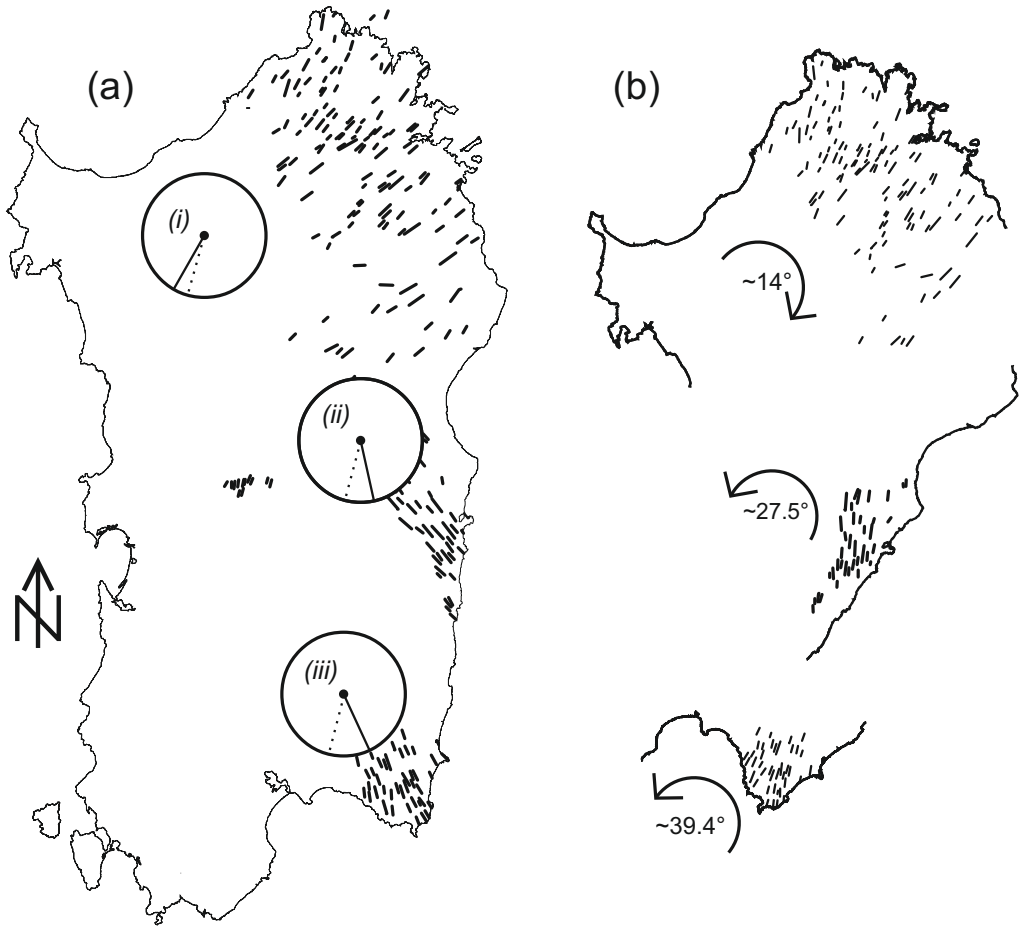

Figure 3.8: (a) Sardinia in its present outline and orientation with the distribution of Early Permian dyke provinces. Stippled: expected Permian declinations for nominal points in (i) a central part of northern Sardinia, (ii) a central part of central-eastern Sardinia and (iii) a central part of south-eastern Sardinia calculated from the 270Ma pole from the Baltica AWPW of Torsvik *et al.* (2012). Solid: observed magnetic declinations of the Early Permian dykes of this study. All declinations are in European coordinates (e. g. corrected for the opening of the Bay of Biscay and of the Liguro-Provençal Basin). (b) Paleogeography of Sardinia restored based on the observed declinations; the arrows indicate the amount and sense of rotation since the magnetization was acquired; see text for discussion.

3.7 Discussion and Conclusions

The observed rotations confirm and further substantiate previous paleomagnetic analyses from Permian and Carboniferous rocks of Sardinia (Zijderveld *et al.*, 1970; Edel *et al.*, 1981; Edel, 2000; Moser, 2004; Moser *et al.*, 2005) that revealed the existence of a complex tectonic history characterized by large-scale differential rotations of crustal blocks.

Regarding the age and tectonic significance of the observed rotations, already in the 1980's, Edel *et al.* (1981) inferred that the rotations between northern and southern Sardinia were due to an "[...] important phase of deformation in Late Variscan times [...]". Subsequent analyses confirmed and better substantiated this conclusion. Kirscher *et al.* (2011) analyzed a total of 280 samples from 44 sites of Middle and Late Jurassic age from Sardinia (Nurra, Baronie-Supramonte, Barbagia-Sarcidano, and Sulcis), obtaining site mean directions and paleomagnetic poles that indicate negligible amounts ($\pm 10^{\circ}$) of post-Jurassic internal rotations within Sardinia. We therefore exclude that the rotations described in this study are related to tectonic processes postdating the Jurassic, such as extensional tectonics affecting the European margin during the Jurassic (Zattin *et al.*, 2008), Alpine tectonics that started roughly during the Late Cretaceous (Carmignani *et al.*, 1994a; Rosenbaum *et al.*, 2002) or transcurrent tectonics in the Cenozoic (Carmignani *et al.*, 1994a; Pasci, 1997; Oggiano *et al.*, 2009). Moreover, Cenozoic subduction rollback tectonics cannot be held responsible for the observed rotations or the curvature of the Gulf of Orosei as proposed by Helbing *et al.* (2006a,b) based on the paleomagnetic data of Kirscher *et al.* (2011) documenting the internal coherence of Sardinia in post-Jurassic times. This opens the possibility that the observed rotations could have occurred during the Permian after the Variscan coalescence of Gondwana and Laurasia.

The block rotations documented in this study are reminiscent of block rotations previously observed in Permian and Triassic sediments and volcanic rocks from the Toulon-Cuers basin of SE France (Aubele *et al.*, 2012), which was located along the European margin immediately to the west of Sardinia in Permian times. Similarly to what is observed in this study, the latitudes of the Early to Middle Permian paleopoles from Toulon-Cuers agree well with the corresponding segment of the APWP of Baltica (Europe), whereas the longitudes are strung out along a small circle segment, indicating relative rotations between the sampled regions and stable Europe. The Triassic poles, instead, plot close to the Triassic segment of the European APWP and provide a strong constraint on the age of the observed rotations, which is likely late Early–Middle Permian. To the west of Toulon-Cuers, a very similar timing of block rotations was observed in the Brive and Saint-Affrique basins of the French

Massif Central where Early Permian rocks show rotated paleomagnetic vectors while Late Permian rocks have not been affected by rotations (Cogné *et al.*, 1990, 1993; Diego-Orozco and Henry, 1998; Henry *et al.*, 1999; Diego-Orozco *et al.*, 2002; Chen *et al.*, 2006). In addition, paleomagnetic data from the Maures-Estérel massif located immediately to the east of the study area in SE France suggest a large clockwise block rotation during the late Early to Middle Permian (Edel, 2000).

Summarizing and expanding the above, paleomagnetic data collected over large parts of the western Mediterranean Variscides seem to indicate the existence of an intra-Pangea belt of tectonic blocks straddling from the Massif Central to southern France and Corsica-Sardinia characterized by complex and differential block rotations that may have largely occurred in post-Early Permian and pre-Early Triassic times. The timing of the transformation from Irving's Pangea B (Irving, 1977) to a Wegenerian Pangea A configuration broadly agrees with the timing of block rotation documented in this and the aforementioned studies. This postulated transformation occurred essentially during the Middle Permian from an Early Permian Pangea B to a Late Permian Pangea A (Muttoni *et al.*, 1996, 2003, 2009). The Middle Permian therefore seems to coincide with a period of major intra-Pangea plate reorganization associated with magmatic activity as suggested by several authors (e. g., Deroin and Bonin (2003); Isozaki (2009)).

We previously illustrated (Aubele *et al.*, 2012) that the simple two-dimensional model developed by McKenzie and Jackson (1983) can explain the existence of differential (clockwise, counter-clockwise) rotations of crustal blocks within a zone of distributed deformation imposed by the relative motion of the bounding plates. Accordingly, we suggest that the various crustal blocks of Sardinia-Corsica and SE France were rotated by variable amounts and sense as they were trapped within a diffuse shear zone between Laurasia and Gondwana (e.g. Arthaud and Matte (1977)) acting during the Permian. In this scenario, an assumed dextral shear between Laurasia and Gondwana would lead to systematic clockwise or counterclockwise rotations about vertical axes of crustal blocks of variable shape and dimension located within the shear zone. We speculate that the large-scale rotations of fault-bounded blocks observed in the Permian dykes of Sardinia, as well as in the Permian series elsewhere in Europe, may have been induced by post-Variscan intra-Pangea wrenching and shearing occurring during Pangea instability and transformation (see Muttoni *et al.* (2003); Aubele *et al.* (2012); Domeier *et al.* (2012) for a detailed discussion on the Pangea debate).

Our working hypothesis of continental-scale shearing between Laurasia and Gondwana occurring as consequence of Pangea transformation during the Permian will benefit from future studies from other dyke provinces potentially caught in the shear zone, e.g. in Calabria (Sila Grande) and Catalonia.

3.8 Acknowledgments

This project has been funded by the German Science Foundation (DFG) Grants BA 1210/8–1 and BA 1210/20–1. Special thanks goes to Dennis Kent whose comments on an earlier version of the manuscript were very helpful. We are indebted to Paola Pittau and Myriam Del Rio for fundamental help in solving burocratic problems during our sampling campaign. Special thanks goes to Barbara Emmer for help in the field and Giuseppe Muttoni for legal advice. We are also thankful for very helpful and substantial reviews provided by J. Gattacceca and C. Mac Niocaill.

4

New Early Permian Paleopoles from Sardinia confirm intra-Pangea Mobility

By ***K. Aubele, V. Bachtadse, G. Muttoni, A. Ronchi and D. V. Kent***
submitted to Tectonics.

Abstract

We present new paleomagnetic poles for the Early Permian from 18 sites (167 samples) from sedimentary and volcanic rocks from northern and southern Sardinia (Italy). Reproducible paleomagnetic component directions have been retrieved using thermal demagnetization. We compare the new paleomagnetic poles - transferred into European coordinates to account for the opening of the Ligurian Sea and the Bay of Biscay in the Cenozoic - with data from stable Europe. Whereas the Early Permian pole for northern Sardinia is rotated clockwise (cw) to the west of the coeval segment of the apparent polar wander path (APWP) of stable Europe, the coeval paleomagnetic pole for central-southern Sardinia is rotated counterclockwise (ccw) away to the east of the APWP, thus suggesting post-Early Permian differential vertical axis rotations between central-southern and northern parts of the island, which is in agreement with earlier paleomagnetic data from Sardinia and the greater Mediterranean realm. In conjunction with previous results, we argue that the observed Permian differential block rotations are the result of post-Variscan intra-Pangea mobility localised inside a wide zone of deformation and that they ended in the Early Mesozoic.

4.1 Introduction

Transform fault activity can lead to differential vertical axis rotations of adjacent tectonic blocks caught within a wider fault zone. In reverse, the absence of such rotations is a strong evidence for the abandonment of the fault activity. The rotations can be quantified by using paleomagnetic techniques. In combination with robust geochronological and stratigraphical control, paleomagnetism allows substantial insights into the spatial and temporal (paleo-)evolution of (transform) fault activity in a given area.

The Pangea A vs. Pangea B controversy provides a classic case of a highly debated large-scale transform fault system, running approximately along the paleoequator and bordering the southern Pangea continents (Gondwana) against the northern ones (Laurasia) in Permian times. The final outcome of this long lasting debate hinges on the question whether the existence of a large-scale transform fault zone can be demonstrated which is required to transfer Pangea from a B type into an A type configuration (Irving, 1977; Morel and Irving, 1981; Muttoni *et al.*, 2003; Domeier *et al.*, 2012). Based on a variety of geological evidences (e. g. Arthaud and Matte (1977); Burg *et al.* (1994); Stampfli (2001); Cassinis *et al.* (2012)), the zone

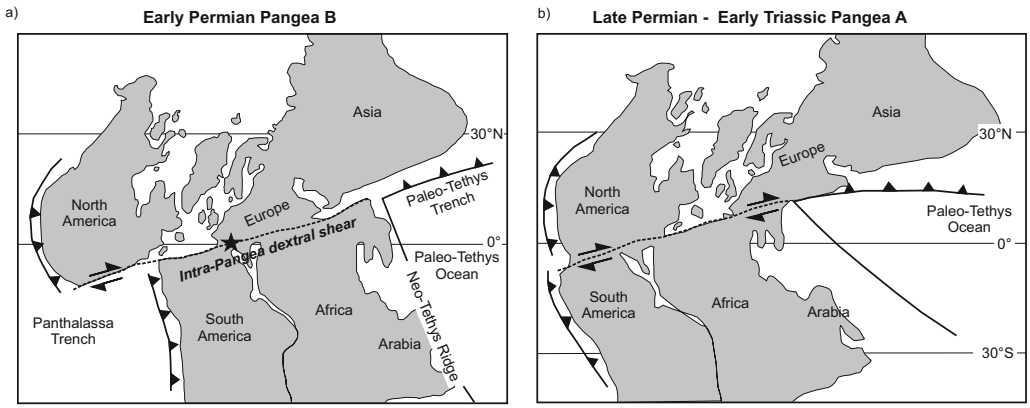

Figure 4.1: Pangea B configuration after Irving (1977) in the Early Permian (a). Star: approximate location of the study area. Wegenarian Pangea A configuration in the late Permian to Early Triassic (b). Modified after Muttoni *et al.* (2009).

of transform fault activity is expected to lie within the present-day Mediterranean realm in southern Europe and/or northern Africa. Previous paleomagnetic studies (Aubele *et al.*, 2012, 2014) support the existence of an intra-Pangea belt of tectonic blocks straddling from the Massif Central to southern France and Corsica-Sardinia characterized by complex and differential clockwise/counterclockwise block rotations that may have largely occurred in post-Early Permian and pre-Middle? Triassic times. The rotations have tentatively been assigned to represent shear stress caused by a large intra-Pangean dextral transform fault system, accomodating the transformation from an Early Permian Pangea B to a Late Permian Pangea A *sensu* Muttoni *et al.* (2003) (Fig. 4.1).

To extend the existing set of Permian paleomagnetic data from Sardinia, a detailed study of paleomagnetic data from sedimentary and volcanic sequences (mainly ingnimbrites) in Sardinia covering early Cisuralian to Guadalupian (Early to Middle Permian) sedimentation and volcanism is presented here. Fig. 4.2 shows a stratigraphic record of the sampled formations, which are described in detail in the following section. Paleontological data as well as the intercalation with volcanic products allows a robust relative and absolute age estimation of the sampled rocks.

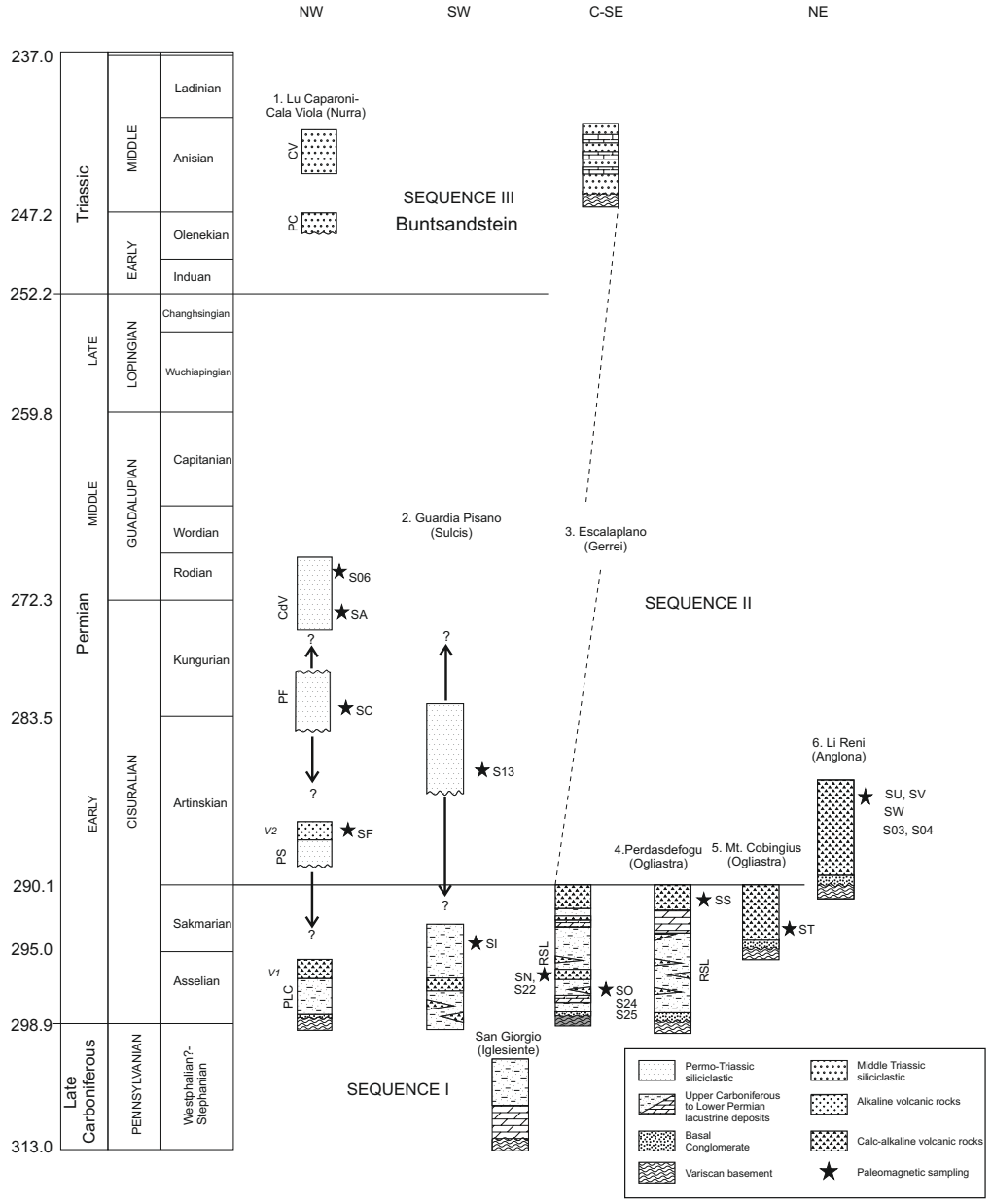

Figure 4.2: Stratigraphy and ages of the sampled formations. PLC: Punta Lu Caparoni; PS: Pedru Siligu Fm.; PF: Porto Ferro Fm; CdV: Cala del Vino Fm.; CP: Porticciolo Conglomerate; CV: Cala Viola Fm.; RSL: Rio su Luda Fm. Stars indicate the statigraphic position of the sampled horizons.

4.2 Geological Setting and Stratigraphy

The Early to Middle Permian geological record of the western Mediterranean domain is dominated by the effects of northward subduction of the Paleotethys active oceanic ridge and the resulting transformation of the western Eurasian sector of the Variscan chain into a dextral strike-slip orogen and diffuse transform margin. Strike-slip tectonic activity caused tilting and subsidence of basement blocks, triggering the formation of numerous pull-apart basins in Sardinia and elsewhere in western Paleoeurope (present day coordinates) (Broutin *et al.*, 1994; Deroin and Bonin, 2003; Ronchi *et al.*, 2008; Cassinis *et al.*, 2012). The progressive transformation of the western Variscan chain from a collisional to a dextral shear margin led to the deposition of thick piles of fluvial-lacustrine sediments in narrow strike-slip basins in many European regions, and especially in Spain, France, Germany and Italy (for example see a review in Cassinis *et al.* (2012)). The following sections describe the lithological characteristics of the sampled Sardinian basins as shown in Fig. 4.2. Sampling localities are given in Fig. 4.3.

4.2.1 Lu Caparoni/Cala Viola Basin (Nurra)

The post-Variscan continental record of Nurra may be subdivided into three distinct tectono-sedimentary cycles (Cassinis *et al.*, 2000, 2003; Ronchi *et al.*, 2008, 2011). At the base of the volcano-sedimentary succession in the northwestern part of Sardinia lie a basal conglomerate and a thin alluvial-to-lacustrine succession composed of dark shales, sandstone layers and conglomerate bodies, named Punta Lu Caparoni Formation ($\sim$ 15m) (Gasperi and Gelmini, 1980; Cassinis *et al.*, 2003). On top of the Punta Lu Caparoni Fm., several meters of volcaniclastic acidic deposits (rhyolitic ignimbrites and tuffs; V1 in Fig. 4.2) are present. The macrofloral association of the sequence is indicative of an Early Permian age and based on close lithological analogies, the Punta Lu Caparoni Fm. is assumed to be coeval with the Les Pellegrins Fm. in the Toulon-Cuers Basin (Cassinis *et al.* (2003); Durand (2006, 2008) and references therein). This sequence is separated by a slight angular unconformity from the overlying sediments.
The following Pedru Siligu Fm. (about 50m thick and lying at the base of Sequence II, as in Fig. 4.2) starts with sediments typical for braided alluvial environments, such as channelized conglomerates and coarse sandstones. After a new volcanic episode (V2 in Fig. 4.2; Casa Satta), it is in turn followed by the Porto Ferro Fm., represented by at least 200m of fluvial fossil-barren red beds. Separated by an angular

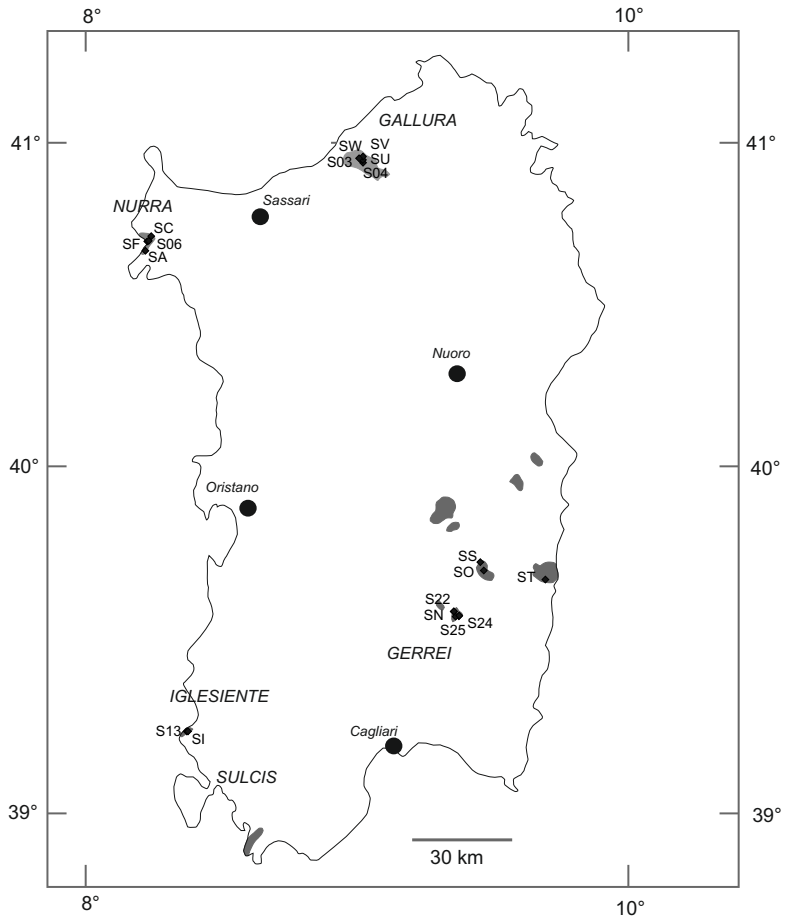

Figure 4.3: Geological sketch map of the Upper Carboniferous-Permian sedimentary and volcanic sections in Sardinia. Diamonds mark the sampling locations from the 2004 and 2011 sampling campaigns on Sardinia.

unconformity, the upper part of Sequence II in Sardinia is represented by stratified green to reddish sandstones and siltstones, typical for sedimentation by meandering rivers (Cala del Vino Fm., about 400m).
Ronchi *et al.* (2011) date the above described units of Sequence I and the first two formations of Sequence II to early and late Cisuralian, while the upper formation of Sequence II is dated to latest Cisuralian- early Guadalupian (Roadian). Also, these three formations can be lithologically compared with the corresponding Transy, Les Salettes and Saint-Mandrier formations in Provence (Cassinis *et al.*, 2003; Durand, 2006, 2008).
The formations of Sequence III (Porticciolo Conglomerate; Arenarie di Cala Viola) rest disconformably on top of the Cala del Vino Fm., and start with a few metres of quartz conglomerate, including wind-worn clasts and arenitic intercalations. Those deposits clearly testify to an arid period, as recognized in many other parts of Europe around Olenekian times (Bourquin *et al.*, 2007, 2011). The conglomerate is followed by medium-to-fine grained floodplain deposits (red sandstones and siltstones), indicating new climatic conditions, from arid to semi-arid. The corresponding formations in the Toulon-Cuers basins are the Poudingue de Port-Issol and the Grés de Gonfaron (Cassinis *et al.*, 2003; Durand, 2006, 2008).

4.2.2 Guardia Pisano (Sulcis)

The 120m thick succession that is exposed in the Guardia Pisano Basin can be subdivided into three informal lithostratigraphic units (the lower, middle and upper), where the latter two units seem to overlie the lower unit unconformably (Barca and Costamagna, 2006). On the basis of regional correlations, Ronchi *et al.* (2008) propose a subdivision of the section into four lithofacies (A to D) ranging in age from the early Cisuralian (facies A to C) to post-Autunian (late Early Permian to Middle Permian; facies D). According to Fischer *et al.* (2010), lithofacies B yields a rich vertebrate paleontological content.
The basal deposits (A and B) are composed of grey-black sandy shales which were deposited in a fluvial-lacustrine to palustrine environment. For this unit of the Guardia Pisano sequence, an early Asselian age is indicated by a rich sporomorph record (Pittau *et al.*, 2002). Unit B contains medium- to coarse-grained pyroclastic deposits and rhyolitic lava flows, which were radiometrically dated to 297 ± 5Ma using SHRIMP and lead-zircon evaporation (Cocherie in Pittau *et al.* (2002)). The upper unit (D) is composed of grey to red sandstones and thin pelites deposited on an alluvial plain under warmer and humid conditions (Ronchi *et al.*, 2008); due to a lack of fossil content, only a post-Asselian age can be constrained. Stratigraphical

correlation with the deposits of Nurra (Pedru Siligu, Porto Ferro and Cala del Vino formations) is, for the time being, premature.

4.2.3 Escalaplano Basin (Gerrei)

In the Escalaplano Basin, located in central-eastern Sardinia, magmatic products clearly dominate over the strictly sedimentary units. The volcano-sedimentary sequence can be subdivided into a lower and upper part (Pecorini, 1974; Cassinis *et al.*, 2000; Ronchi *et al.*, 2008). In general, the two sequences start with coarse-grained sedimentary rocks followed by reworked volcaniclastic deposits and tuffs which in turn are followed by finer-grained lacustrine to palustrine deposits. The lower sequence is topped by a rhyolitic ignimbrite, the upper one by an andesite lava flow (Cortesogno & Gaggero in Cassinis *et al.* (2000)). The two sequences can in turn be subdivided into nine lithostratigraphic units, seemingly separated by paraconformities, described in detail by Ronchi *et al.* (2008). On the basis of scarce (bio-)stratigraphical data, and mainly from correlation with the nearby Mulargia lake Autunian deposits and the late Palaeozoic volcano-sedimentary successions in the area, the Escalaplano deposits have been assigned an Early Permian (late? "Autunian") age.

4.2.4 Perdasdefogu Basin (Ogliastra)

The largest of the Permian sedimentary basins in south-eastern Sardinia hosts a Lower Permian volcano-sedimentary succession, non-conformably overlying the lower Paleozoic metamorphic basement and, in turn, unconformably covered by the Middle to Upper Jurassic coarse-grained quartz conglomerates and/or dolostones (Genna Selole Fm. and Dorgali Fm.). The basin fill is strongly influenced by contemporaneous volcanism, represented by calc-alkaline extrusives and dykes (Cortesogno & Gaggero in Cassinis *et al.* (2000)). The sedimentary and volcanic succession of the Perdasdefogu Basin has a total average thickness of 250m. In this study, the Riu Su Luda Fm. (150m) was sampled. For a detailed lithological description, the reader is referred to Ronchi *et al.* (2008). Significant similarities in the paleofloral record exist between the Perdasdefogu succession and the sedimentary sequence in NW Sardinia (Nurra, Lu Caparoni/Cala Viola Basin (Ronchi *et al.*, 1998; Pittau *et al.*, 2008; Galtier *et al.*, 2011)).
The age of the Riu su Luda Fm. can be constrained by the co-occurrence of three amphibian species which can also be found in the Upper Goldlauter Fm. in the Thuringian Forest Basin, Germany (Werneburg *et al.*, 2007). The felsic tuff layers intercalated into the middle part of the Goldlauter Fm. have been dated to 288±7Ma

(U/Pb on zircon separates; Lützer *et al.* (2007)) and the volcanic rocks in the overlying Oberhof Fm. (Reifstieg Rhyolite) yielded an age of 287 ± 2Ma (Ar/Ar; Goll and Lippolt (2001)).

4.2.5 Monte Cobingius (Ogliastra)

The Permian sedimentary section at Monte Cobingius, only a few kilometers to the east of the main Perdasdefogu Basin, is mainly composed of fluvial whitish conglomerates and sandstones (about 20m thick) and unconformably overlies the Variscan basement. It is in turn covered by about 30m of andesite breccias and lavas. A more detailed description of the sequence can be found in Ronchi *et al.* (2008).

4.2.6 Li Reni (Anglona)

In the Coghinas Valley (Li Reni-Azzagulta area, Anglona) crops out the only Lower Permian volcano-sedimentary sequence of NE Sardinia, represented by very scattered sedimentary deposits and large volcanic effusive bodies (Traversa, 1979). Radiometric ages, performed on azoic sandstones at the base of the sequence and on the overlying ignimbrites (Rb/Sr on mineral separates, Muscovite and Biotite: 288 ± 3 and 286 ± 3 Ma; Del Moro *et al.* (1996)) indicate an early-middle Artinskian age (Ronchi *et al.*, 2008).

4.3 Field and Laboratory Methods

All samples were taken using a gasoline-powered, water-cooled drill and oriented using a standard magnetic compass. Subsequently, samples were cut into standard 11cc cylindrical specimens. All samples were studied in the paleomagnetic laboratory of the University of Munich. The specimens were thermally demagnetized using a Schoenstedt furnace with increments of $30°C$ up to maximum temperatures of $700°C$. Temperature steps were variably adjusted to sample behaviour during the demagnetization process and were decreased to 5 to $10°C$ intervals approaching the unblocking temperature of the respective sample. After each heating step, the natural remanent magnetization was measured with a 2G Enterprises cryogenic magnetometer mounting SQUID (Superconducting Quantum Interference Device) sensors located in a magnetically shielded room. Demagnetization results were plotted on orthogonal projection diagrams (Zijderveld, 1967) and analyzed using the least square method (Kirschvink, 1980) on linear portions of the demagnetization paths defined by at

least four consecutive demagnetization steps (Fig. 4.4). Linear fits were anchored to the origin of the demagnetization axes where appropriate. Paleomagnetic site mean directions were calculated using the paleomagnetic software of Bachtadse and Maier (1994), and were used to calculate regional mean directions according to age and tectonic affiliation. Table 4.1 lists all relevant paleomagnetic data. Table 4.2 lists the resulting paleopoles of this study together with other published paleomagnetic data from the Sardinia-Corsica region. The paleomagnetic poles for Sardinia were transferred into European coordinates using the rotation parameters of Gong *et al.* (2008) to accomodate the opening of the Bay of Biscay and of Gattacceca *et al.* (2007) for the opening of the Ligurian sea. The resulting combined rotation pole has the coordinates lat=41.93°, lon=4.61°, angle=-79.8° (clockwise). In addition to paleomagnetic analyses, rock-magnetic data were determined using a Variable Field Translation Balance (Krása *et al.*, 2007) (Fig. 4.5). Rock magnetic analyses include hysteresis measurements, isothermal remanent magnetization (IRM) acquisition in fields up to 700 mT, backfield magnetization for the definition of the coercivity of remanence, and in-field heating (up to 700°C) and cooling cycles (hereafter referred to as thermomagnetic measurements) in order to estimate the Curie temperatures of the magnetic minerals (Moskowitz, 1981), as well as to identify possible mineralogical transformations during heating. Analysis of the rockmagnetic parameters was carried out using the software by Leonhardt (2006). In this paper, we present combined results from two field campaings from 2004 and 2011. This is reflected in the nomenclature of sample labelling. Samples labelled "S" plus a capital letter were collected in 2004 and samples labelled "S" plus a number were collected in 2011 (see Fig. 4.3).

4.4 Results

4.4.1 NRM Demagnetization Behaviour/Magnetic Mineralogy

Northern Sardinia (Gallura and Nurra)

Fig. 4.4 shows six representative orthogonal projection diagrams from the sites in northern Sardinia (S03-7A, S03-4A, S04-5A from Gallura and S06-7A, SA-6A and SC-14B from Nurra). The samples from Gallura show similar demagnetization behaviour with essentially two directional components. The first directional component in samples S03-7A and S03-4A is removed by heating up to 250°C. It points roughly towards the direction of the present day magnetic field for Sardinia which

Table 4.1: Geographic coordinates and paleomagnetic data of sites from the 2004 and the 2011 sampling campaigns on Sardinia.

Site					In Situ				Bedding corrected			
Name	*N/N'*	*Lithology*	*GLat°*	*GLon°*	$D°$	$I°$	k	α_{95}°	$D°$	$I°$	k	α_{95}°
SA	9/13	Redbeds	N40.64	E8.19	115.6	-26.6	26.1	10.3	116.2	-20.3	26.1	10.3
SC	14/14	Red Siltstone	N40.68	E8.20	87.9	-60.3	10.9	12.6	124.1	-39.9	11.7	12.2
S06	7/10	Redbeds	N40.68	E8.20	113.3	-16.5	10.3	19.7	114.3	-9.7	10.9	19.2
SF	9/15	Volcanics	N40.70	E8.22	129.6	-3.5	6.2	22.5	130.8	-14.1	6.3	22.4
SU	7/12	Ignimbrites	N40.94	E8.90	142.5	-8.0	40.5	9.6	142.5	-8.0	40.5	9.6
SV	21/23	Ignimbrites	N41.00	E8.90	137.7	-7.6	22.4	6.9	137.7	-7.6	22.4	6.9
SW	7/8	Ignimbrites	N40.95	E8.87	145.5	2.9	16.5	15.3	145.5	2.9	16.5	15.3
S03	5/13	Ignimbrites	N40.93	E8.89	150.4	-10.2	23.3	16.2	150.4	-10.2	23.3	16.2
S04	4/8	Ignimbrites	N40.94	E8.89	145.5	-4.1	72.2	10.9	145.5	-4.1	72.2	10.9
Northern Sardinia	9		N40.65	E8.20	132.8	-15.0	10.5	16.7	135.0	-14.6	14.4	14.0
SI	16/33	Redbeds	N39.25	E8.46	85.6	3.3	21.6	8.1	86.9	18.8	20.6	8.3
S13	6/10	Redbeds	N39.25	E8.45	78.9	-10.3	24.8	13.7	81.1	-8.4	25.7	13.5
SN	8/20	Ignimbrites	N39.62	E9.32	68.5	2.2	310.5	3.1	68.4	7.1	129.0	4.9
SO	9/14	Rhyolitic Tuffs	N39.61	E9.35	92.2	15.3	9.2	17.9	96.4	20.1	9.2	17.9
SS	20/20	Dacite	N39.70	E9.43	82.9	-10.0	40.3	5.2	84.5	-4.3	40.3	5.2
ST	4/8	Andesite	N39.63	E9.55	81.2	12.2	61.4	11.8	76.4	27.3	61.4	11.8
S22	7/9	Ignimbrites	N39.62	E9.32	72.3	-8.9	17.9	14.7	73.5	-3.6	27.5	11.7
S24	8/8	Rhyolitic Tuffs	N39.60	E9.34	86.0	0.3	16.3	14.1	82.8	2.9	13.7	15.5
S25	6/7	Rhyolitic Tuffs	N39.60	E9.33	81.3	-9.0	47.5	9.8	82.9	-6.4	19.5	15.5
Southern Sardinia	9		N39.65	E9.40	81.0	-0.6	45.1	7.7	81.1	7.7	28.9	9.7

GLat/GLon: Geographic latitude/longitude of sampling site; $D°/I°$: Paleomagnetic declination/inclination; α_{95}: Circle of 95% confidence; N/N': number of specimens used in the calculation of the mean data/number of measured specimens.

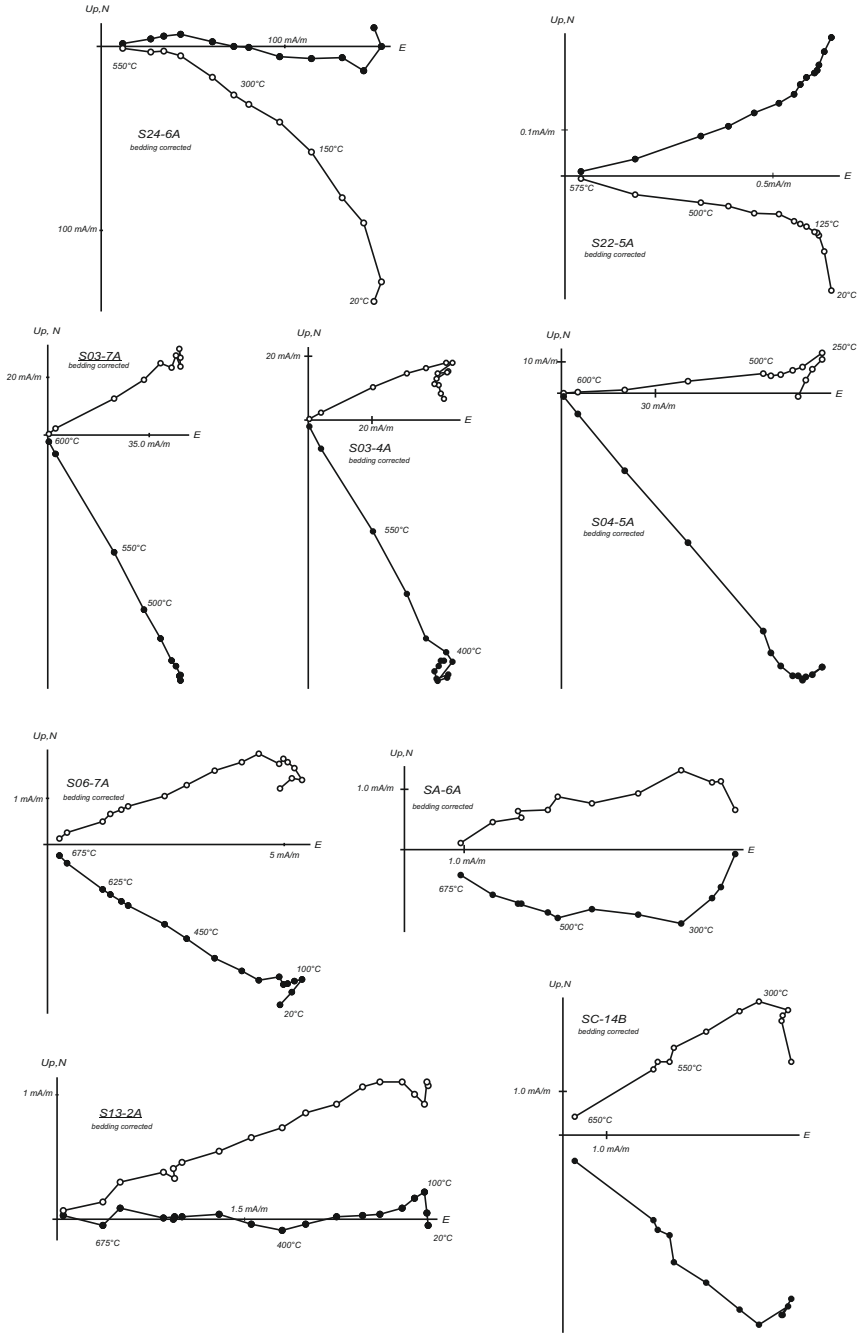

Figure 4.4: Results of thermal demagnetization experiments plotted as orthogonal vector diagrams in bedding corrected coordinates. Solid and open dots represent vector endpoints projected onto the horizontal and vertical planes, respectively.

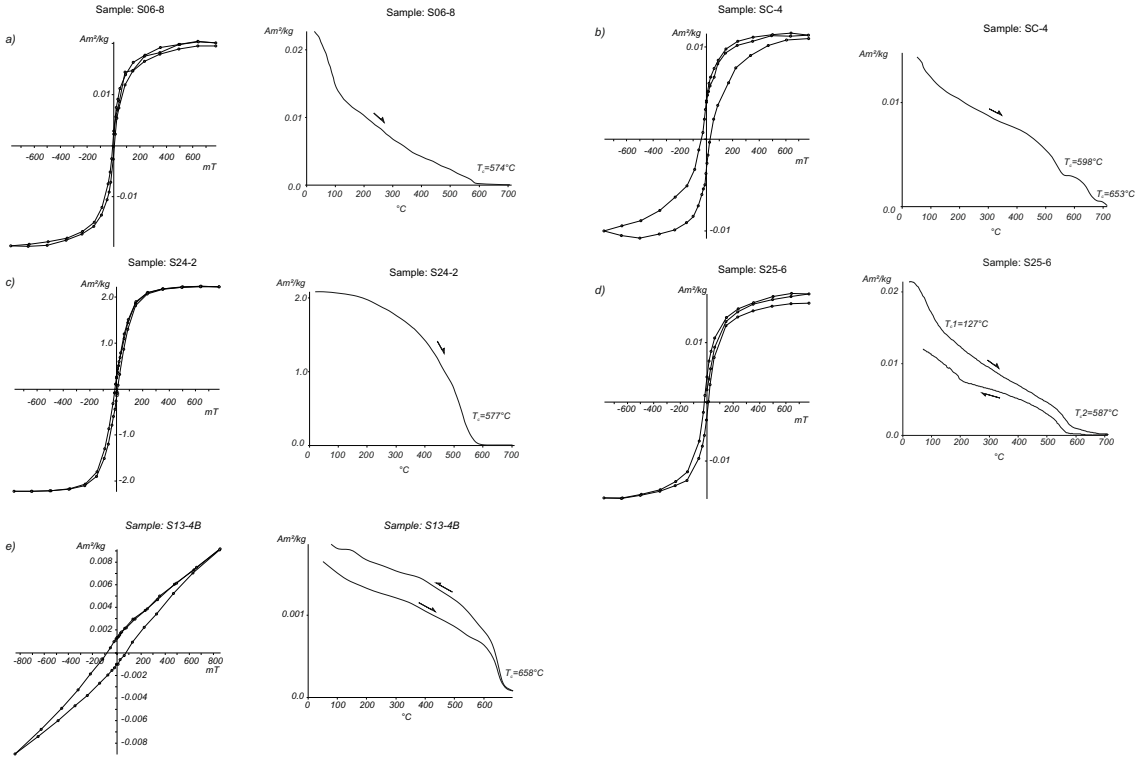

Figure 4.5: Results of rock-magnetic experiments on representative samples. Hysteresis loops (left) and thermomagnetic curves (right). [J/J$_{max}$]: normalized magnetization intensities, [Am^2/kg]: absolute magnetization intensities.

is $D = 2.0°$, $I = 55.6°$ (as calculated from the 2014 version of the international geomagnetic reference field model IGRF-12[1]). The second directional component shows a clear trend towards the origin of the vector end point diagram with magnetization intensity gradually decreasing during stepwise heating up to 600°C. Sample S04-5A also shows two directional components during thermal demagnetization. The first component is removed by heating up to 250°C, and the second one again shows a clear trend towards the origin of the diagram with a gradual decrease in magnetization intensity up to 625°C. The samples from the Nurra region show more variable demagnetization behaviours with more than one directional components. In samples S06-7A and SC-14B, no clear low temperature directional component can be defined. However, from 300°C onward, a single component trending toward the origin of the diagram can be clearly defined in both samples. Magnetization intensity gradually decreases during stepwise heating up to $650 - 675$°C. Sample SA-6A arguably shows three overlapping directional components. The first component is removed at 300°C, the second one at 500°C. Up to 675°C, the third component trends toward the origin of the demagnetization diagram.

Fig. 4.5 shows representative results from rock-magnetic experiments. The results from sample S06-8 give a clear indication of magnetite as the main carrier of magnetization (see Fig. 4.5 a). The Curie temperature of 574°C and the coercivity of remanence (obtained from backfield curve measurements) of ~ 30 mT support this interpretation. The results for sample SC-4 (Fig. 4.5 b) also from the northwestern sampling area, on the other hand, strongly suggest the presence of two coercivity fractions. The wasp-waisted shape of the hysteresis loop as well as the two-step decrease in the thermomagnetic heating curve at 598°C and 653°C, respectively, indicate magnetite and haematite as main magnetic carriers. The coercivity of remanence of ~ 140 mT is the weighted result of the contributing high- and low-coercivity fractions. Values for magnetite typically lie in the range of a few tens of mT, while haematite is typified by values of a few hundreds of mT (Dunlop and Özdemir, 1997). The obtained value of ~ 140 mT is therefore likely to be the result of a combination of both carriers.

Southern Sardinia (Gerrei and Iglesiente/Sulcis)

Fig. 4.4 displays two representative demagnetization diagrams from samples from the Gerrei sites (Escalaplano: S24-6A and S22-5A). Both samples show two overlapping directional components. The low temperature component, pointing roughly towards the direction of the present day magnetic field for Sardinia (again calculated from

[1] http://www.ngdc.noaa.gov/IAGA/vmod/igrf.html, 01/27/2015

the IGRF-12 model), is removed at 125°C. In both samples, the second component shows a clear trend toward the origin of the demagnetization diagram, with gradually decreasing magnetization intensity up to 550 − 575°C. Directional data from site S13 (Sulcis) are also presented in Fig. 4.4. A low stability secondary component is removed at 100°C. A vector end point trajectory trending toward the origin of the orthogonal projection can be defined for the demagnetization steps from 200 to 700°C. Rock-magnetic results from the samples from southern Sardinia are displayed in Fig. 4.5 c - e. The samples from the Gerrei area (Fig. 4.5 c and d) provide clear evidence of magnetite as the main magnetic carrier. This is especially evident in sample S24-2, where the rather low coercivity of remanence of $\sim$ 45 mT and the typical convex decrease in magnetization intensity displayed by the heating portion of the thermomagnetic curve, culminating in a Curie temperature of 577°C, provide substantial evidence for this observation. The picture is a little less clear in sample S25-6, where two coercivity fractions are observed. The hysteresis loop does not reach saturation in the applied maximum field of 800 mT, indicating a high coercive fraction. Here, we speculate on the presence of goethite in accordance with the initial decrease in magnetization at 127°C, as displayed in the heating portion of the thermomagnetic curve. The second decrease in magnetization intensity at 587°C, however, is indicative of magnetite. Fig. 4.5 e shows data from site S13 from the Sulcis area. The strong paramagnetic content and high coercive fraction are clearly visible in the hysteresis curve. The sudden drop in intensity at about 660°C provides clear evidence for the existence of haematite as primary magnetic phase.

4.4.2 Paleomagnetic Data

A low temperature component (up to 300°C) was identified in the majority of the samples. It clusters around the present day field direction calculated for a nominal point at 40°N/9°E in Sardinia using the IGRF-12 model (Fig. 4.6). Samples from the Iglesiente/Sulcis area in the SW of the island do not display these low temperature component directions.

Northern Sardinia (Gallura and Nurra)

A total of 83 samples from 9 sites from northern Sardinia were included in the analysis (Fig. 4.3 and Table 4.1). In northwest Sardinia, samples were taken from the Pedru Siligu, Porto Ferro and Cala del Vino Formations (Fig. 4.2). In addition, we sampled the Permian ignimbrites in Gallura, which were previously studied by, among others, Zijderveld *et al.* (1970) and Westphal *et al.* (1976a). As the ignimbritic formation lies approximately horizontal and the local structural setting appears undeformed, no

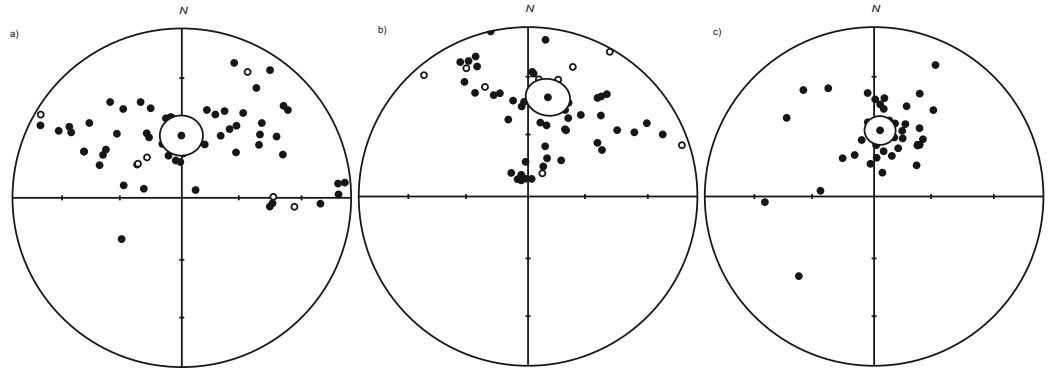

Figure 4.6: Stereographic projections in bedding corrected coordinates of the low temperature magnetic component directions of samples from this study. Solid and open dots represent projections on the upper and lower hemispheres, respectively. LT component directions from a) Gerrei ($D = 359.6°$, $I = 59.7°$, $\alpha_{95} = 10.0°$, $k = 3.8$), b) Nurra ($D = 11.3°$, $I = 39.8°$, $\alpha_{95} = 9.7°$, $k = 4.6$), c) Gallura ($D = 5.2°$, $I = 57.8°$, $\alpha_{95} = 7.2°$, $k = 10.5$).

tectonic correction was applied here. The site mean directions in in situ and bedding corrected coordinates are shown in Fig. 4.7. The Permian site mean direction from northern Sardinia yields a bedding corrected regional mean direction for the area of Dec = $135.0°E$, Inc = $-14.6°$ (N = 9, $\alpha_{95} = 14.0°$, k = 14.4). This is in substantial agreement with the previous results for Gallura (Dec = $142.0°E$, Inc = $-2.0°$ (N = 6, $\alpha_{95} = 12.0°$, k = 34) after Zijderveld *et al.* (1970) and Dec = $145.0°E$, Inc = $0.0°$ (N = 4, $\alpha_{95} = 27.0°$, k = 1) after Westphal *et al.* (1976a)).

Southern Sardinia (Iglesiente/Sulcis and Gerrei/Ogliastra)

A total of 84 samples from 9 sites ranging in age from Early to Middle Permian from southern Sardinia were included in the analysis (Figs. 4.2, 4.3 and Table 4.1). 22 samples from two sites from the Iglesiente/Sulcis and 62 samples from 7 sites from the Gerrei/Ogliastra region yield a bedding corrected mean direction for southern Sardinia of Dec = $81.1°E$, Inc = $7.7°$ (N = 9, $\alpha_{95} = 9.7°$, k = 28.9) (Fig. 4.8). This is in substantial agreement with the previous results for central-eastern Sardinia from our study on Paleozoic dykes on Sardinia of Dec = $91.9°E$, Inc = $-4.8°$ (N = 6, α_{95} = $13.6°$, k = 25.3) (Aubele *et al.*, 2014) and also with results from southeast Sardinia from Edel *et al.* (1981) of Dec = $85.0°E$, Inc = $-7.0°$ (N = 27, $\alpha_{95} = 5.5°$, k = 27) (see Table 4.2).

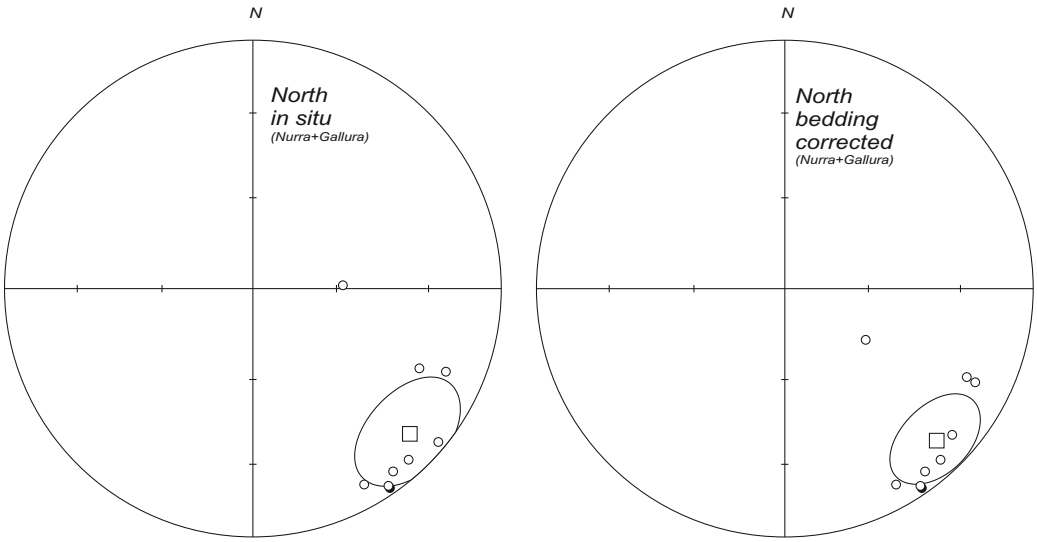

Figure 4.7: Stereographic projections in in situ and bedding corrected coordinates of the Permian characteristic paleomagnetic directions from northern Sardinia. Solid and open dots represent projections on the upper and lower hemispheres, respectively.

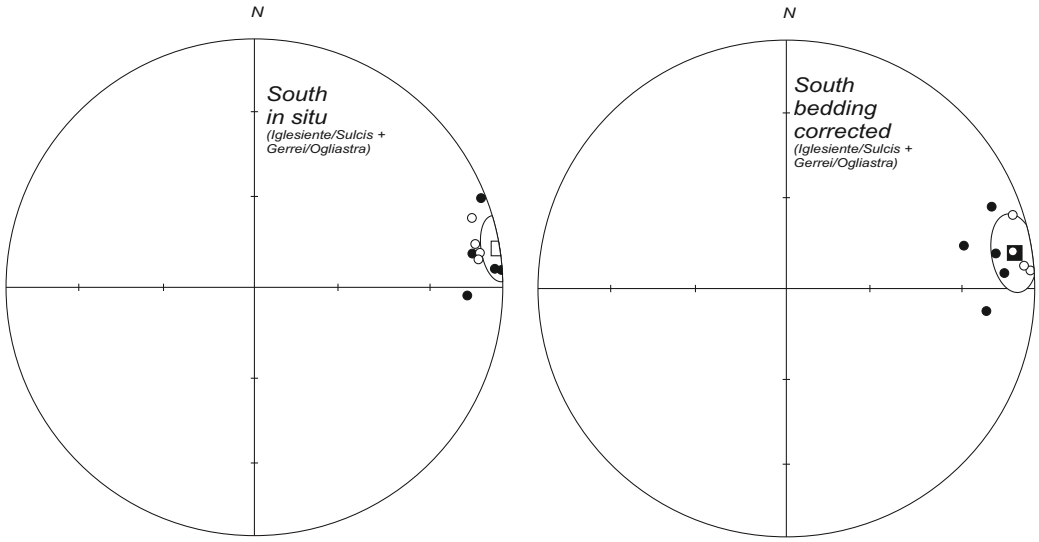

Figure 4.8: Stereographic projections in in situ and bedding corrected coordinates of the characteristic paleomagnetic directions from southern Sardinia. Solid and open dots represent projections on the upper and lower hemispheres, respectively.

Table 4.2: Permo-Triassic pole positions for Corsica-Sardinia from the literature and from the present study rotated to European coordinates, using rotation parameters of Gattacceca *et al.* (2007) (rotation pole coordinates $\lambda = 43.50°$, $\varphi = 9.50°$, angle 45.00° cw) in order to close the Ligurian ocean and Gong *et al.* (2008) (rotation pole coordinates $\lambda = 43.00°$, $\varphi = -2.00°$, angle 35.00° cw) to account for the opening of the Bay of Biscay. All poles are projected to the southern hemisphere. Labels refer to the poles as plotted in Fig. 4.10.

Region	Label	Age mag. (Ma)	Dec/Inc	α_{95}	Paleomagnetic Pole		Reference[1]
					Original	*Rotated*	
Corsica	1	320-250	134.7/-11.3	6.8	36.26°S/70.4°E	46.51°S/44.51°W	1
Sardinia	2	320-250	132.7/-1.6	7.3	31.24°S/68.36°E	43.60°S/38.13°W	1
Nurra	3	296 ± 9	126/-1	n. s.	26.57°S/73.86°E	46.63°S/29.73°W	2
SE Sardinia	5	300-280	85/-7	5.5	1.34°S/75.6°W	51.03°S/33.57°E	2
Nurra	4	Permian (n. s.)	110/-15.5	n. s.	20.0°S/91.0°E	58.24°S/9.2°W	3
Gallura	6	Permian (n. s.)	142.5/-2	11.5	38.0°S/59.0°E	38.8°S/52.8°W	3
Gallura	7	Permian	145.0/0.0	27.0	37.0°S/58.0°E	37.03°S/48.73°W	4
NE Sardinia	n	282 ± 4-268 ± 4	133.1/-1.2	15.0	31.5°S/67.9°E	43.3°S/38.7°W	5
E Sardinia	c	298 ± 5-289 ± 4	91.9/-4.8	13.6	3.0°S/100.1°E	52.7°S/24.0°E	5
SE Sardinia	s	298 ± 5-289 ± 4	80.0/-20.6	24.2	0.9°S/66.0°W	54.9°S/48.2°E	5
N Sardinia	north	295-270	135.0/-14.6	14.0	38.0°S/71.4°E	47.6°S/46.77°W	6
S Sardinia	south	298-290	81.1/7.7	9.7	9.3°S/78.3°W	42.76°S/35.04°E	6

[1] References always refer to the unrotated and unprocessed poles as calculated from the given Dec/Inc and the geographic position of the respective investigated region. 1: Vigliotti *et al.* (1990), 2: Edel *et al.* (1981), 3: Zijderveld *et al.* (1970), 4: Westphal (1976), 5: Aubele *et al.* (2014), 6: This Study. n. s.: not specified.

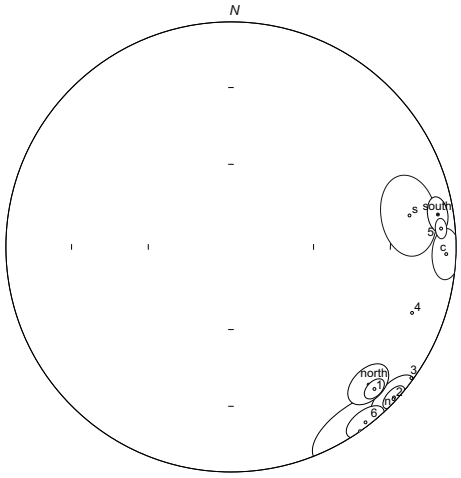

Figure 4.9: Mean paleomagnetic directions from this and other studies from the literature. The labelling follows Table 4.2. Solid and open dots represent projections on the upper and lower hemispheres, respectively.

4.5 Data Interpretation

The ChRM components from this study show shallow (negative and positive) inclinations with easterly and south-easterly declinations. The mean directions from this and other paleomagnetic studies from the Permian and Early Triassic of Sardinia and Corsica as listed in Table 4.2 are shown in Fig. 4.9.

It appears that Permian mean directions from the northern and southern parts of Sardinia from rocks of volcanic and sedimentary provencance cluster in the SE and E of the equal area projection of Fig. 4.9, respectively. The declinations differ by $\sim 45°$, while the differences in inclination are negligible with respect to error limits. The only exception is represented by direction #4 from Zijderveld *et al.* (1970), discussed below.
The paleomagnetic poles form two distinct clusters: the Permian paleomagnetic poles from northern Sardinia lie to the west of the apparent polar wander path of the South Pole of Baltica (Torsvik *et al.*, 2012), whereas the Permian poles from the south of the island cluster to the east of the APWP (Fig. 4.10). The paleomagnetic pole from Permian redbeds in Nurra from Zijderveld *et al.* (1970) (direction and pole with #4 in Table 4.2) plots in agreement with the uppermost Permian/lowermost Triassic poles for Baltica/stable Europe. This pole is only defined by two site mean

directions and thus appears to be of questionable reliability. Furthermore, the age of the pole is given as "Permian" and not further specified by Zijderveld *et al.* (1970). Assuming an uppermost Permian age, relative block rotations can be excluded for at least the Nurra region in post-Permian times on the basis of these data.
The poles from this study as well as the published poles of similar age are strung out along a small circle cutting the 250-290 Ma segment of the South Pole APWP of Baltica, in broad agreement with the mean ages of the sampled rocks (taking into account the inherent uncertainties associated with the different dating techniques as well as potential errors in the Baltica APWP arising from the time-averaging of paleopoles that are not always sufficiently well dated). A single Euler pole of rotation, calculated as the pole to the small circle best fitting the paleomagnetic poles, can account for the differential block rotations observed; this Euler pole lies in Sardinia at Latitude = 40°N, Longitude = 9°E (Fig. 4.10, study area). From this observation, we infer differential true vertical axis rotations between the southern and northern parts of Sardinia during the Early Permian in agreement with earlier studies.

In order to estimate the Permian rotations of northern and southern Sardinia relative to stable Europe, we restored those regions to European coordinates using the rotation parameters of Gattacceca *et al.* (2007) and Gong *et al.* (2008), obtaining a position for a nominal point at the centre of northern Sardinia of Lat = 38.6°N, Long = 4.2°E and for a nominal point at the centre of southern Sardinia of Lat = 37.9°N, Long = 2.8°E. These restored coordinates were then used to calculate the declinations and inclinations expected from the Early Permian paleomagnetic poles of this study, again rotated to European coordinates. The resulting directions are: Dec = 211.9°E, Inc = −14.6° for northern Sardinia and Dec = 156.9°E, Inc = 8.3° for southern Sardinia. The expected directions for the different parts of Sardinia (restored to Europe) calculated from the 270 Ma paleopole of Baltica (Torsvik *et al.*, 2012) are Dec = 195.7°E, Inc = −5.7° for northern and Dec = 194.9°E, Inc = −3.8° for southern Sardinia, which implies differences in declinations of 16.2° for northern and 38.0° for southern Sardinia. Fig. 4.11 shows northern and southern Sardinia in its present outline (a) and restored to the Early Permian paleogeography (b). In the restored configuration, the Early Permian dykes, rotated by 16° cw for northern Sardinia and 38° ccw for southern Sardinia, show a much better alignment which is in agreement with what we observed before (Aubele *et al.*, 2014).

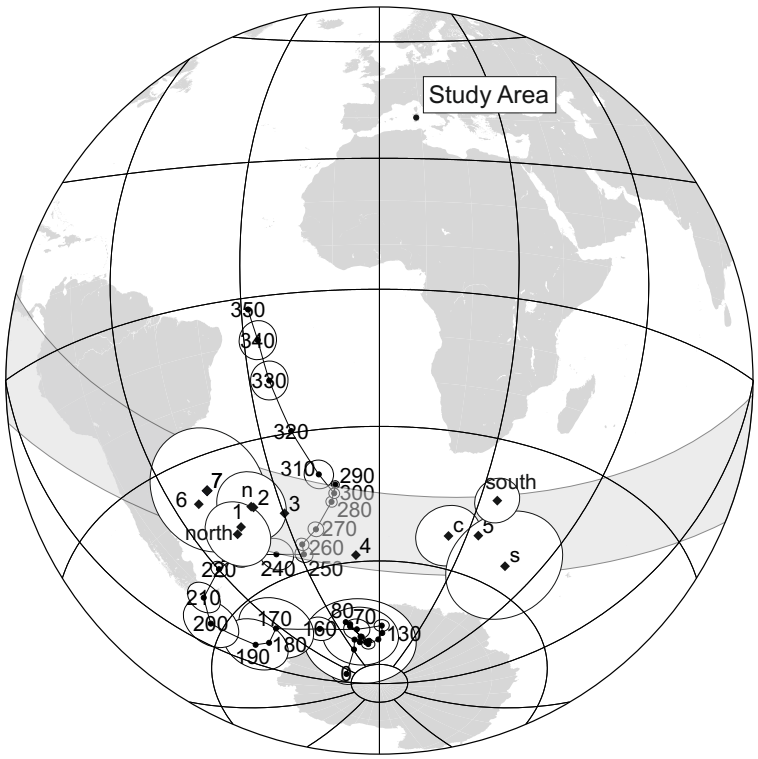

Figure 4.10: Paleomagnetic poles from this study for northern and southern Sardinia in combination with various published poles from different parts of Sardinia. The labelling follows Table 4.2. All poles are shown in European coordinates, i. e. they have been corrected for the opening of the Ligurian Ocean and the Bay of Biscay. These poles plot within a small circle band centered on the 250-290 Ma time window of the Baltica apparent polar wander path of Torsvik *et al.* (2012). The pole of rotation to the small circles (solid polygon) lies within Sardinia (study area), indicating true vertical axis rotations between northern and central–southern Sardinia in Early Permian times.

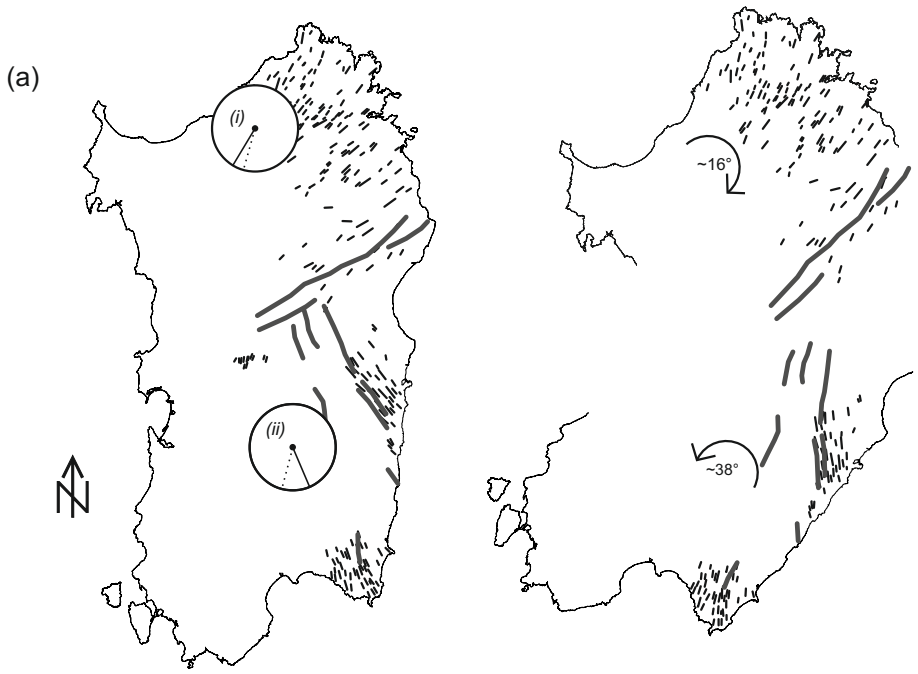

Figure 4.11: (a) Sardinia in its present outline and orientation with the distribution of Early Permian dyke provinces. Stippled: expected Permian declinations for (i) northern Sardinia and (ii) southern Sardinia calculated from the 270Ma pole from the Baltica AWPW of Torsvik *et al.* (2012). Solid: observed magnetic declinations of the Early Permian samples of this study. All declinations are in European coordinates (e. g. corrected for the opening of the Bay of Biscay and of the Liguro-Provençal Basin). (b) Paleogeography of Sardinia restored based on the observed declinations; the arrows indicate the amount and sense of rotation since the magnetization was acquired.

4.6 Conclusions

In conclusion, the results of this study confirm previous results from various regions within Sardinia and obtained from different rock types. The paleomagnetic mean direction from southern Sardinia is virtually identical with the direction from the eastern dyke province from Sardinia (Aubele *et al.*, 2014), which is an independent validation that the dykes were not tilted about horizontal axes. This is a confirmation for the suitability of dykes for paleomagnetic sampling, as long as a reference surface for tectonic correction can be reliably defined. With this study, we substantiate the observation of true vertical axis rotations (clockwise and counterclockwise) within a broad band of crustal segments in the western Mediterranean during Early and Middle Permian times. This observation testifies to general intra-Pangea mobility associated with large-scale shearing between Laurasia and Gondwana. In fact, we can define three crustal blocks within the study areas in the western Mediterranean as indicated in Fig. 4.12. The southern block 1 rotated counterclockwise with respect to stable Europe and the adjacent blocks after magnetization of the sampled rocks in the Early Permian. The middle block 2 on the other hand shows a slight clockwise rotation with respect to stable Europe and block 1 after magnetization of the sampled rocks in the Early Permian. Early Permian results from the northern block 3 show a large clockwise rotation with respect to stable Europe as well as blocks 1 and 2. We conclude in favour of a decreasing N-S gradient (in Late Paleozoic/Early Mesozoic coordinates) in rotation rates towards the south and away from the northern boundary of the large-scale transform fault zone. The counterclockwise rotation of block 1 nicely confirms the ball bearing model that we recently proposed (Aubele *et al.*, 2012), which leads to clockwise and counterclockwise rotations of blocks of different aspect ratios caught within large-scale transform fault zones.

We know from earlier studies (Advokaat, 2011; Kirscher *et al.*, 2011; Aubele *et al.*, 2012) that the western Mediterranean area - namely the Maures-Esterél Massif, the Toulon-Cuers Basin, Corsica and Sardinia - acted as a single tectonic block from at least 260 ± 10 Ma until the Cenozoic counterclockwise rotation of Corsica-Sardinia away from the European mainland. Including the questionable paleomagnetic pole from Zijderveld *et al.* (1970) for the Nurra region (Sardinia), the upper age constraint of the observed rotations can be put in the uppermost Permian ($\sim$ 260 Ma). This upper time limit for transform fault activity between Laurasia and Gondwana is perfectly reconcilable with paleogeographic reconstructions based on paleomagnetic data for the Late Permian, which allow a Pangea A configuration

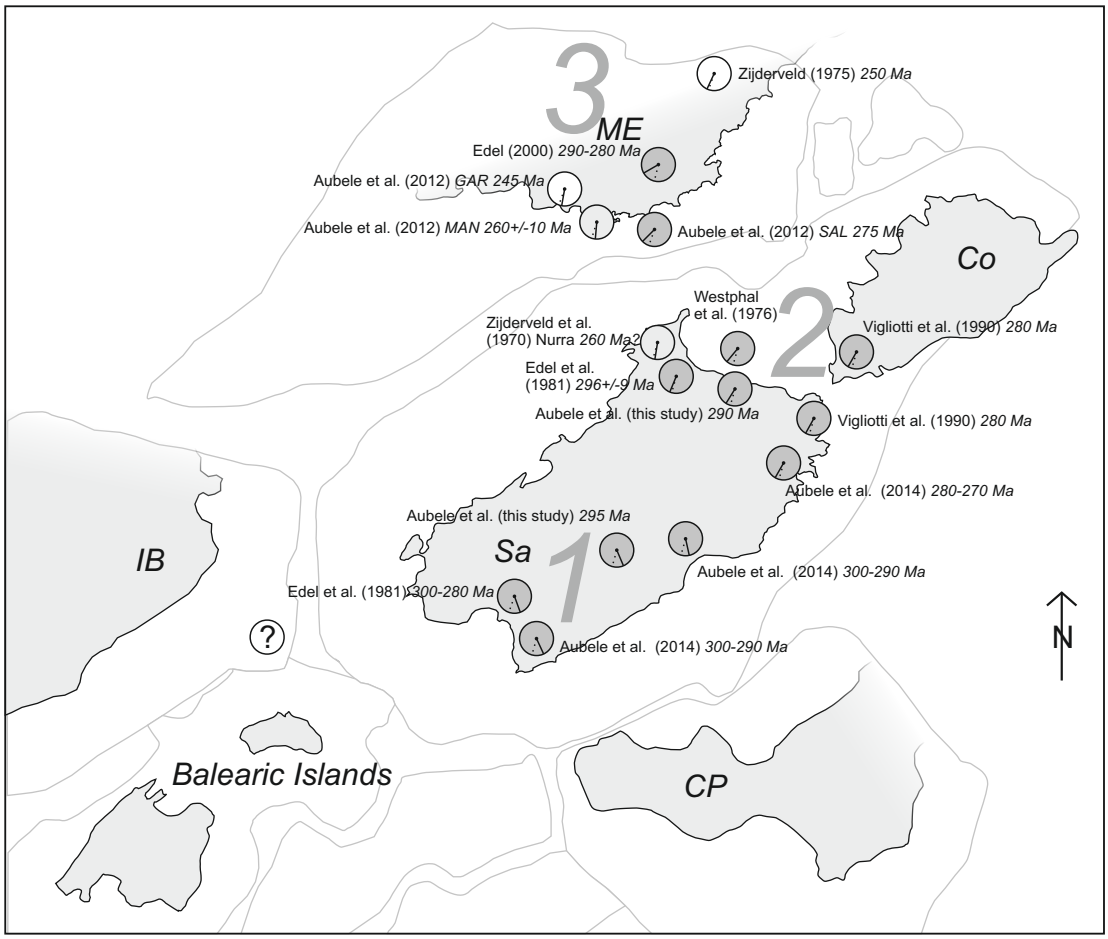

Figure 4.12: Late Paleozoic to Early Mesozoic reconstruction of Maures-Estérel (ME), Corsica (Co), Sardinia (Sa), Iberia (IB), the Balearic islands and the Calabria-Peloritani terrane (CP). Circular diagrams display observed (solid lines) and expected (stippled lines) declinations from the studies presented here and from the literature (Zijderveld *et al.*, 1970; Zijderveld, 1975; Westphal, 1976; Edel *et al.*, 1981; Vigliotti *et al.*, 1990; Edel, 2000; Aubele *et al.*, 2012, 2014). All declinations are given in European coordinates, i. e. we used the parameters of Gattacceca *et al.* (2007) (rotation pole coordinates $\lambda = 43.50°$, $\varphi = 9.50°$, angle 45.00° cw) in order to close the Ligurian ocean and Gong *et al.* (2008) (rotation pole coordinates $\lambda = 43.00°$, $\varphi = -2.00°$, angle 35.00° cw) to account for the opening of the Bay of Biscay.

(Muttoni *et al.*, 2003; Domeier *et al.*, 2011b).

4.7 Acknowledgments

This project has been funded by the German Science Foundation (DFG) Grants BA 1210/8–1 and BA 1210/20–1. Special thanks goes to Barbara Emmer and Elmar Moser for help in the field campaign of 2004 and to Matthias Hackl for assistance in the field in 2011.

5

Paleomagnetism of Jurassic Carbonate Rocks from Sardinia - No Indication of Post Jurassic Internal Block Rotations

By ***U. Kirscher, K. Aubele, G. Muttoni, A. Ronchi and V. Bachtadse*** *published in* Journal of Geophysical Research Solid Earth, *2011,* ***116*** *(B12), 1978-2012, doi:10.1029/2011JB008422.*

5 PALEOMAGNETISM OF JURASSIC CARBONATE ROCKS FROM SARDINIA - NO INDICATION OF POST JURASSIC INTERNAL BLOCK ROTATIONS

Abstract

Several paleomagnetic studies on Carboniferous and Permian sedimentary and volcanic rocks from Sardinia and Corsica have recently demonstrated (I) the tectonic coherence between southern Corsica and northern Sardinia and (II) significant rotations between individual crustal blocks within Sardinia itself. The geodynamic significance of these rotations, however, is not clearly understood mainly because of uncertainties in defining their timing and causes. In order to contribute to these issues, a pioneering paleomagnetic study on Jurassic carbonates from the Baronie-Supramonte region of eastern-central Sardinia has been extended regionally and stratigraphically. A total of 280 oriented drill cores were taken from 44 sites of Middle and Late Jurassic age in the Nurra, Baronie-Supramonte, Barbagia-Sarcidano and Sulcis regions. Despite generally weak remanent magnetization intensities, on the order of less than 1mA/m, thermal and alternating field demagnetizations were successfully applied to define a characteristic remanent magnetization component in about 60% of the samples.

Site mean directions show rather good agreement after correction for bedding tilt, and yield Middle and Late Jurassic overall mean directions of $D = 269.7°$ and $I = 45.0°$ ($\alpha_{95} = 8.0°$, $k = 14$, $n = 25$ sites) and $D = 275.5°$ and $I = 50.7°$ ($\alpha_{95} = 7.2°$, $k = 45.3$, $n = 10$ sites), respectively. Positive regional and local fold and reversal tests demonstrate the primary character of the natural magnetic remanence, which is carried by magnetite. These results indicate only insignificant amounts ($\pm 10°$) of post-Jurassic rotations within the island of Sardinia. The resulting Middle and Late Jurassic paleopoles ($Lat = 16.5°$, $Long = 299.1°$, $dp = 6.4°$, $dm = 10.1°$ and $Lat = 23.4°$, $Long = 301.2°$, $dp = 6.5°$, $dm = 9.7°$), corrected for the opening of (1) the the Liguro-Provençal Basin and (2) the Bay of Biscay using rotation parameters from the literature fall near the coeval segment of the European apparent polar wander path.

These results constrain the timing of large differential block-rotations found in Late Carboniferous- Permian rocks to a pre Middle- Jurassic age, and lead to exclude tectonics related to the Alpine orogeny for such rotations.

5.1 Introduction

The Paleozoic to Cenozoic tectonic and geodynamic evolution of Sardinia has been studied since the early 1970's. Plate tectonic models based on geologic evidence have been used to relate the counterclockwise rotation of the Sardinia block with respect

to Europe north of the Pyrenees, to the opening of the Bay of Biscay (Van der Voo, 1969; Cohen, 1981; Olivet, 1996) during the Aptian (Gong *et al.*, 2008), whereas a wealth of paleomagnetic, radiometric, and marine geophysical data revealed the subsequent counterclockwise rotation of the Sardinia and Corsica blocks during the opening of the Liguro-Provençal Basin in the Miocene (Alvarez *et al.*, 1973; de Jong *et al.*, 1973; Manzoni, 1975; Cohen, 1981; Montigny *et al.*, 1981; Vigliotti *et al.*, 1990; Ferrandini *et al.*, 2003). Paleomagnetic data from Permian and Carboniferous rocks of Sardinia (Zijderveld *et al.*, 1970; Edel *et al.*, 1981; Edel, 2000; Moser *et al.*, 2005; Emmer *et al.*, 2005) (and references therein) revealed the existence of a complex tectonic history characterized by large scale differential block rotations between individual basins. The origin and geodynamic significance of these differential block rotations observed in Permian rocks of Sardinia are not clearly understood nor is their timing accurately constrained. These rotations may have originated as a consequence of (I) transpressive dextral wrenching related to the late Variscan orogeny (Edel, 2000), (II) Late Paleozoic post-Variscan shearing between Laurasia and Gondwana (Arthaud and Matte, 1977) possibly related to the Pangea B to Pangea A transformation (see section 5.5 and references in (Muttoni *et al.*, 2003)), (III) extensional tectonics that characterized the European passive margin during Early and Middle Jurassic times (Zattin *et al.*, 2008), (IV) subduction rollback tectonics in the Tyrrhenian Sea since Oligocene times (Helbing *et al.*, 2006b), or (V) Cenozoic transcurrent tectonics (Carmignani *et al.*, 1992; Pasci *et al.*, 1998; Oggiano *et al.*, 2009; Faccenna *et al.*, 2002; Dieni *et al.*, 2008). In order to discern whether these block rotations are Permian features within a dynamic Pangea or are linked to subsequent geodynamic events, a detailed paleomagnetic study has been carried out on well-dated Jurassic sediments from four areas of Sardinia (Nurra, Baronie, Barbagia-Sarcidano, and Sulcis; Fig. 5.1). This study complements the previous results obtained in the Baronie-Supramonte region by Horner and Lowrie (1981).

5.2 Local geological setting and sampling

The geological record of Sardinia during the Late Carboniferous to Permian is characterized by the emplacement of granitic batholiths, the effusion of volcanic rocks of intermediate geochemistry, as well as the deposition of continental sediments of variable composition (e.g., Cortesogno *et al.* (1998); Cassinis *et al.* (2000); Ronchi *et al.* (2008); Rossi *et al.* (2009)). Marine sedimentation started in the Middle Triassic with the deposition of Muschelkalk-type limestones (Posenato *et al.*, 2002) and

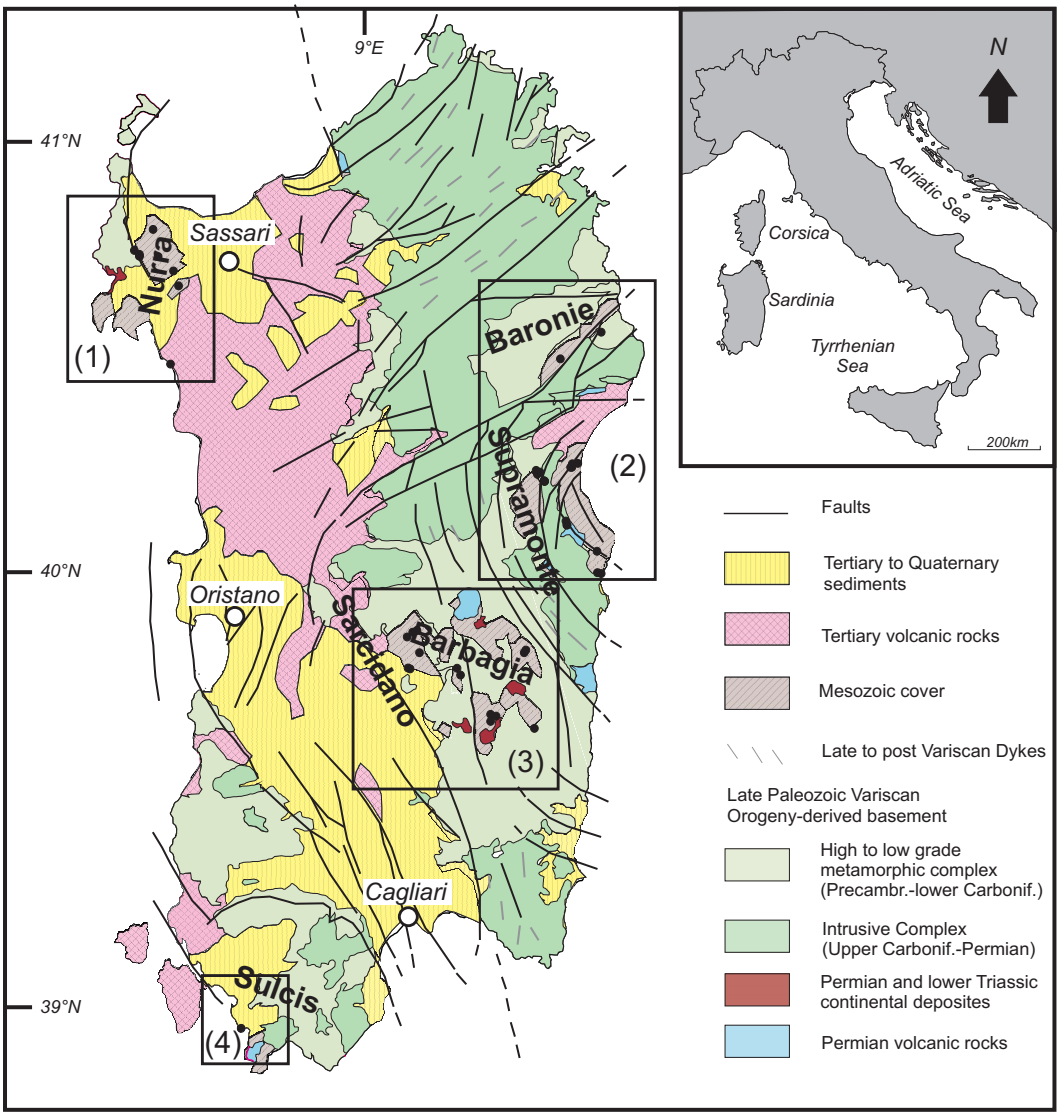

Figure 5.1: Simplified geological sketch map of Sardinia with major faults and dykes (modified after Cherchi *et al.* (2010)). The four black boxes indicate the study areas: (1) Nurra, (2) Supramonte (Gulf of Orosei) and Monte Albo (Baronie), (3) Barbagia-Sarcidano, (4) Sulcis. Small black dots represent sampling sites.

ensued during the Jurassic with various sedimentary units outcropping in the Nurra, Baronie-Supramonte, Barbagia-Sarcidano, and Sulcis areas (Fig. 5.1) (Cherchi *et al.*, 2010; Jadoul *et al.*, 2010; Dieni and Massari, 1986; Dieni *et al.*, 1983; Costamagna, 2000). In the North-Western basin (Nurra), Jurassic sedimentation started with $\sim$ 50m of oolitic and bioclastic limestones with at the top reddish sandstones with fossiliferous calcarenites of Early Jurassic age (Unit1 after Cherchi *et al.* (2010)), followed by 400–575m of Middle Jurassic oolithic and marly carbonates (Unit2-11 after Cherchi *et al.* (2010)). The Upper Jurassic part of the sequence is comprised of 250–300m of neritic carbonates and micritic limestones extending up to the Cretaceous (Unit12+13 after Cherchi *et al.* (2010)).
In the central (Barbagia and Sarcidano) and eastern (Gulf of Orosei) basins, the Variscan basement is disconformably overlain by the Bajocian–Bathonian conglomerates and sandstone of the Genna Selole Formation (Dieni *et al.*, 1983), followed by several hundred meters of Bathonian–Kimmeridgian dolostones and limestones of the Dorgali, Genna Silana, and S'Adde Formations, followed at the top by the Tithonian–Berriasian limestones of the Monte Bardia Formation (Fig. 5.2) (Costamagna and Barca, 2004; Costamagna *et al.*, 2007; Jadoul *et al.*, 2010).

The southwestern basin (Sulcis) is characterized by two sedimentary sequences of Mesozoic age (Barca and Costamagna, 1997). The Cala Su Trigu Unit is composed of dolomites and marls with a thickness of $\sim$ 120m, indicating deposition in carbonate platform settings. The Guardia Sa Perda Unit, with a total thickness of $\sim 300 - 350$m, consists of limestones (Punta Tonnara Formation), dolomites (Monte Zari Formation) and marly limestones (Guardia Sa Barracca Formation). They document an evolution from carbonate platform conditions to an environment of middle to outer carbonate shelf (Fig. 5.2).
In this paper, we present paleomagnetic data from Middle and Late Jurassic sediments from all of the four Jurassic outcrop areas of Sardinia (Fig. 5.1 and Tab. 5.1).

5.3 Field and Laboratory Methods

Paleomagnetic cores were taken in the field using a portable gasoline powered drill and oriented using a standard magnetic compass.
All samples were studied in the paleomagnetic laboratory of the University of Munich. Standard $\sim$ 10cc cylindrical cores were stepwise demagnetized using thermal (TH) or Alternating Field (AF) techniques. For TH and AF demagnetization, a Schoenstedt oven and a 2G Enterprises AF device were used, respectively. The

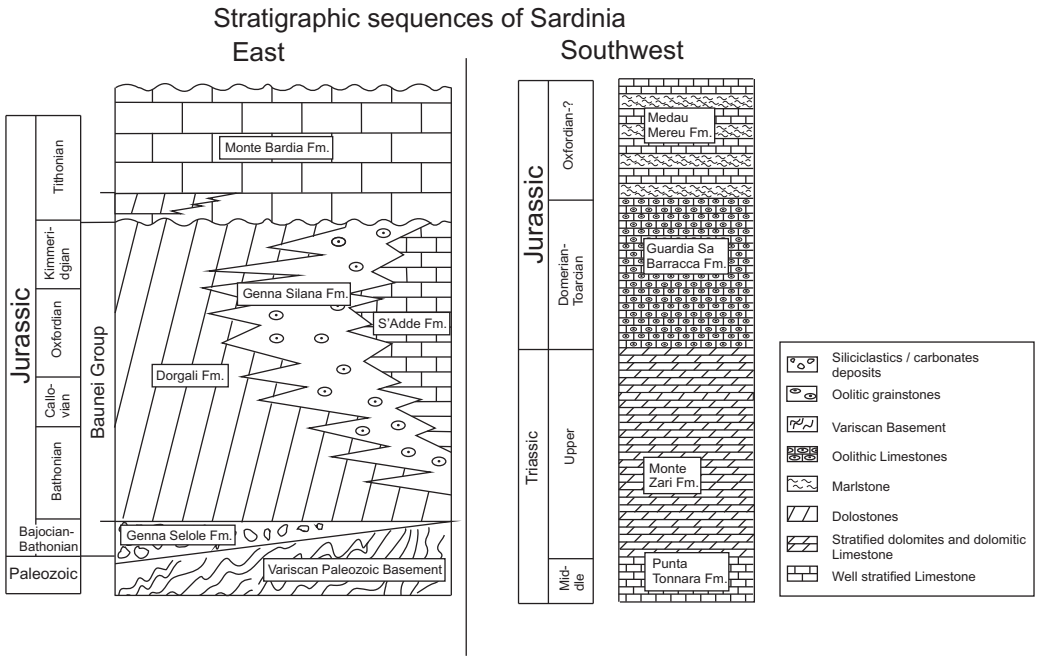

Figure 5.2: Stratigraphic sections of the Jurassic of Central/Eastern and Southwestern Sardinia, modified after Costamagna *et al.* (2007); Barca and Costamagna (1997).

Table 5.1: Geographic location of sampling sites.

Site	Lat. [°N]	Long. [°E]	Site	Lat. [°N]	Long. [°E]	Site	Lat. [°N]	Long. [°E]
Nurra Region			OLI2	40.13081	9.58188	TIS3	40.23021	9.51227
OLM	40.67522	8.39143	OLI3	40.13977	9.57725	Barbagia and Sarcidano		
CAS	40.70938	8.37628	ULA1	39.83755	9.44949	BSM1	39.80065	9.10017
CAM	40.74210	8.32900	ULA2	39.84388	9.45470	CAN1	39.87437	9.09104
CCU1	40.75512	8.25665	ULA2	39.84388	9.45470	CAN2	39.88484	9.10814
CCU2	40.74224	8.27200	RIF1	40.07037	9.67221	CAN3	39.88891	9.12213
CCU3	40.74307	8.27193	CAL	40.27126	9.61375	MSA1	39.68027	9.34734
CCU4	40.80273	8.31397	BAU1	40.02197	9.67358	MSA2	39.69184	9.36326
GRI	40.49788	8.36782	BAU2	40.01940	9.68568	MSA3	39.69615	9.34747
Sulcis			BUE1	40.26205	9.59512	PER1	39.66186	9.41847
MSP	38.99334	8.57973	BUE2	40.27052	9.59682	PER2	39.66449	9.48054
Baronie			OHE	40.25556	9.48653	VNT	39.83845	9.12923
SIN	40.57006	9.68499	GOR1	40.25151	9.49765	SUL	39.80268	9.09363
LUL	40.50956	9.55992	GOR2	40.24687	9.49020	SAD	39.80359	9.26015
Supramonte			TIS1	40.23105	9.50923			
OLI1	40.13044	9.57942	TIS2	40.23157	9.51057			

magnetization was measured with a 2G Enterprises cryogenic SQUID (Superconducting QUantum Interference Device) magnetometer in a magnetically shielded room. Isothermal remanent magnetizations (IRM) were imparted with a Magnetic Measurements Pulse Magnetizer (MMPM) with peak fields of 2.3T. Hysteresis parameters were determined using a Variable Field Translation Balance (VFTB, Krása *et al.* (2007)).
Demagnetization results were plotted on orthogonal vector diagrams (Zijderveld, 1967) and analyzed using the least square method (Kirschvink, 1980) on linear portions of the demagnetization paths defined by at least four consecutive demagnetization steps. The linear fits were anchored to the origin of the demagnetization axes where appropriate.
Only occasionally the combined use of demagnetization great-circles and endpoint data (McFadden and McElhinny, 1988) was used to retrieve component directions with overlapping coercivity spectra.
Pilot studies demonstrate the superiority of TH on AF-demagnetization, and thus the vast majority of the specimens was thermally demagnetized using increments of 30°C in a temperature range from 100°C up to a maximum of 600°C.

5.4 Results

5.4.1 Rock magnetic results

Rock magnetic measurements were performed on representative samples of the different sampled rock types. Due to the overall weakness of the magnetic signal, VFTB experiments turned out to be extremely difficult to perform. However, using also information from IRM acquisition curves, an adequate description of the magnetic carriers of the samples was possible to achieve.
The data were corrected for diamagnetic and/or paramagnetic contributions. In general, the hysteresis loops as well as the thermomagnetic curves show the presence of at least two different magnetic phases with both varying coercivity spectra and Curie temperatures (Fig. 5.3). Important results of these measurements are (1) the presence of a high coercivity mineral, (2) Curie temperatures in the range of 100 to 150°C (goethite) and (3) at $\sim 550 - 580°$ (magnetite), (4) a hump in the thermomagnetic curves (compare (c) and (d) in Figure 5.3) starting at ~ 420°C with a maximum at ~ 520°C, and (5) an occasional decrease of intensity at ~ 650°C (Fig. 5.3). The latter can only be observed during 'in-field' heating experiments on the VFTB and is attributed to mineralogical alterations during heating such as forma-

tion of secondary magnetite from a ferric sulfate phases, which is also indicated by the sharp increase of intensity after cooling to room temperature ((d) in Figure 5.3).

5.4.2 Paleomagnetic results

Detailed thermal demagnetization experiments show the presence of two different magnetic components with overlapping unblocking temperature spectra, indicated by the curved shape of some orthogonal vector diagrams (Fig. 5.4). An initial low temperature component (LTC) with high intensity values and generally aligned along the present-day field (in *in situ* coordinates) was removed at low demagnetization temperatures between 100°C up to ∼ 210°C. Eleven sites are characterized by the sole presence of the LT component pointing towards the origin of the projection. The resulting *in situ* LTC site-mean directions are in agreement within error with the present-day field direction for a reference site in central Sardinia, and were therefore excluded from further analysis as they are considered to represent a recent overprint. A high temperature characteristic component (HTC) of dual polarity broadly oriented to the west and up or east and down in tilt corrected coordinates was identified as linear segments from ∼ 240°C up to ∼ 600°C in 33 sites. Some ∼ 50% of the samples display unblocking temperatures, which are in a temperature range from 520 to 580°C and are clearly indicative for magnetite. The remaining samples lost all the detectable remanent magnetization at ∼ 450°C, which might be caused by a contamination of the magnetite phase. Samples with different unblocking temperatures, however, do not show different magnetization directions of the HTC (compare (e) and (f) in Figure 5.4). AF demagnetization was usually not effective in isolating the magnetic components observed during thermal demagnetization experiments. Only occasionally, AF and TH demagnetization experiments yielded comparable results (Fig. 5.4).

Nurra Region

Jurassic rocks of the Nurra region in the northwestern part of Sardinia ((1) in Fig. 5.1) were sampled at eight sites (mostly in the area of Mt. Alvaro-Mt. Nurra, Tab. 5.1). A single site (CCU1) of Early Jurassic age (Unit 2 of Cherchi *et al.* (2010); (Fig. 5.5)) did not yield reliable demagnetization results. Four out of a total of six sites of Middle Jurassic age (Units 3-5, 8 and 11 of Cherchi *et al.* (2010); Fig. 5.5), and one site (OLM) of Late Jurassic age (Unit 13 of Cherchi *et al.* (2010); Fig. 5.5), are characterized by weak but stable HT component directions (Tab. 5.2).
Basically, only two of these sites (OLM, GRI) show statistically reliable results including demagnetization data of more than two samples. The additional three sites

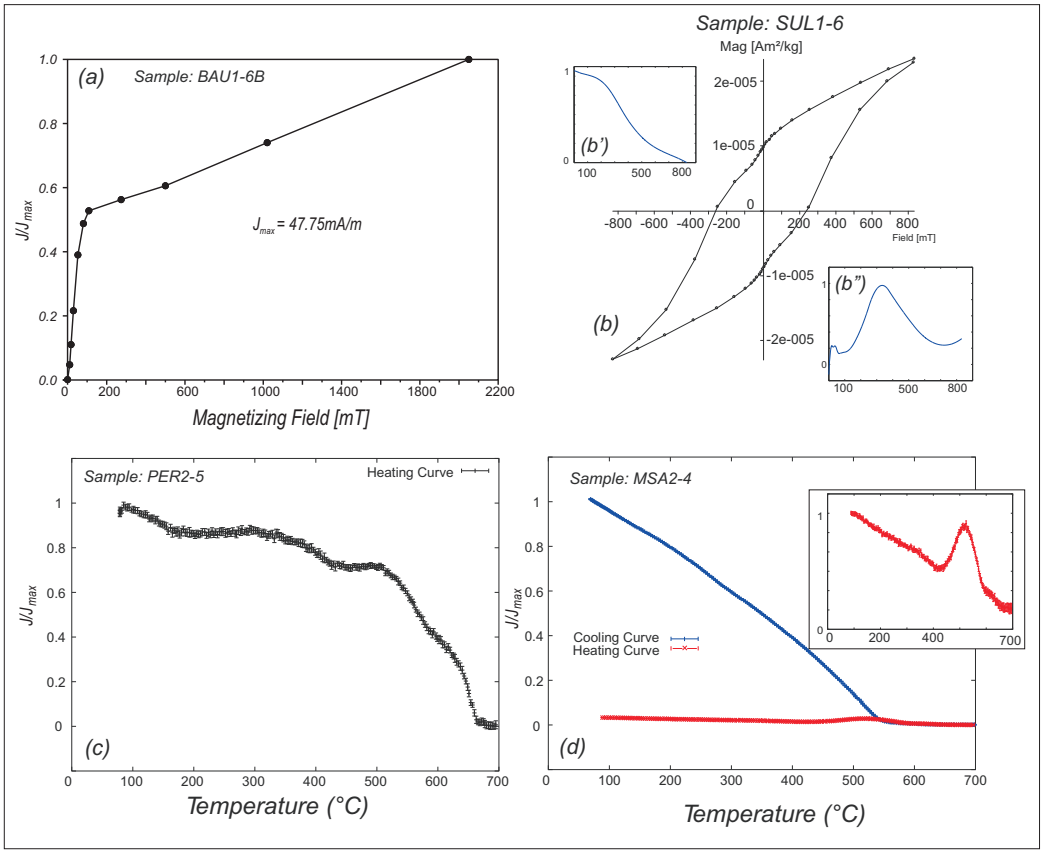

Figure 5.3: Rock magnetic analysis of representative samples. (a) IRM acquisition curve, (b) Hysteresis loop, measured after heating to 150°C. Also shown are the difference of the descending and ascending branches of the hysteresis loop for positive field values (b'), and the first derivative of the latter (b"), (c) and (d) Thermomagnetic curves. At (d) both heating and subsequent cooling curves are shown; inset: only normalized heating curve is shown with same axis.

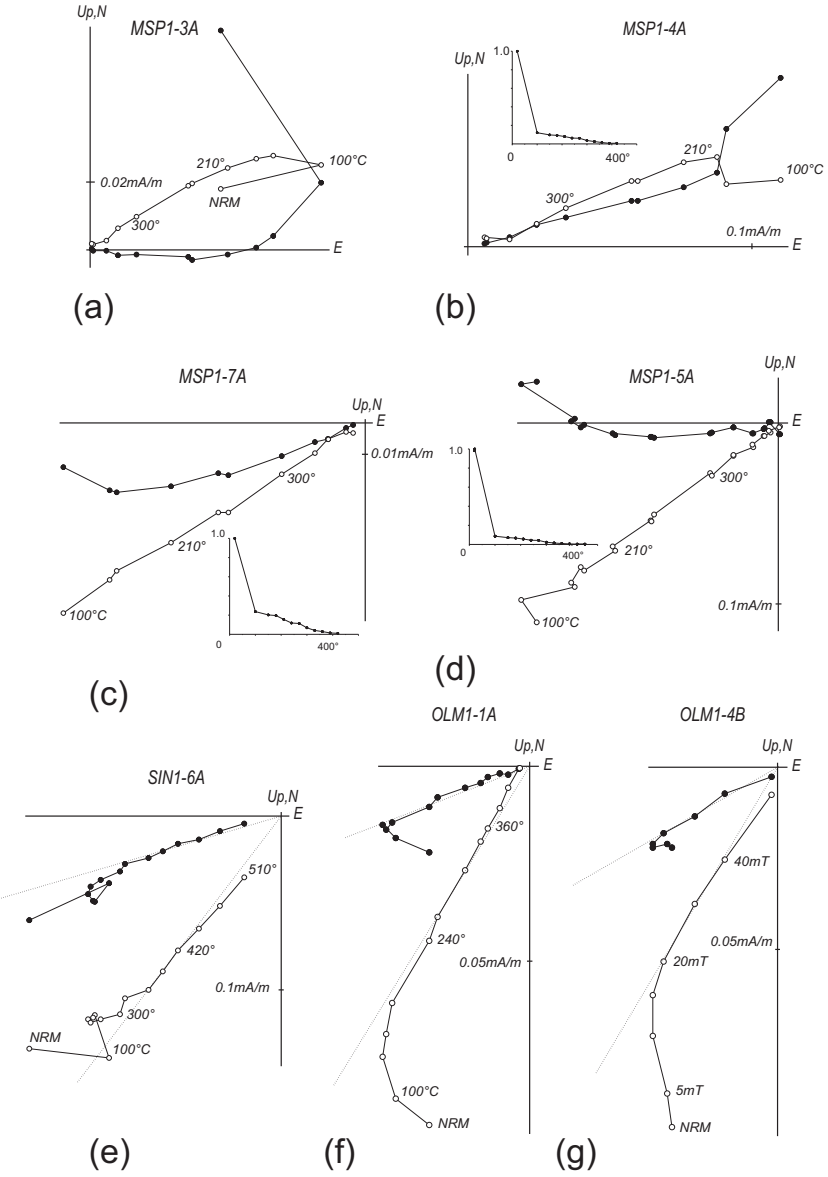

Figure 5.4: Results of thermal (a)-(f) and alternating field (g) demagnetization experiments plotted as orthogonal vector diagrams (Zijderveld, 1967) in stratigraphic coordinates using the paleomagnetic software of Wack (2010). Full (open) dots represent vector endpoints projected onto the horizontal (vertical) plane. (b)-(d): For clarity, high NRM values due to strong viscous component are not plotted.

Table 5.2: Paleomagnetic directions from Jurassic sediments of the Nurra Region.

Site	Age	N	P	In situ				Bedding-corrected			
				$D[^\circ]$	$I[^\circ]$	k	α_{95} $[^\circ]$	$D[^\circ]$	$I[^\circ]$	k	α_{95} $[^\circ]$
OLM	L	5/9	N	286.6	50.9	169.7	5.9	243.4	58.3	196.7	5.9
CAS[a]	M	1/7	N	7.2	60.1			18.1	29.7		
CAM	M	2/6	M	280.3	39.4	658.6	9.7	259.9	57.6	658.5	9.7
CAM[a]	M	2/6	N	334.4	38.1			351.8	56.6		
CCU1[a]	E	3/6	N	347.0	51.8	19.7	47.7	9.9	62.8	19.7	47.7
CCU2[a]	M	3/5	N	15.0	62.5	1513.1	17.1	328.9	76.3	1507.7	17.1
CCU3	M	1/7	N	261.2	55.3			245.5	63.0		
CCU4	M	2/3	N	258.6	16.5			247.9	24.3		
GRI	M	5/10	N	288.4	50.2	263.5	4.7	278.0	25.3	263.5	4.7

Site: sampling sites, Age: E for Early, M for Middle and L for Late Jurassic. N: number of samples used for calculating site mean directions/number of measured samples. P: magnetic polarity; N = normal, M = mixed. Declination (D) and Inclination (I) in degrees, Fisher precision parameter k (Fisher, 1953), Fisher circle of 95% confidence (α_{95}) in geographic (*in situ*) and bedding corrected (TC) coordinates, respectively.
([a]) well defined paleomagnetic directions with values in geographic coordinates close to the present day field direction.

of Middle Jurassic age (CAM, CCU3, CCU4) are based on only one or two samples, which show reliable demagnetization behaviour. However, their results were included in the calculation of the mean directions only because of their broad coherence with the two trustable sites and because of the good quality of these individual samples. Because of homogeneous bedding attitudes, no fold test was possible to perform. However, one site where normal and reversed polarities of magnetization were observed, (CAM, Unit 3, Fig. 5.5) passes the reversal test, classified as C according to the criteria of McFadden and McElhinny (1990), whereas the other sites show only normal polarity characteristic components.
The mean direction for rocks of Middle Jurassic age in the area is $D = 259.4^\circ$, $I = 43.4^\circ$, $\alpha_{95} = 27.7$, $k = 12.0$, $n = 4$ sites (Tabs. 5.1, 5.2), for sites of Late Jurassic age in the area the mean direction is $D = 243.4^\circ$, $I = 58.3^\circ$, $\alpha_{95} = 14.5$, $k = 29.0$, $N = 5$ samples (Tabs. 5.1, 5.2).

Supramonte (Gulf of Orosei) and Baronie (Monte Albo)

In the Orosei Gulf area of Supramonte ((2) in Fig. 5.1), two parallel and continuous mountain ridges, composed of carbonates mostly of Jurassic age, extend from north to south exhibiting an overall curvature with radius on the order of $\sim 30km$ and convexity facing the Tyrrhenian sea in the East. Thirteen of the nineteen sites sampled in the Dorgali and S'Adde Formations of the Supramonte show the presence of a dual polarity characteristic HT component. To the North of the Supramonte area, starting from the town of Siniscola, another ridge of Jurassic rocks (Mt. Albo) extends $\sim 20km$ in a southwestward direction. Only two sites were accessible for sampling in this area. Site SIN in the S'Adde Formation yielded characteristic HTC directions. Site LUL consisting of sandy carbonates of the Dorgali Formation (Bathonian after Jadoul *et al.* (2010) or Bathonian–Kimmeridgian after Costamagna *et al.* (2007)) is

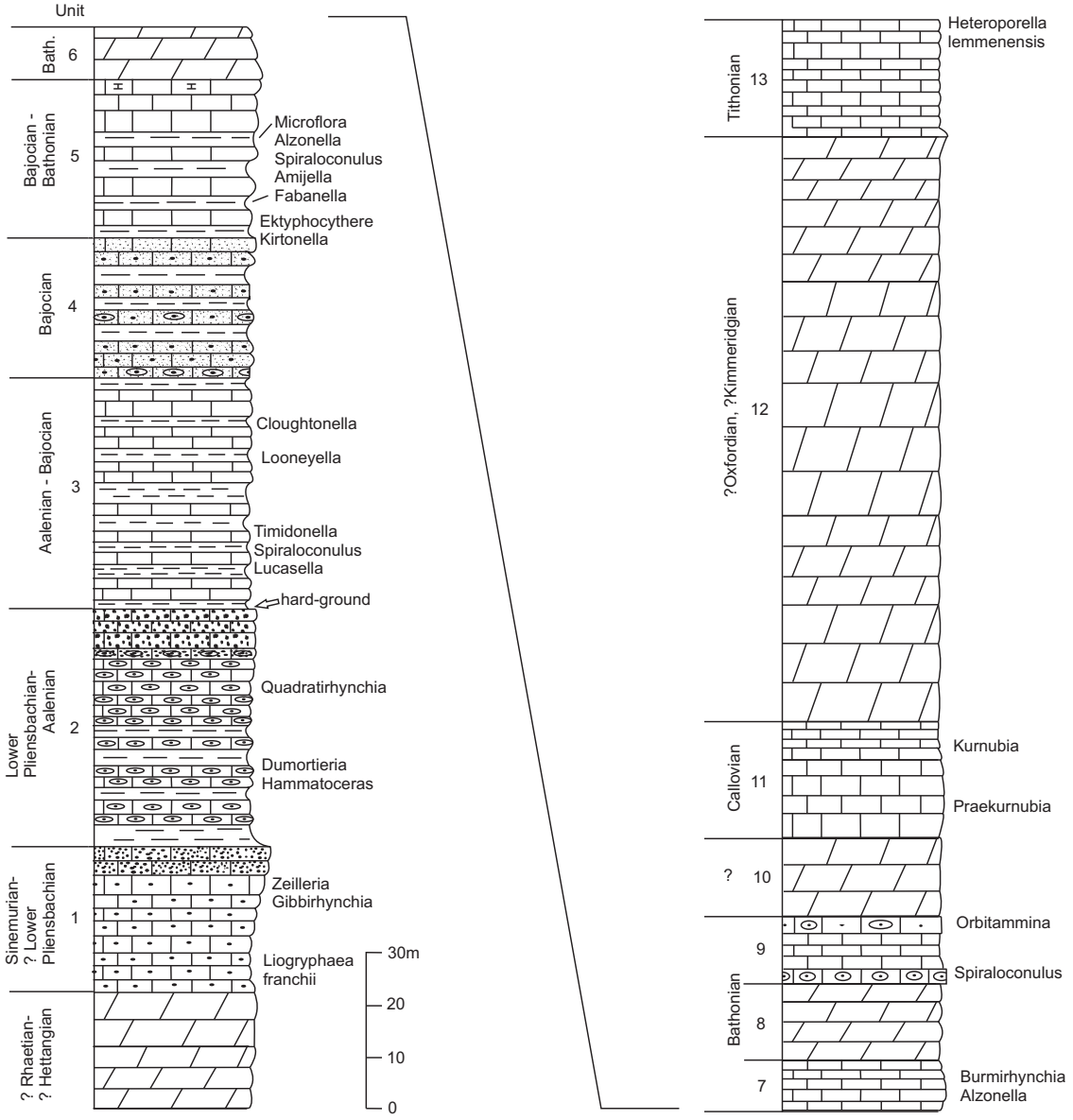

Figure 5.5: Synthetic stratigraphic section of the Jurassic of the Nurra region (NW Sardinia), modified after Cherchi *et al.* (2010); numbered units explained therein.

Table 5.3: Paleomagnetic directions from Jurassic sediments from the Gulf of Orosei.

Site	Age	N	P	In situ				Bedding-corrected			
				$D[^\circ]$	$I[^\circ]$	k	α_{95} $[^\circ]$	$D[^\circ]$	$I[^\circ]$	k	α_{95} $[^\circ]$
Baronie and Supramonte											
OLI1	M	2/5	N	267.7	11.2	16.5	14.1	279.2	34.9	16.5	14.1
OLI2*	M	3/6	M	111.1	-16.6	12.6	12.7	124.7	-26.7	12.6	12.7
OLI3	M	4/8	N	277.4	37.2	13.9	19.3	279.0	52.1	13.9	19.3
ULA1[b]	M	3/8	M	249.2	40.5	22.0	16.6	249.2	40.5	22.0	16.6
ULA2	M	6/7	M	93.2	-46.0	140.4	5.8	94.6	-49.8	140.4	5.8
URZ	L	3/6	N	279.6	30.1	5.6	42.8	278.0	39.9	22.0	27.0
RIF[b]	L	7/7	M	259.3	47.3	9.4	16.0	276.2	51.8	9.4	16.0
CAL	L	5/6	M	287.5	14.9	20.8	14.9	285.7	46.8	20.8	14.9
BAU1[a]	M	4/7	N	352.9	56.7	34.5	15.9	351.9	46.5	35.0	15.8
BAU2	M	5/8	N	280.4	46.7	11.7	24.0	294.3	59.8	11.8	11.8
BUE1[a]	M	6/9	N	332.7	31.0	45.0	10.3	319.7	-10.6	37.6	11.3
BUE2	M	7/23	M	113.0	-24.2	40.1	14.8	113.1	-20.1	40.1	14.8
BUE2[a]	M	13/23	N	352.2	52.2	18.3	10.1	48.8	50.3	17.1	10.5
OHE[a]	M	3/5	N	331.5	55.6	46.6	18.3	9.1	61.1	46.6	18.3
GOR1	L	3/5	N	215.7	57.4	21.4	27.3	268.8	38.2	21.8	21.8
GOR2	L	1/3	N	259.0	32.4			277.7	56.5		
GOR2[a]	L	2/3	N	4.8	57.7	589.5	10.3	23.1	32.9	589.5	10.3
TIS1	L	2/4	N	292.7	19.9	59.0	33.1	302.3	43.8	59.0	20.0
TIS2	L	7/8	N	271.2	32.8	50.1	8.6	282.1	55.3	65.8	7.5
TIS3	L	5/8	N	268.7	20.4	77.9	8.7	268.0	51.4	77.9	8.7
SIN	L	5/7	N	269.6	45.4	55.7	10.3	262.4	55.9	49.6	11.0
LUL	M	2/6	N	270.4	12.9	1061.8	171.9	265.4	31.5		
LUL[a]	M	2/6	N	339.7	44.1	24.2	53.2	1.2	58.5	24.2	53.2

Site: sampling sites, Age: M for Middle, L for Late Jurassic. N: number of samples used for calculating site mean directions/number of measured samples. P: magnetic polarity; N = normal, M = mixed. Declination (D) and Inclination (I) in degrees, Fisher precision parameter k (Fisher, 1953), Fisher circle of 95% confidence (α_{95}) in geographic (*in situ*) and bedding corrected coordinates, respectively. ([a]) well defined paleomagnetic directions with values in geographic coordinates in vicinity to the present day field, supposing an overprint of the magnetic signal. ([b]) paleomagnetic mean direction calculated by combining linear trajectories of demagnetization paths with remagnetization circles, using the technique of McFadden and McElhinny (1988). (*) biased direction of Jurassic mean (this study) with component of present day field direction of the study area.

characterized by very weak magnetizations; two samples from this site yielded stable component directions oriented along the present day field in *in situ* coordinates, whereas two other samples treated with the great circle analysis (McFadden and McElhinny, 1988) yield an intersection close to the HTC site mean direction of site SIN. In summary, sites from Supramonte and Baronie show similar HTC directions (Tab. 5.3). Both mean *in situ* HTC directions show no similarity with the direction of the present day field and are thought to reflect primary magnetizations.

Grouped according to age, Late Jurassic site mean directions of the area show an increase of the Fisher precision parameter k (Fisher, 1953) from 14.3 to 60.4 after 100% tilt correction. Middle Jurassic site mean directions show no substantial changes of the precision parameter k, which can be explained by rather similar bedding characteristics of these sites (dip directions of 60° to 100° and dips of 15° to 35°).

The mean direction for rocks of Middle Jurassic age in the area is $D = 277.1°$, $I = 41.2°$, $\alpha_{95} = 15$, $k = 14.6$, $n = 8$ sites (Tabs. 5.1, 5.3). The mean direction for rocks of Late Jurassic age in the area is $D = 278.2°$, $I = 49.4°$, $\alpha_{95} = 6.7$, $k = 60.4$, $n = 9$ sites (Tabs. 5.1, 5.3).

Table 5.4: Paleomagnetic directions from Jurassic sediments of Barbagia-Sarcidano and Sulcis Regions.

Site	Age	N	P	In situ				Bedding-corrected			
				D[°]	I[°]	k	α_{95} [°]	D[°]	I[°]	k	α_{95} [°]
Barbagia and Sarcidano											
BSM*	M	5/20	M	44.0	-20.0	88.6	8.2	41.0	-22.2	88.6	8.2
CAN1*	M	3/6	N	314.1	46.0	1127.5	19.8	314.1	46.0	1127.5	19.8
CAN2[b]	M	5/7	M	293.5	44.4	12.6	23.0	278.3	38.4	12.6	23.0
CAN3[b]	M	4/6	R	78.1	-41.3	26.8	11.4	73.1	-33.7	26.8	11.4
MSA1	M	10/10	M	288.2	55.6	9.7	15.7	294.1	58.9	9.7	15.7
MSA2	M	5/6	R	105.5	-54.6	29.0	14.5	94.4	-53.9	29.0	14.5
MSA3	M	6/7	R	86.6	-47.3	34.7	10.7	85.3	-44.6	34.7	10.7
PER1	M	5/10	M	81.9	-50.1	24.5	16.2	75.4	-43.5	24.5	16.2
PER2	M	11/12	M	96.5	-60.8	61.4	6.0	86.2	-47.6	61.4	6.0
VNT[b]	M	3/6	M	243.2	63.8	13.4	30.0	238.1	44.2	13.4	30.0
SUL*	M	6/11	M	139.7	-60.3	66.4	31.2	139.7	-60.3	66.4	31.2
SAD[b]	M	5/15	M	269.6	58.0	44.9	11.9	265.3	62.3	44.9	11.9
Sulcis											
MSP	M	8/9	M	93.0	65.9	7.9	21.0	257.8	25.6	30.5	10.2

Site: sampling sites, Age: M for Middle L for Late Jurassic. N: number of samples used for calculating site mean directions/number of measured samples. P: magnetic polarity; N = normal, R = reverse, M = mixed. Declination (D) and Inclination (I) in degrees, Fisher precision parameter k (Fisher, 1953), Fisher circle of 95% confidence (α_{95}) in geographic (*in situ*) and bedding corrected (TC) coordinates, respectively.
([b]) paleomagnetic mean direction calculated by combining linear trajectories of demagnetization paths with remagnetization circles, using the technique of McFadden and McElhinny (1988). (*) biased direction of Jurassic mean (this study) with component of present day field direction of the study area.

Barbagia-Sarcidano Region

In the Barbagia and Sarcidano regions, i.e. in the area of the towns of Isili, Laconi and Nurri ((3) in Fig. 5.1), twelve sites were sampled in Middle Jurassic sediments of the Dorgali Formation. Three of these sites were rejected due to a strongly developed present-day LT component overprint or because of the poor quality of the demagnetization data. The remainder of the sites yields well-defined dual polarity HT component directions (Tab. 5.4). At eight sites, these directions pass the reversal test in tilt corrected coordinates (classified C after McFadden and McElhinny (1988)). The tilt-corrected Middle Jurassic mean direction for the area is $D = 273.2°$, $I = 49.7°$,$\alpha_{95} = 12.3$, $k = 13.2$ and $n = 12$ sites (Tabs. 5.1, 5.4).

Sulcis region

In the far southwestern part of the island ((4) in Fig. 5.1), to the west of the Campidano graben, Jurassic rocks are only exposed immediately to the north of the village of Porto Pino. In this area, 9 samples in a small-scale syncline in the Medau Mereu Formation (Middle Jurassic after Costamagna (2000)) were collected. Eight of these samples yield usable HT component directions [maximum angular deviation (MAD) values between 1.6° and 4.4° based on at least 8 demagnetization steps] that yield positive reversal and fold tests (Fig. 5.6 and Tab. 5.4). The tilt-corrected site-mean characteristic HT component direction is $D = 257.8°$ and $I = 25.6°$ ($\alpha_{95} = 10.2°$; $k = 30.5$; $N = 8$ samples, Tabs. 5.1, 5.4).

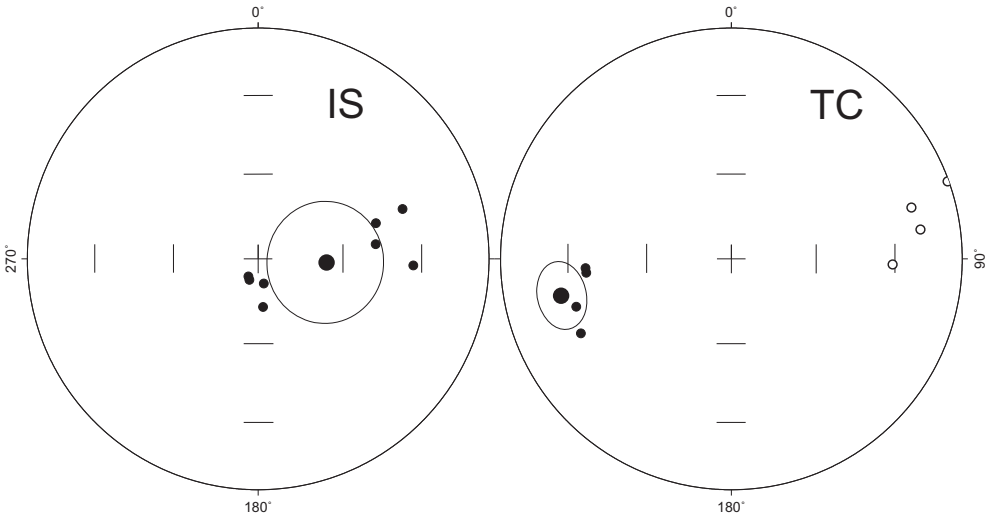

Figure 5.6: Stereoplots of individual sample directions of site MSP in the South West of Sardinia in geographic (IS=in situ) and stratigraphic (TC=tilt corrected) coordinates. Full (open) dots represent projection on the upper (lower) hemisphere. Large black dots indicate site mean direction with 95% confidence circles (α_{95}).

5.4.3 Data summary

Except for two sites of Early Jurassic age, all other sites of Middle and Late Jurassic age from the four investigated regions yield reliable HTC-directions (Tab. 5.5, Fig. 5.7).

When grouped according to age, the total of 25 Middle Jurassic site-mean directions from the four investigated regions show an increase of the Fisher precision parameter k from 10 to 14 after 100% tilt correction, and the reversal test after tilt correction is positive (classified as C according to the criteria of McFadden and McElhinny (1990)). The resulting Middle Jurassic overall mean direction is $D = 269.7°$, $I = 45.0°$, $k = 14.0$, $\alpha_{95} = 8.0°$, $n = 25$ sites.

Similarly, the total of 10 Late Jurassic site-mean directions from the four investigated regions show an increase of the Fisher precision parameter k from 25.3 to 45.3 after 100% tilt correction, and a positive reversal test (classified as C according to the criteria of McFadden and McElhinny (1990)). The resulting Late Jurassic overall mean direction is $D = 275.5°$, $I = 50.7°$, $k = 45.3$, $\alpha_{95} = 7.2°$, $n = 10$ sites.

It has to be noted, that Nurra and Sulcis Regions might contain uncertainties, originated from insufficient statistical coverage of several sites and/or areas. To improve the spatial distribution, site mean directions obtained from only one or two

Table 5.5: Overall site mean directions

Region	Jurassic Age	n	In situ			Bedding-corrected		
			$D[°]$	$I[°]$	α_{95} [°]	$D[°]$	$I[°]$	α_{95} [°]
Nurra	Middle	4	268.7	41.2	23.7	259.4	43.4	27.7
Region	Late	1	286.6	50.9	5.9	243.4	58.3	5.9
Supramonte-	Middle	8	275.8	30.1	13.4	277.1	41.2	15.0
Baronie	Late	9	269.5	34.8	14.1	278.2	49.4	6.7
Barbagia- Sarcidano	Middle	12	273.2	53.5	11.6	273.2	49.7	12.3
Sulcis	Middle	1	93.0	65.9	21.0	257.8	25.6	10.2
Mean	Middle	25	273.9	46.0	9.5	269.7	45.0	8.0
Mean	Late	10	271.9	36.6	13.0	275.5	50.7	7.2

n: number of sites used for calculating overall mean directions, mean Declination (D), mean Inclination (I) and Fisher circle of 95% confidence (α_{95}) (Fisher, 1953) in degrees in *in situ* coordinates and after bedding correction.

samples are included in the study. This might obscure a regional systematic deviation in the order of some 10°. However, excluding all site mean directions based on less than three samples would bias the overall mean directions for Middle and Late Jurassic rocks only by less than 5° (Middle: $\Delta D = 2.4°, \Delta I = 0.5°$, Late: $\Delta D = 4.0°, \Delta I = 0.4°$).
The resulting Middle and Late Jurassic paleopole positions plot at $Lat = 16.5°$, $Long = 299.1°$ ($dp = 6.4°$, $dm = 10.1°$) and at $Lat = 23.4°$, $Long = 301.2°$ ($dp = 6.5°$, $dm = 9.7°$), respectively.
These results indicate a pre-tilting origin of the characteristic component directions retrieved in the Jurassic carbonates and substantial tectonic coherence of the four investigated areas with only minor amounts of possible internal post-Jurassic rotations of ±10° (Fig. 5.7, Tab. 5.5).

5.5 Discussion and Conclusions

Paleomagnetic analysis of Middle and Late Jurassic sedimentary rocks from 44 sites, sampled in four regions of Sardinia (Nurra, Baronie-Supramonte, Barbagia-Sarcidano and Sulcis) reveals the presence of reliable characteristic component directions carried essentially by magnetite. The uniform distribution of directional data from allover Sardinia and especially around the arc shaped Gulf of Orosei, yields no evidence for oroclinal bending as proposed by Helbing *et al.* (2006b).

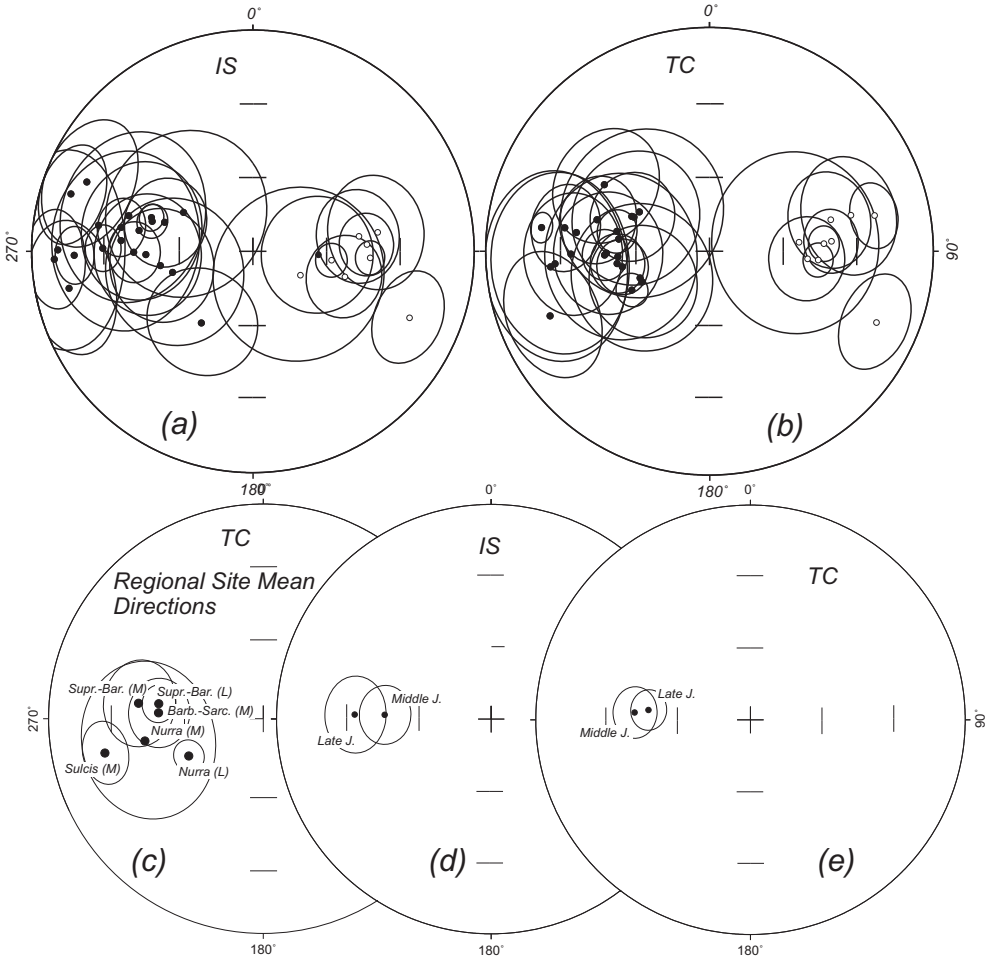

Figure 5.7: Stereographic projection of all site mean directions (a, b), grouped by region and age (c) and according to age (d, e) only. IS refers to *in situ*, TC to tilt corrected data. Shown are also 95% confidence circles. Full (open) dots represent projection on the upper (lower) hemisphere. Regional site mean directions (c) for Supramonte-Baronie (Supr.-Bar.), Barbagia-Sarcidano (Barb.-Sarc.), Sulcis and Nurra regions for Middle (M) and Late (L) Jurassic age, respectively.

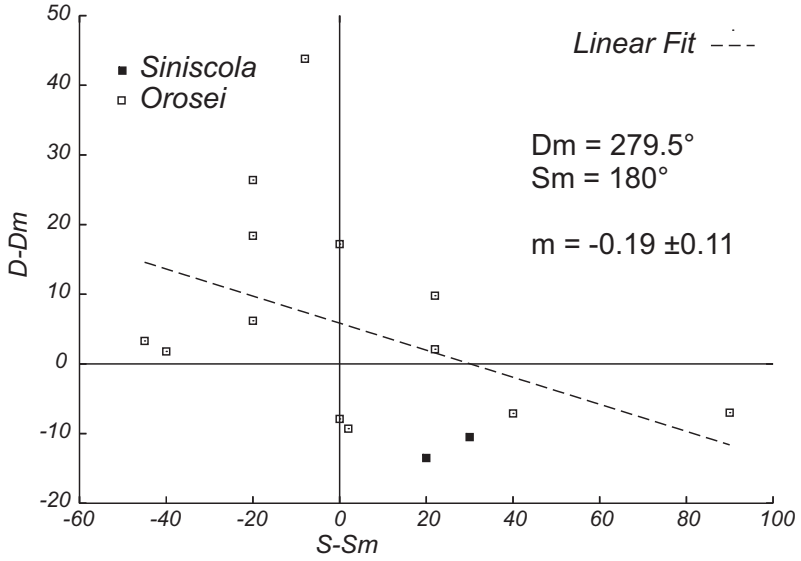

Figure 5.8: Deviations from mean values of declination (Dm) versus strike (Sm) for the data from the Gulf of Orosei (Supramonte). The linear fit shows no correlation between strike and declination and therefore suggests, that no oroclinal bending is present in the area (method after Schwartz and Van der Voo (1983)).

No correlation between deviation in strike and declination (Schwartz and Van der Voo, 1983) was identified when analyzing the directional data from Baronie and Supramonte (Fig. 5.8).

Coherent site mean directions obtained from the characteristic magnetization components allow to calculate Middle and Late Jurassic regional mean directions which are statistically indistinguishable and result in the corresponding Middle and Late Jurassic paleopoles.
Middle and Late Jurassic Sardinian paleopoles were rotated into European coordinates by closing the Liguro-Provençal Basin and the Bay of Biscay using rotation parameters of Gattacceca *et al.* (2007) and Van der Voo (1969) assuming a two-step rigid-body model. In a first step a rotation was applied to close the younger Liguro-Provençal Basin about an Euler pole located at $Lat = 43.5°$, $Long = 9.5°$ and a clockwise angle of rotation of 45° (Gattacceca *et al.*, 2007), followed by a second rotation closing the older Bay of Biscay with an Euler pole located at $Lat = 43.0°$, $Long = -2°$ and a clockwise angle of rotation of 35° (Van der Voo, 1969; Gong *et al.*, 2008). The rotated paleopoles were then compared to the coeval paleopoles of the

apparent polar wander (APW) path of Europe of Besse and Courtillot (2002). Inspection of Figure 5.9 reveals that the imposed rotations bring the Sardinian paleopoles very close to the European APW path, a relatively limited statistical discrepancy seems however to persist between the rotated Sardinian paleopoles and the coeval $\sim 170 - 140$Ma poles of Europe. An explanation for this discrepancy might be an underestimation of the assumed rotation angle for the Sardinian microblock during the opening of the Bay of Biscay. Assuming a larger angle of rotation in the order of $\sim 60^\circ$ and a similar pole of rotation would decrease the displacement of the Middle and Late Jurassic poles of Sardinia and the coeval poles of Europe (grey poles in Figure 5.9).

Alternatively, the Middle and Late Jurassic reference paleopoles of Europe are misplaced insofar as they are based on paleopole entries from limestones from central Europe that have an ambiguous smeared distribution with a suspicion of remagnetization, as extensively discussed in Muttoni *et al.* (2005).
Acknowledging these uncertainties, the following conclusions can be drawn:
1) Only negligible amounts of differential block rotations occurred within Sardinia since the Jurassic.
2) No oroclinal bending in the Gulf of Orosei as proposed by Helbing *et al.* (2006b).
3) Sardinia as a whole shows clear tectonic coherence with Europe during the Jurassic, and subsequently underwent a first counterclockwise rigid body rotation (juxtaposed to Iberia) during the opening of the Bay of Biscay (Van der Voo, 1969; Cohen, 1981; Olivet, 1996) in the Aptian (Gong *et al.*, 2008), and a subsequent counterclockwise rotation (jointly together with Corsica) during the opening of the Liguro-Provençal Basin in the Miocene (Gattacceca *et al.*, 2007).
4) As a consequence of the internal tectonic coherence of Sardinia since the Middle Jurassic, the timing of large differential rotations of up to 110° found in Permian rocks from different regions of Sardinia (Edel *et al.*, 1981; Edel, 2000; Moser *et al.*, 2005; Emmer *et al.*, 2005) are constrained to a generic Permian - Early Jurassic age. These large internal rotations can therefore neither be due to extensional tectonics at the European margin during the Jurassic (Zattin *et al.*, 2008), nor to Alpine tectonics that started broadly in the Late Cretaceous (Rosenbaum *et al.*, 2002), nor to subduction-related oroclinal bending in the Cenozoic ((Helbing *et al.*, 2006b), Fig. 5.8), nor to, finally, Cenozoic transcurrent tectonics (Carmignani *et al.*, 1994a). Consequently, the internal rotations observed in Permian units must have taken place in Permian-Triassic times, after the end of the Variscan orogeny and well before the Jurassic opening of the Penninic Ocean and its subsequent closure during the Alpine orogeny.
The post-Variscan period was one of intense crustal reorganization in transtensional

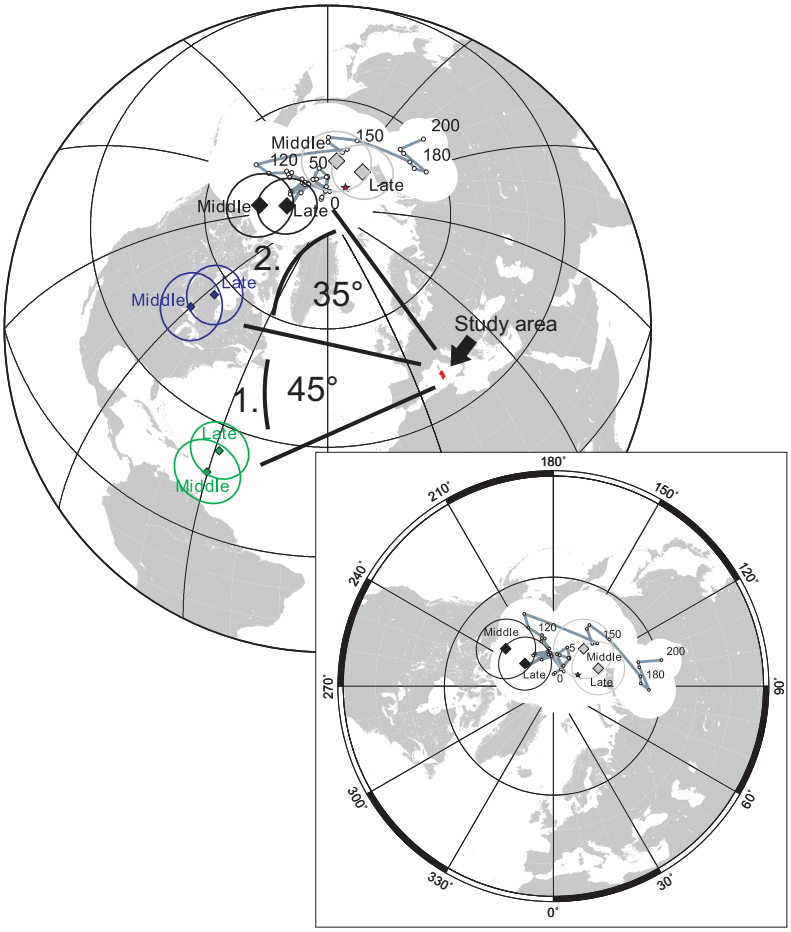

Figure 5.9: Paleomagnetic poles with associated α_{95} circles of confidence calculated from the overall mean Middle and Late Jurassic directions of Sardinia (green diamonds) have been rotated by closing the Liguro-Provençal Basin using rotation parameters of Gattacceca *et al.* (2007) (blue diamonds) and the Bay of Biscay using rotation parameters of Van der Voo (1969) (black diamonds). Grey diamonds represent poles, corrected for the opening of the Bay of Biscay with a overestimated rotation amount (60°). The APW path of Europe with associated α_{95}'s for the last 200 Ma (Besse and Courtillot, 2002) is indicated by white circles. Red star indicates the present day geomagnetic north pole.

and/or transpressional tectonic regimes. During the latest Carboniferous and Early Permian, the convergence of Gondwana and Laurussia changed from oblique collision to dextral translation along continental-scale dextral shear systems linked by secondary sinistral shears that developed in Europe and North Africa between the Uralides in the east and the Appalachians in the west (Arthaud and Matte, 1977; Blès *et al.*, 1989; Ziegler and Dëzes, 2006; McCann *et al.*, 2006; Cassinis *et al.*, 2011). This period of wrench tectonics may have culminated with the transformation of Pangea from a Pangea 'B' configuration to a Pangea 'A-2' configuration that took place mostly during the Middle Permian (e.g. Muttoni *et al.* (2003, 2009) and references therein). Sardinia and Corsica, together with the Little and Great Kabylie, and the Calabria basement, were members of the same Alboran micro-plate (Rosenbaum *et al.*, 2002), which was attached to the French-Catalan margin prior to Alpine-Apennine deformation in the Cenozoic (Westphal *et al.*, 1973, 1976b; Arthaud and Matte, 1977). They were therefore located just where most of the inferred shearing between Gondwana and Laurussia is expected to have taken place. We therefore speculate that post-Variscan intra-Pangea wrenching and shearing may have induced the large scale rotations of fault-bounded blocks observed in Permian units of Sardinia as well as elsewhere in Europe, e.g. in the Saint-Affrique and Brive basins of the French Massif Central (Chen *et al.*, 2006), as preliminarily discussed in Emmer *et al.* (2005). This inference, which remains at present speculative, however, will be explored in detail in a paleomagnetic work (now in progress) on Late Paleozoic–Middle Triassic rocks of Sardinia, which we consider as geological key witnesses of a major African-European contact zone.

5.6 Acknowledgments

We thank the Editor André Revil, J.-B. Edel, A. Smirnov and one anonymous reviewer for their very constructive comments on the manuscript. An earlier version was read by D. Bilardello and his comments lead to a significant improvement of the manuscript. Support in the field by M. Hackl is gratefully acknowledged. The study was funded by a research grant (Ba1210/8-1) to V.B. of the German Research funding agency (DFG).

6
Conclusions

The previous chapters demonstrate that large-scale diffuse and segmented transform fault zones can cause true vertical axis rotations of the involved crustal segments. The rotations can be quantified using paleomagnetic data. This is important, as major strike-slip faults may not be preserved through time (Umhoefer, 2000), and paleomagnetic studies may be the only successful approach to identify ancient large-scale strike-slip fault systems.
The Pangea transform zone - running approximately along the paleoequator during the late Paleozoic - is a highly debated continental-scale strike-slip fault system for which only scarce direct geological evidence can be found. Therefore, in the framework of the thesis presented here, several paleomagnetic studies on late Paleozoic/early Mesozoic volcanic and sedimentary rocks were carried out in the southwestern Mediterranean region. All sampling areas lie within the putative transform fault zone and were presumably affected by fault activity. Fig. 6.1 shows a synthesis of late Paleozoic/early Mesozoic paleomagnetic declinations from the presented studies in conjunction with data from the literature. We document relative rotations of varying amount both between crustal blocks and with respect to reference declinations for the study areas in the Early Permian. We define three crustal blocks within the study areas in the western Mediterranean as indicated in Fig. 6.1. The southern block 1 (mainly consisting of southeastern Sardinia) rotated counterclockwise with respect to stable Europe and the adjacent blocks after magnetization of the sampled rocks in the Early Permian. The middle block 2 (containing southern Corsica and northern Sardinia) on the other hand shows a slight clockwise rotation with respect to stable Europe and block 1 after magnetization of the sampled rocks in the Early Permian. Early Permian results from the northern block 3 (Toulon basin and Maures massif) show a large clockwise rotation with respect to stable Europe and blocks 1 and 2. We conclude in favor of a decreasing N-S gradient (in Late Paleozoic/Early Mesozoic coordinates) in rotation rates towards the south away from the northern boundary of the large-scale transform fault zone. The rotation pattern of the blocks nicely confirms the ball bearing model that we recently proposed (Aubele *et al.*, 2012), which results in clockwise and counterclockwise rotations of blocks caught within large-scale transform fault zones. More data from a larger area are needed in order to refine and further validate this model.

Data from rocks that acquired their magnetization at 260 ± 10 Ma and younger show no rotations. In agreement with several paleomagnetic studies on Mesozoic rocks from the area (e. g. Advokaat (2011); Kirscher *et al.* (2011)), we infer the crustal coherence of the blocks with stable Europe from the Early Mesozoic until

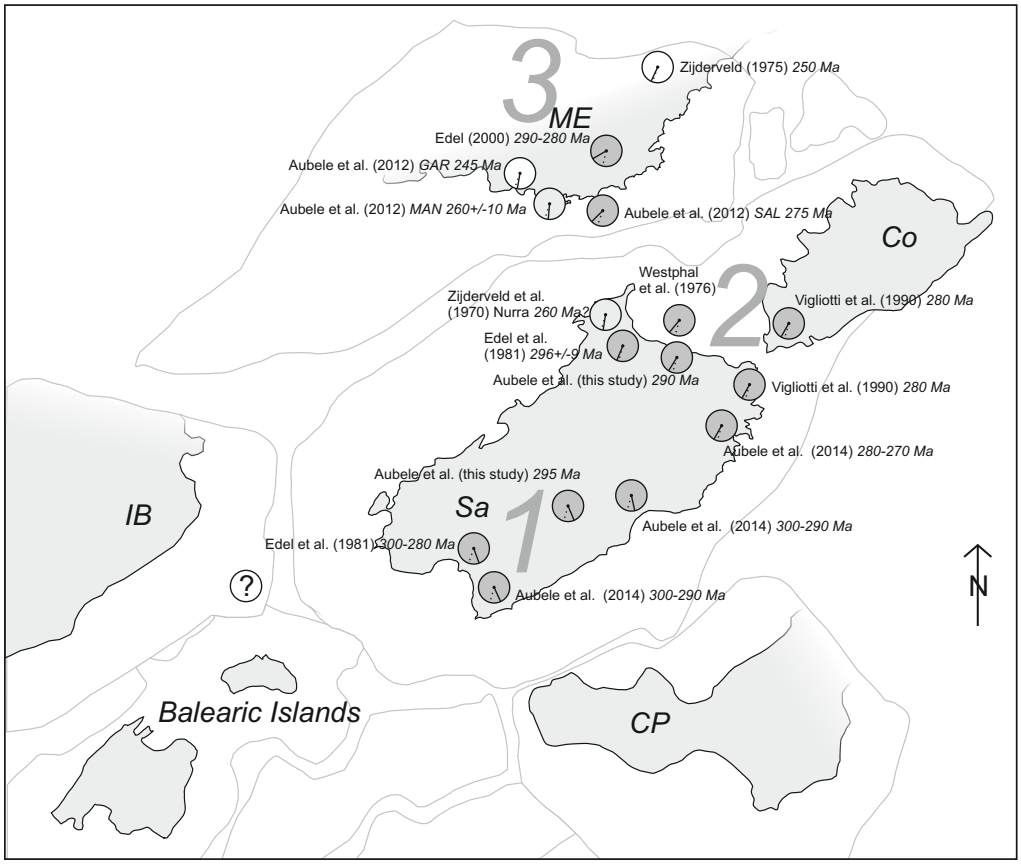

Figure 6.1: Late Paleozoic to Early Mesozoic reconstruction of Maures-Estérel (ME), Corsica (Co), Sardinia (Sa), Iberia (IB), the Balearic islands and the Calabria-Peloritani terrane (CP). Circular diagrams display observed (solid lines) and expected (stippled lines) declinations from the studies presented here and from the literature (Zijderveld *et al.*, 1970; Zijderveld, 1975; Vigliotti *et al.*, 1990; Edel, 2000; Aubele *et al.*, 2012, 2014). All declinations are given in European coordinates, i. e. we used the parameters of Gattacceca *et al.* (2007) (rotation pole coordinates $\lambda = 43.50°$, $\varphi = 9.50°$, angle 45.00° cw) in order to close the Ligurian ocean and Gong *et al.* (2008) (rotation pole coordinates $\lambda = 43.00°$, $\varphi = -2.00°$, angle 35.00° cw) to account for the opening of the Bay of Biscay.

the Cenozoic counterclockwise rotation of Corsica-Sardinia associated with the opening of the Ligurian ocean. The observed vertical axis rotations are interpreted as evidence for intra-Pangea mobility possibly associated with the 2000 to 3000 km dextral megashear between Laurasia and Gondwana active during the Middle Permian.

References

Advokaat, E. L. (2011). *New Paleomagnetic Data show no Mesozoic Rotation of Corsica-Sardinia Microplate.* Diplomarbeit, University of Utrecht, The Netherlands.

Alvarez, W., Franks, S., and Nairn, A. (1973). Palaeomagnetism of Plio-Pleistocene Basalts from North-west Sardinia. *Nature*, **243**, 10–11.

Angiolini, L., Gaetani, M., Muttoni, G., Stephenson, M. H., and Zanchi, A. (2007). Tethyan oceanic currents and climate gradients 300 m. y. ago. *Geology*, **35**, 1071–1074.

Arthaud, F. and Matte, P. (1977). Late Paleozoic strike-slip faulting in southern Europe and northern Africa: Result of a right-lateral shear zone between the Appalachians and the Urals. *Geological Society of America Bulletin*, **88**, 1305–1320.

Atzori, P. and Traversa, G. (1986). Post-granitic permo-triassic dyke magmatism in eastern Sardinia (Sarrabus p.p., Barbagia, Mandrolisai, Goceano, Baronie and Gallura). *Periodico di Mineralogia*, **55**, 203–231.

Atzori, P., Cirrincione, R., Del Moro, A., and Mazzoleni, P. (2000). Petrogenesis of late Hercynian calc-alkaline dykes of mid-eastern Sardinia: petrographical and geochemical data constraining hybridization process. *Eur. J. Mineral.*, **12**, 1261–1282.

Aubele, K. (2010). *A Paleomagnetic Study on Mesozoic Carbonate Rocks from Sardinia: New Paleomagnetic Results and Geodynamic Implications.* Diplomarbeit, Ludwig-Maximilians-Universität München.

Aubele, K., Bachtadse, V., Muttoni, G., Ronchi, A., and Durand, M. (2012). A Paleomagnetic Study of Permian and Triassic Rocks from the Toulon-

Cuers Basin, SE France: Evidence for intra-Pangea Block Rotations in the Permian. *Tectonics*, **31**.

Aubele, K., Bachtadse, V., Muttoni, G., and Ronchi, A. (2014). Paleomagnetic data from late Paleozoic dykes on Sardinia: evidence for intra-Sardinian block rotations and implications on the Pangea megashear system. *G-cubed*.

Bachtadse, V. and Maier, F. (1994). PALMAG, Paleomagnetic Measuring Software.

Baldelli, C., Bigazzi, G., Elter, F., and Macera, P. (1987). Description of a permo-trias alkaline lamprophyre embedded into the micaschists of garnet-staurolite-kyanite grade of North-eastern Sardinia island. In F. P. Sassi and R. Bourrouilh, Herausgeber, *IGCP n 5 Newsletter*, Ausgabe 7, Seiten 7–10.

Barca, S. and Costamagna, L. (1997). Compressive 'Alpine' tectonics in Western Sardinia (Italy): geodynamic consequences. *Comptes Rendus de l'Academie des Sciences, Serie II.*, **325**, 791–797.

Barca, S. and Costamagna, L. G. (2006). Stratigrafia, analisi di facies ed architettura deposizionale della successione permiana di Guardia Pisano (Sulcis, Sardegna SW). *Boll.Soc.Geol.It. (Ital.J.Geosci.)*, **125**, 3–19.

Bard, J.-P. (1997). Démembrement anté-mésozoïque de la chaîne varisque d'Europe occidentale et d'Afrique du Nord: rôle essentiel des grands décrochements transpressifs dextres accompagnant la rotation-translation horaire de l'Afrique durant le Stéphanien. *C. R. Acad. Sci. Paris*, **324**, 693–704.

Bassot, A.-M. (1987). Les formations carbonifères de la Provence orientale (Sud-Est de la France). *Géologie Alpine, Grenoble, Mém. h. s.*, **13**, 19–24.

Begassat, P. (1985). *Les bassins stéphaniens des Maures et de Tanneron; pétrologie, géochimie du volcanisme, métallogénie.* Dissertation, Paris VI. 163 p.

Besse, J. and Courtillot, V. (2002). Apparent and true polar wander and the geometry of the geomagnetic field over the last 200 Myr. *Journal of Geophysical Research*, **107**.

Blès, J., Bonijoly, D., and Gros, C. C. Y. (1989). Successive post-Variscan stress fields in the French Massif Central and its borders (Western European plate): comparison with geodynamic data. *Tectonophysics*, **169**, 79–111.

Bouillet, G. and Lutaud, L. (1958). Contribution à l'étude paléogéographique de la péeriode permienne dans la Provence cristalline. *Bull. Soc. géol. France*, **8**(5), 447–462.

Bourquin, S., Durand, M., Diez, J.-B., Broutin, J., and Fluteau, F. (2007). The Permian-Triassic boundary and lower Triassic sedimentation in western European basins: an overview. *J. Iber. Geol.*, **33**(2), 221–236.

Bourquin, S., Bercovici, A., López-Gómez, J., Diez, B., Broutin, J., Ronchi, A., Durand, M., Arche, A., Linol, B., and Amour, F. (2011). The Permian-Triassic transition and the onset of Mesozoic sedimentation at the northwestern peri-Tethyan domain scale: Paleogeographic maps and geodynamic implications. *Paleogeography, Paleoclimatology, Paleoecology*, **299**(1-2), 265–280.

Broutin, J. and Durand, M. (1995). First paleobotanical and palynological data on the Les Salettes Formation uppermost member (Permian Toulon Basin, Southeastern France). *Intern. Congr. on Carboniferous-Permian.*

Broutin, J., Cabanis, B., Chateauneuf, J.-J., and Deroin, J.-P. (1994). Évolution biostratigraphique, magmatique et tectonique dy domain paléotéthysien occidental (SW de l'Europe): implications paléogéographiques au Permien inférieur. *Bull. Soc. Géol. France*, **165**(2), 163–179.

Burg, J. P., van den Driessche, J., and Brun, I. P. (1994). Syn- to post-thickening extension in the Variscan belt of Western Europe: modes and structural consequences. *Géologie de la France*, **3**, 33–51.

Carmignani, L., Cocozza, T., Minzoni, N., and Pertusati, P. C. (1978). The Hercynian orogenic revolution in Sardinia. *Zeitschrift der deutschen Geologischen Gesellschaft*, **129**, 485–493.

Carmignani, L., Carosi, R., Disperati, L., Funedda, A., Musumeci, G., Pasci, S., and Pertusati, P. (1992). Tertiary transpressional tectonics in NE Sardinia, Italy. In L. Carmignani and F. Sassi, Herausgeber, *Contributions to the Geology of Italy with special regard to the Paleozoic Basements. A volume dedicated to Tommaso Cocozza.*, Ausgabe IGCP No. 276. Newsletter.

Carmignani, L., Barca, S., Disperati, L., Fantozzi, P., Funedda, A., Oggiano, G., and Pasci, S. (1994a). Tertiary compression and extension in the Sardinian basement. *Boll. Geofis. Teor. Appl.*, **36**, 45–62.

Carmignani, L., Carosi, R., and Di Pisa, A. (1994b). The Hercynian chain in Sardinia (Italy). *Geodinamica Acta*, **7**, 31–47.

Casini, L., Cuccuru, S., Maino, M., Oggiano, G., and Tiepolo, M. (2012). Emplacement of the Arzachena Pluton (Corsica-Sardinia Batholith) and the geodynamics of incoming Pangaea. *Tectonophysics*, **544-545**, 31–49.

Cassinis, G., Durand, M., and Ronchi, A. (2000). Permian continental basins of sardinia and provence: Stratigraphic and paleogeographic implications. In 15^{th} *Journée thém. Assoc. Géol. Permien, Paris.*

Cassinis, G., Durand, M., and Ronchi, A. (2003). Permian-Triassic continental sequences of Northwest Sardinia and South Provence: stratigraphic correlations and palaeogeographical implications. *Bull. Soc. Geol. It.*, **2**, 119–129.

Cassinis, G., Perotti, C., and Ronchi, A. (2011). Permian continental basins in the Southern Alps (Italy) and peri-Mediterranean correlations. *Int J Earth Sci*, Seiten 1–29.

Cassinis, G., Perotti, C., and Ronchi, A. (2012). Permian continental basins in the Southern Alps (Italy) and peri-mediterranean correlations. *International Journal of Earth Sciences*, **101**(1), 129–157.

Channel, J. E. T. (1996). Palaeomagnetism and Palaeogeography of Adria. In T. D. H. Morris, A, Herausgeber, *Palaeomagnetism and Tectonics of the Mediterranean Region*, Ausgabe 105, Seiten 119–135. Geological Society London, Special Publication.

Chen, Y., Henry, B., Faure, M., Becq-Giraudon, J.-F., Talbot, J.-Y., Daly, L., and Le Goff, M. (2006). New Early Permian paleomagnetic results from the Brive basin (French Massif Central) and their implications for Late Variscan tectonics. *Int. J. Earth Sci. (Geol. Rundsch.)*, **95**, 306–317.

Cherchi, A., Simone, L., Schroeder, R., Carannante, G., and Ibba, A. (2010). I sistemi carbonatici giurassico - cretacei della Nurra (Sardegna settentrionale). *Geol.F.Trips*, **2**(2.1), 122.

Cocherie, A., Rossi, P., Fanning, C., and Guerrot, C. (2005). Comparative use of TIMS and SHRIMP for U-Pb zircon dating of A-type granites and mafic tholeiitic layered complexes and dykes from the Corsican batholith (France). *Lithos*, **82**, 185–219.

Cogné, J. P., Brun, J. P., and Van den Driessche, J. (1990). Paleomagnetic evidence for rotation during Stephano-Permian extension in southern Massif Central (France). *Earth and Planetary Science Letters*, **101**, 272–280.

Cogné, J. P., Van den Driessche, J., and Brun, J. P. (1993). Syn-extension rotations in the Permian St. Affrique basin (Massif Central, France): paleomagnetic constraints. *Earth and Planetary Science Letters*, **115**, 29–42.

Cohen, C. (1981). Plate Tectonic Model for the Oligo-Miocene Evolution of the Western Mediterranean. *Tectonophysics*, **68**, 283–311.

Conti, P., Carmignani, L., Oggiano, G., Funedda, A., and Eltrudis, A. (1999). From thickening to extension in the Variscan belt - kinematic evidence from Sardinia (Italy). *Terra Nova*, **11**, 93–99.

Cortesogno, L., Cassinis, G., Dallagiovanna, G., Gaggero, L., Oggiano, G., Ronchi, A., Seno, S., and Vanossi, M. (1998). The Variscan post-collisional volcanism in Late Carboniferous-Permian sequences of Ligurian Alps, Southern Alps and Sardinia (Italy): a synthesis. *Lithos*, **45**, 305–328.

Costamagna, L. (2000). Analisi di facies della successione triassico-giurassica di Porto Pino (Sardegna sud-occidentale). *Atti Ticinesi Sc. Terra*, **41**, 65–82.

Costamagna, L. and Barca, S. (2004). Stratigrafia, analisi di facies, paleogeografia ed inquadramento regionale della successione giurassica dell'area dei Tacchi (Sardegna Orientale). *Boll. Soc. Geol. It.*, **123**, 477–495.

Costamagna, L., Barca, S., and Lecca, L. (2007). The Bajocian - Kimmeridgian Jurassic sedimentary cycle of eastern Sardinia: Stratigraphic, depositional and sequence interpretation of the new 'Baunei Group'. *Comptes Rendus Geoscience*, **339**, 601–612.

Davies, J. H. and von Blanckenburg, F. (1995). Slab breakoff; a model of lithosphere detachment and its test in the magmatism and deformation of collisional orogens. *Earth and Planetary Science Letters*, **129**, 85–102.

de Jong, K., Manzoni, M., Stavenga, T., van Dijk, F., van der Voo, R., and Zijderveld, J. (1973). Palaeomagnetic evidence for rotation of Sardinia during early Miocene. *Nature*, **243**, 281–283.

Del Moro, A., Di Simplicio, P., Ghezzo, C., Guasparri, G., Rita, F., and Sabatini, G. (1975). Radiometric data and intrusive sequence in the Sardinia batholith. *Neues Jahrbuch Mineral.*, **126**, 28–44.

Del Moro, A., Di Pisa, A., and Oggiano, G. (1996). Relationship between an Autunian volcano-sedimentary succession and the Tempio Massif Granites (northern Sardinia). Geochronological and field constraints. *Plinius*, (16), 94–95.

Demathieu, G. and Durand, M. (1991). Les traces de pas de Tétrapodes dans le Trias détritique du Var et des Alpes maritimes (France). *Bull. Mus. Hist. Nat. Paris*, **13, sect. C**, 115–133.

Demathieu, G., Gand, G., and Toutin-Morin, N. (1992). La palichnofaune des bassins permiens provençaux. *Geobios*, **25**(1), 19–54.

Deroin, J. P. and Bonin, B. (2003). Late Variscan tectonomagmatic activity in Western Europe and surrounding areas: the Mid-Permian Episode. *Boll Soc Geol It (Special Volume)*, **2**, 169–184.

Diego-Orozco, A. and Henry, B. (1998). Palaeomagnetic data from the Permian Rodez basin and rotations in the southwestern border of the Massif Central. *Comptes Rendus de l'Academie des Sciences Series IIA Earth and Planetary Science*, **327**, 225–229.

Diego-Orozco, A., Chen, Y., Henry, B., and Becq-Giraudon, J.-F. (2002). Paleomagnetic results from the Permian Rodez basin implications: the Late Variscan tectonics in the southern French Massif Central. *Geodinamic Acta*, **15**, 249–260.

Dieni, I. and Massari, F. (1986). Mesozoic of Eastern Sardinia. *In: 19th Micropaleontological Colloquium, Guide-Book, A. Cherchi Ed., Sardinia, October 1985*, Seiten 66–77.

Dieni, I., Fischer, J., Massari, F., Salard-Cheboldaeff, M., and Vozenin-Serra, C. (1983). La succession de Genna Selole (Baunei) dans le cadre de la palogographie msojurassique de la Sardaigne orientale. *Mem. Sci. Geol., Padova*, **36**, 117–148.

Dieni, I., Massari, F., and Médus, J. (2008). Age, depositional environment and stratigraphic value of the Cuccuru 'e Flores Conglomerate: insight into the Palaeogene to Early Miocene geodynamic evolution of Sardinia. *Bulletin de la Société géologique de la France*.

Domeier, M., Van der Voo, R., Tohver, E., Tomezzoli, R. N., Vizan, H., H., T. T., and Kirshner, J. (2011a). New Late Permian paleomagnetic data from Argentina: Refinement of the apparent polar wander path of Gondwana. *G-Cubed*, **12**.

Domeier, M., Van der Voo, R., Tomezzoli, R. N., Tohver, E., Hendriks, B. W. H., Torsvik, T. H., Vizan, H., and Dominguez, A. (2011b). Support for an 'A-type' Pangea reconstruction from high-fidelity Late Permian and Early to Middle Triassic paleomagnetic data from Argentina. *Journal of Geophysical Research*, **116**.

Domeier, M., Van der Voo, R., and Denny, F. B. (2011c). Widespread inclination shallowing in Permian and Triassic paleomagnetic data from Laurentia: Support from new paleomagnetic data from Middle Permian shallow intrusions in southern Illinois (USA) and virtual geomagnetic pole distributions. *Tectonophysics*, **511**, 38–52.

Domeier, M., Van der Voo, R., and Torsvik, T. (2012). Paleomagnetism and Pangea: The road to reconciliation. *Tectonophysics*, **514-517**, 14–43.

Dominguez, A. R., Van der Voo, R., Torsvik, T. H., Hendriks, B. W. H., Abrajevitch, A., Domeier, M., Larsen, B. T., and Rousse, S. (2011). The $\sim$ 270 Ma palaeolatitude of Baltica and its significance for Pangea models. *Geophysical Journal International*.

Dunlop, D. J. and Özdemir, O. (1997). *Rock Magnetism: Fundamentals and Frontiers*. Cambridge University Press.

Durand, M. (1993). Un exemple de sédimentation continental permienne dominée par l'activité de chenaux méandriformes: La formation de Saint-Mandrier (Bassin de Toulon, Var). *Géologie de la France, Orléans*, **2**, 43–55.

Durand, M. (2001). The Continental Permian-Triassic Series of Provence (Southeast France). Field Trip Guidebook. International Field Conference on "The Stratigraphic and Structural Evolution of the Late Carboniferous to Triassic Continental and Marine Successions in Tuscany (Italy). Regional Reports and General Correlations".

Durand, M. (2006). The problem of the transition from the Permian to the Triassic Series in southeastern France: comparison with other Peritethyan regions. *Geological Society, London, Special Publications*, **265**, 281–296.

Durand, M. (2008). Permian to Triassic continental successions in southern Provence (France): an overview. *Boll. Soc. Geol. It. (Ital. J. Geosci.)*, **127**(3), 697–716.

Durand, M., Avril, G., and Meyer, R. (1988). Paléogéographie des premiers dépôts triasiques dans les Alpes externes méridionales: Importance de la Dorsale delphino-durancienne. *Cr. R. Acad. Sci. Paris*, **306**(sér. II), 557–560.

Durand, M., Meyer, R., and Avril, G. (1989). Le Trias Détritique de Provence, du dome de Barrot et du Mercantour, journal = Publ. Assoc. Sédimentol. Français.

Edel, J. B. (1980). *Etude paléomagnétique en Sardaigne. Conséquences pour la géodynamique de la Méditerranée occidentale.* Dissertation, Strasbourg I. 310 p.

Edel, J.-B. (2000). Hypothèse d'une ample rotation horaire tardi-varisque du bloc Maures-Estérel-Corse-Sardaigne. *Géologie de la France*.

Edel, J. B., Montigny, R., and Thuizat, R. (1981). Late Paleozoic rotations of Corsica and Sardinia: new evidence from paleomagnetic and K-Ar studies. *Tectonophysics*, **79**, 201–223.

Emmer, B., Bachtadse, V., Muttoni, G., Ronchi, A., and Kent, D. V. (2005). Paleomagnetism of Late Paleozoic Dyke Swarms from Sardinia. *AGU Fall Meeting*, # **GP11A-0015**. Poster.

Faccenna, C., Speranza, F., D'Ajello Caracciolo, F., Mattei, M., and Oggiano, G. (2002). Extensional tectonics on Sardinia (Italy): insights into the arc - back-arc transtensional regime. *Tectonophysics*.

Ferrandini, J., Gattacceca, J., Ferrandini, M., Deino, A., and Janin, M. (2003). Chronostratigraphie et paléomagnétisme des dépôts Oglio-Miocènes de Corse: implications géodynamiques pour l'ouverture du bassin liguro-provençal. *Bulletin de la Société Géologique de France*, **174**, 357–371.

Fischer, J., Schneider, J. W., and Ronchi, A. (2010). New hybondontoid shark from the Permocarboniferous (GzhelianAsselian) of Guardia Pisano (Sardinia, Italy). *Acta Paleontologica Polonica*, **55**(2), 241–264.

Fisher, R. (1953). Dispersion on a sphere. *Proceedings of the Royal Society London*, **A217**, 295–305.

Funedda, A. and Oggiano, G. (2009). Outline of the Variscan basement of Sardinia. *Rendiconti della Società Paleontologica Italiana*, **3**(1), 23–35.

Gaggero, L., Oggiano, G., Buzzi, L., Slejko, F., and Cortesogno, L. (2007). Post-Variscan Mafic Dikes from the late Orogenic Collapse to the Tethyan Rift: Evidence from Sardinia. *Ofioliti*, **32**(1), 15–37.

Galtier, J., Ronchi, A., and J., B. (2011). Early Permian silicified floras from Perdasdefogu Basin (SE Sardinia): comparison and bio-chronostratigraphic correlation with the floras of the Autun Basin (Massif Central, France). *Geodiversitas*, **33**(1), 43–69.

Gand, G. and Durand, M. (2006). Tetrapod footprint ichnoassociations from French Permian basins: comparisons with other Euramerican ichnofaunas. In S. Lucas, G. Cassinis, and J. Schneider, Herausgeber, *Non-marine Permian Biostratigraphy and Biochronology*, Ausgabe 265, Seiten 157–177. Geol. Soc. London, Spec. Publ.

Gasperi, G. and Gelmini, R. (1980). Ricerche sul Verrucano. 4. Il Verrucano della Nurra (Sardegna nord-occidentale). *Mem. Soc. Geol. It.*, **20**(1979), 215–231.

Gattacceca, J., Deino, A., Rizzo, R., Jones, D. S., Henry, B., Beaudoin, B., and Vadeboin, F. (2007). Miocene rotation of Sardinia: New paleomagnetic and geochronological constraints and geodynamic implications. *Earth and Planetary Science Letters*, **258**, 359–377.

Glinzboeckel, C. and Durand, M. (1984). Provence et chaines subalpines méridionales. In *Synthèse géologique du Sud-Est de la France, 1) Stratigraphie et paléogéographie*.

Goll, M. and Lippolt, H. J. (2001). Biotit-Geochronologie ($^{40}Ar_{rad}$/K, $^{40}Ar_{rad}/^{39}Ar_K$, $^{87}Sr_{rad}/^{87}Rb$) spät-variszischer Magmatite des Thüringer Waldes. *N. Jahrbuch Geol. Paleont., Abhandlungen*, **222**, 353–405.

Gong, Z., Langereis, C. G., and Mullender, T. A. T. (2008). The rotation of Iberia during the Aptian and the opening of the Bay of Biscay. *Earth and Planetary Science Letters*, **273**, 80–93.

Gradstein, F. M., Ogg, J. G., and Smith, A. G. e. a. (2005). *A Geologic Time Scale*. Cambridge University Press.

Helbing, H., Frisch, W., and Bons, P. D. (2006a). South Variscan terrane accretion: Sardinian constraints on the intra-Alpine Variscides. *Journal of Structural Geology*, **28**, 1277–1291.

Helbing, H., Frisch, W., Bons, P. D., and Kuhlemann, J. (2006b). Tension gash-like back-arc basin opening and its control on subduction rollback inferred from Tertiary faulting in Sardinia. *Tectonics*, **25**.

Henry, B., Becq-Giraudon, J.-F., and Rouvier, H. (1999). Paleomagnetic studies in the Permian Basin of Largentière and implications for the Late Variscan rotations in the French Massif Central. *Geophysical Journal International*, **138**, 188–198.

Horner, F. and Lowrie, W. (1981). Paleomagnetic Evidence from Mesozoic Carbonate Rocks for the Rotation of Sardinia. *Journal of Geophysics*, **49**, 11–19.

Irving, E. (1977). Drift of the major continental blocks since the Devonian. *Nature*.

Irving, E. (2005). The role of latitude in mobilism debates. *Proceedings of the Nationla Academy of Sciences*, **102**(6), 1821–1828.

Isozaki, Y. (2009). Illawarra reversal: the fingerprint of a superplume that triggered Pangean breakup and the end-Guadalupian (Permian) mass extinction. *Gondwana Research*, **15**, 421–432.

Jackson, M., Worm, H.-U., and Banerjee, S. (1990). Fourier analysis of digital hysteresis data: rock magnetic applications. *Physics of the Earth and Planetary Interiors*, **65**, 78–87.

Jadoul, F., Lanfranchi, A., Casellato, C., Berra, F., and Erba, E. (2010). I sistemi carbonatici giurassici della Sardegna orientale (Golfo di Orosei). *Geol.F.Trips*, **2**(2.1), 122.

Kirscher, U., Bachtadse, V., Aubele, K., and Muttoni, G. (2011). Paleomagnetism of Jurassic Carbonate Rocks from Sardinia - No Indication of Post Jurassic Internal Block Rotations. *Journal of Geophysical Research*, **116**.

Kirschvink, J. L. (1980). The least-square line and plane and the analysis of paleomagnetic data. *The Geophysical Journal of the Royal Astronomical Society*, **62**, 699–718.

Klitgord, K. and Schouten, H. (1986). Plate kinematics of the Central Atlantic. In P. Vogt and B. Tucholke, Herausgeber, *The Geology of North America: The Western North Atlantic Region*. Geol. Soc. Am., Boulder, CO (USA).

Krása, D., Petersen, K., and Petersen, N. (2007). Variable Field Translation Balance. In D. Gubbins and E. Herrero-Bervera, Herausgeber, *Encyclopedia of Geomagnetism and Paleomagnetism. Encyclopedia of Earth Sciences Series*. Springer.

Lamb, S. H. (1987). A model for tectonic rotations about a vertical axis. *Earth and Planetary Science Letters*.

Leonhardt, R. (2006). Analyzing rock magnetic measurements: The RockMagAnalyzer 1.0 software. *Computers and Geosciences*.

Leroy, S. and Cabanis, B. (1993). Le volcanisme permien du bassin de Toulon: un jalon septentrional du volcanisme permien de l'Ouest méditerranéen. *Géologie de la France*, **2**, 57–66.

Lethiers, F., Damotte, R., and Sanfourche, J. (1993). Premières données sur les ostracodes du permien supérieur continental de l'Estérel (SE de la France): Systématique, biostratigraphie, paléoécologie. *Géologie Méditerranéenne*, **20**(2), 109–125.

Lützer, H., Littmann, S., Mädler, J., Romer, R. I., and Schneider, J. (2007). Radiometric and biostratigraphic data on the Permocarboniferous reference section Thüringer Wald. In T. E. Wong, Herausgeber, *Proc. XVth Int. Congr. Carboniferous and Permian Strat. Utrecht, The Netherlands*, Seiten 161–174. Royal Netherl. Acad. Art and Sci.

Manzoni, M. (1975). Paleomagnetic Data from Tertiary Volcanics of the Campidano and Associated Grabens, Sardinia. *Earth and Planetary Science Letters*, **27**, 275–282.

McCann, T., Pascal, C., Timmermann, M. J., Krzywiec, P., López-Gómez, J., Wetzel, A., Krawczyk, C. M., Rieke, H., and Lamarche, J. (2006). Post-Variscan (end Carboniferous - Early Permian) Basin Evolution in Western and Central Europe. *European Lithosphere Dynamics*.

McFadden, P. and McElhinny, M. (1988). The combined analysis of remagnetization circles and direct observations in palaeomagnetism. *Earth and Planetary Science Letters*, **87**, 161–172.

McFadden, P. and McElhinny, M. (1990). Classification of the reversal test in paleomagnetism. *Geophysical Journal International*, **103**, 725–729.

McKenzie, D. P. and Jackson, J. A. (1983). The relationship between strain rates, crustal thickening, paleomagnetism, finite strain, and fault movement within a deforming zone. *Earth and Planetary Science Letters*, **65**, 182–202.

Merabet, N. and Daly, L. (1986). Détermination d'un pôle paléomagnétique et mise en évidence d'aimantations à polarité normale sur les formations du Permien supérieur du Massif des Maures (France). *Earth Planet. Sci. Lett.*, **80**, 156–166.

Montigny, R., Edel, J., and Thuizat, R. (1981). Oligo-Miocene rotation of Sardinia: K-Ar ages and paleomagnetic data of Tertiary volcanics. *Earth and Planetary Science Letters*, **54**, 261–271.

Morel, P. and Irving, E. (1981). Paleomagnetism and the Evolution of Pangea. *Journal of Geophysical Research*, **86**(B3), 1858–1872.

Moser, E. (2004). *Paleomagnetic Study of Permian Sediments and Volcanic Rocks from Sardinia - Testing the Pangea B Hypothesis*. Diplomarbeit, Ludwig-Maximilians-University Munich.

Moser, E., Emmer, B., Bachtadse, V., Kent, D. V., Muttoni, G., and Ronchi, A. (2005). Paleomagnetism of Permian sediments and volcanic rocks from Sardinia. *AGU Fall Meeting Abstracts*.

Moskowitz, B. M. (1981). Methods for estimating Curie Temperatures of Titanomaghemites from experimental J_s-T Data. *Earth and Planetary Science Letters*, **53**, 84–88.

Muttoni, G., Kent, D. V., and Channell, J. E. T. (1996). Evolution of Pangea: paleomagnetic constraints from the Southern Alps, Italy. *Earth and Planetary Science Letters*, **140**, 97–112.

Muttoni, G., Kent, D. V., Garzanti, E., Brack, P., Abrahamsen, N., and Gaetani, M. (2003). Early Permian Pangea B to Late Permian Pangea A. *Earth and Planetary Science Letters*, **215**(3), 379–394.

Muttoni, G., Kent, D. V., Garzanti, E., Brack, P., Abrahamsen, N., and Gaetani, M. (2004). Erratum to "Early Permian Pangea B to Late Permian Pangea A": [Earth and Planetary Science Letters, v. 215, no. 3, p. 379-394]. *Earth and Planetary Science Letters*.

Muttoni, G., Erba, E., Kent, D., and Bachtadse, V. (2005). Mesozoic Alpine facies deposition as a result of past latitudinal plate motion. *Nature*, **434**, 59–63.

Muttoni, G., Gaetani, M., Kent, D. V., Sciunnach, D., Angiolini, L., Berra, F., Garzanti, E., Mattei, M., and Zanchi, A. (2009). Opening of the Neo-Tethys Ocean and the Pangea B to Pangea A transformation during the Permian. *GeoArabia*, **14**(4), 17–48.

Nelson, M. R. and Jones, C. H. (1987). Paleomagnetism and crustal rotations along a shear zone, Las Vegas Range, Southern Nevada. *Tectonics*.

Ogg, J. G., Ogg, G., and Gradstein, F. M. (2008). *The Concise Geologic Time Scale*. Cambridge University Press.

Oggiano, G., Funedda, A., Carmignani, L., and Pasci, S. (2009). The Sardinia-Corsica microplate and its role in the Northern Apennine. Geodynamics: new insights from the Tertiary intraplate strike-slip tectonics of Sardinia. *Ital.J.Geosci. (Boll.Soc.Geol.It.)*, **128**(2), 527–539.

Olivet, J.-L. (1996). La cinématique de la plaque ibérique. *Bull. Centres Rech. Expl. -Prod. Elf Aquitaine*, **20**(1), 131–195.

Paquette, J.-L., Ménot, R.-P., Pin, C., and J.-B., O. (2003). Episodic and short-lived granitic pulses in a postcollisional setting: evidence from precise U-Pb zircon dating through a crustal cross section in Corsica. *Chemical Geology*, **198**(1, 2), 1–20.

Parent, H. (1932). Le terrain houllier à Collobrières et en environs d'Hyères. *C. R. som. Soc. géol. France*, **11**, 159–161.

Pasci, S. (1997). Tertiary transcurrent tectonics of North-Central Sardinia. *Bull. Soc. Géol. France*, **168**, 301–312.

Pasci, S., Oggiano, G., and Funedda, A. (1998). Rapporti tra tettonica e sedimentazione lungo le fasce trascorrenti oligo-aquitaniane della Sardegna NE. *Boll. Soc. geol. it.*, **117**, 443–453.

Pecorini, G. (1974). Nuove osservazioni sul Permo-Trias di Escalaplano (Sardegna sud-orientale). *Boll. Soc. Geol. It.*, **93**, 991–999.

Pittau, P., Barca, S., Cocherie, A., Del Rio, M., Fanning, M., and Rossi, P. (2002). Le bassin permien de Guardia Pisano (Sud-Ouest de la Sardaigne, Italie): palynostratigraphie, paléophytogéographie, corrélations et âge radiométrique des produits volcaniques associés. *Geobios*, **35**, 561–580.

Pittau, P., Del Rio, M., and Funedda, A. (2008). Relationships between plant communities characterization and basin formation in the Carboniferous-Permian of Sardinia. *Boll. Soc. Geol. It.*, **127**(3), 637–653.

Platt, J. P. (1986). Dynamics of orogenic wedges and the uplift of high-pressure metamorphic rocks. *Bull. Geological Society of America*, **97**, 1037–1053.

Platt, J. P. and England, P. C. (1994). Convective removal of lithosphere beneath mountain belts; thermal and mechanical consequences. *American Journal of Science*, **294**, 307–336.

Poli, G., Ghezzo, C., and Conticelli, S. (1989). Geochemistry of granitic rocks from the Hercynian Sardinia-Corsica batholith: Implication for magma genesis. *Lithos*, **23**(4), 247–266.

Posenato, R., Simone, L., Urlichs, M., and Ibba, A. (2002). The Ladinian 'Muschelkalk' of Punta del Lavatoio (Alghero, NW Sardinia). *Rend.Soc.Paleont.Ital.*, **1**, 283–291.

Rochette, P. and Vandamme, D. (2001). Pangea B: an artifact of incorrect paleomagnetic assumptions? *Anali Geofisica*, **44**, 649–658.

Ron, H., Freund, R., and Garfunkel, Z. (1984). Block Rotation by Strike-Slip Faulting: Structural and Paleomagnetic Evidence. *Journal of Geophysical Research*, **89**, 6256–6270.

Ronchi, A., Broutin, J., Diez, J. B., Freytet, B., Galtier, J., and Lethiers, F. (1998). New palaeontological discoveries in some Early Permian sequences of Sardinia. Biostratigraphic and palaeogeographic implications. *C. R. Acad. Sci. Paris*, **327**, 713–719.

Ronchi, A., Sarria, E., and Broutin, J. (2008). The Autuniano Sardo: basic features for a correlation through the Western Mediterranean and Paleoeurope. *Boll.Soc.Geol.It. (Ital.J.Geosci.)*, **127**(3), 655–681.

Ronchi, A., Sacchi, E., Romano, M., and Nicosia, U. (2011). A huge caseid pelycosaur from north-western Sardinia and its bearing on European Permian stratigraphy and palaeobiogeography. *Acta Palaeontologica Polonica*, **56**(4), 723–738.

Rosenbaum, G., Lister, G. S., and Duboz, C. (2002). Relative motions of Africa, Iberia, and Europe during Alpine orogeny. *Tectonophysics*, **359**, 117–129.

Rossi, P., Oggiano, G., and Cocherie, A. (2009). A restored section of the 'southern Variscan realm' across the Corsica-Sardinia microcontinent. *C.R.Geoscience*, **341**, 224–238.

Schwartz, S. Y. and Van der Voo, R. (1983). Paleomagnetic evaluation of the orocline hypothesis in the central and southern Appalachians. *Geophysical Research Letters*, **10**, 505–508.

Smethurst, M. A., Khramov, A. N., and Pisarevsky, S. (1998). Paleomagnetism of the Lower Ordovician Orthoceras Limestone, St. Petersburg, and a revised drift history for Baltica in the early Palaeozoic. *Geophys. J. Int.*, **133**, 44–56.

Stampfli, G. M., Herausgeber (2001). *Geology of the western Swiss Alps*, Ausgabe 36, Seiten 1–41. Mémoires de Géologie (Lausanne).

Tauxe, L., Mullender, T. A. T., and Pick, T. (1996). Potbellies, wasp-waists, and superparamagnetism in magnetic hysteresis. *Journal of Geophysical Research*, **101**, 571–583.

Torsvik, T. H. and Van der Voo, R. (2002). Refining Gondwana and Pangea paleogeography: Estimates of Phanerozoic non-dipole (octupole) fields. *Geophys. J. Int.*, **151**, 771–794.

Torsvik, T. H., Van der Voo, R., Preeden, U., Mac Niocaill, C., Steinberger, B., Doubrovine, P. V., van Hinsbergen, D. J. J., Domeier, M., Gaina, C., Tohver, E., Meert, J. G., McCausland, P. J. A., and Cocks, L. R. M. (2012). Phanerozoic polar wander, palaeogeography and dynamics. *Earth-Science Reviews*, **114**, 325–368.

Traversa, G. (1979). Permian volcanism in Sardinia. *IGCP Project, Newsletter 1*, **5**, 127–140.

Traversa, G. and Vaccaro, C. (1992). REE distribution in the late Hercynian dikes from Sardinia. In *IGCP n 276 Newsletter*, Ausgabe 5, Seiten 241–262.

Traversa, G., Ronca, S., Del Moro, A., Pasquali, C., Buraglini, N., and Barabino, G. (2003). Late to post-Hercynian dyke activity in the Sardinia-Corsica domain: a transition from orogenic calc-alkaline to anorogenic alkaline magmatism. *Boll Soc Geol It (Special Volume)*, **2**, 131–152.

Umhoefer, P. J. (2000). Where are the missing faults in translated terranes? *Tectonophysics*, **326**, 23–25.

Vaccaro, C., Atzori, P., Del Moro, A., Oddone, M., Traversa, G., and Villa, I. M. (1991). Geochronology and Sr isotope geochemistry of late-Hercynian dykes from Sardinia. *Schweiz. Mineral. Petrogr. Mitt.*, **71**, 221–230.

Van der Voo, R. (1969). Paleomagnetic Evidence for the Rotation of the Iberian Peninsula. *Tectonophysics*, **7**(1), 5–56.

Van der Voo, R. (1993). *Paleomagnetism of the Atlantic, Tethys and Iapetus Oceans*. Cambridge University Press.

Van der Voo, R. and Torsvik, T. H. (2001). Evidence for Permian and Mesozoic Non-dipole Fields Provides an Explanation for the Pangea Reconstruction Problems. *Earth and Planetary Science Letters*, **187**, 71–81.

Van Hilten, D. (1964). Evaluation of some geotectonic hypotheses by paleomagnetism. *Tectonophysics*, **1**(1), 3–71.

Vigliotti, L., Alvarez, W., and McWilliams, M. O. (1990). No relative rotation detected between Corsica and Sardinia. *Earth and Planetary Science Letters*, **98**, 313–318.

Visscher, H. (1968). On the Thuringian age of the Upper Palaeozoic sedimentary and volcanic deposits of the Estérel, Southern France. *Rev. Palaeobot. Palynol.*, **6**, 71–83.

Wack, M. (2010). A new software for the measurement of magnetic moments using SQUID and spinner magnetometers. *Computers & Geosciences*.

Wegener, A. (1920). Die Entstehung der Kontinente und Ozeane. In P. D. E. Wiedemann, Herausgeber, *Die Wissenschaft - Sammlung von Einzeldarstellungen aus den Gebieten der Naturwissenschaft und der Technik*, Ausgabe 66. Druck und Verlag von Friedr. Vieweg & Sohn, Braunschweig.

Weil, A. B., Van der Voo, R., and Van der Pluijm, B. A. (2001). Oroclinal bending and evidence against the Pangea megashear: The Cantabria-Asturias arc (northern Spain). *Geology*, **29**(11), 991–994.

Werneburg, R., Ronchi, A., and Scheider, J. W. (2007). The Early Branchiosaurids (Amphibia) of Sardinia (Italy): Systematic Palaeontology, Palaeoecology, Biostratigraphy and Palaeobiogeographic Problems. *Paleogeography, Paleoclimatology, Paleoecology*, **252**(3-4), 383–404.

Westphal, M. (1976). Paléomagnetisme des formations permiennes de Corse. Comparaison avec la Sardaigne et l'Estérel. *Bull. Soc. géol. Fr.*, **18**(5), 1209–1215.

Westphal, M., Bardon, C., Bossert, A., and Hamzeh, R. (1973). A computer fit for Corsica and Sardinia against Southern France. *Earth and Planetary Science Letters*, **18**, 137–140.

Westphal, M., Orsini, J., and Vellutini, P. (1976a). Le micro-continent corso-sarde, sa position initiale: données paleomagnétiques et raccords géologiques. *Tectonophysics*, **30**, 141–157.

Westphal, M., Orsini, J., and Vellutini, P. (1976b). Le microcontinent corso-sarde, sa position initiale: Donnees paléomagnétiques et raccords géologiques. *Tectonophysics*, **30**, 141–157.

Yuan, K., Van der Voo, R., Bazhenov, M. L., Bakhmutov, V., Alekhin, V., and Hendriks, B. W. H. (2011). Permian and Triassic palaeolatitudes of the Ukrainian shield with implications for Pangea reconstructions. *Geophysical Journal International*, **184**, 595–610.

Zattin, M., Massari, F., and Médus, J. (2008). Thermochronological evidence for Mesozoic-Tertiary tectonic evolution in the eastern Sardinia. *Terra Nova*, **20**, 469–474.

Zheng, J., Mermet, J.-F., Toutin-Morin, N., Hanes, J., Gondolo, A., Morin, R., and Feraud, G. (1992). Datation 40Ar-39Ar du magmatisme et de filons minéralisés permiens en Provence orientale (France). *Geodinamica Acta*, **5**(3), 203–215.

Ziegler, P. and Dëzes, P. (2006). Crustal evolution of Western and Central Europe. *Geological Society, London, Memoirs*, **32**, 43–56.

Zijderveld, J. D. A. (1967). A. C. demagnetization of rocks: Analysis of results. In D. W. Collinson, K. M. Creer, and S. K. Runcorn, Herausgeber, *Methods in Paleomagnetism*, Seiten 254–286. Elsevier, Amsterdam.

Zijderveld, J. D. A. (1975). *Paleomagnetism of the Estérel rocks*. Dissertation, Utrecht. 199 p.

Zijderveld, J. D. A., De Jong, K. A., and Van der Voo, R. (1970). Rotation of Sardinia: palaeomagnetic evidence from Permian rocks. *Nature*, **226**, 993–994.

Acknowledgements

First of all I would like to thank my supervisor Prof. Valerian Bachtadse. He invited me to work in the magnetism group at the chair of Geophysics at the LMU and initialized the Pangea project early on in 2003 in which my work is embedded. He provided constant motivation and fruitful discussions. Financial support through him by the German Science Foundation (DGF grants BA 1210/20-1 and BA 1210/8-1)) who partly funded this work is greatly acknowledged. I truly appreciate his support and belief in me.
Special thanks go to Prof. Giovanni Muttoni. Discussions with him always were intense, challenging and a great inspiration. He is a great teacher and always provided very valuable advice, scientific and beyond. He also taught me patience and to ALWAYS take a final look. Thanks, Gio!
Special thanks also go to Prof. Dennis Kent who has been part of the Pangea project from the very beginning. His great expertise in many fields of science was an invaluable input at all times.
This work would not have been possible without the help of many people, great scientists, who I had the chance to work with. Special thanks go to Prof. Ausonio Ronchi for his valuable help in the field and geologic expertise. The help of his student Nicola Gretter is also greatly appreciated. Further thanks go to Dr. Antonio Langone and Prof. Vincenzo Festa for their very valuable support during field work in Calabria. Thanks also go to my colleagues Uwe Kirscher, Matthias Hackl and Edoardo Dallanave with whom I had the pleasure to share an office, many days in the field and one or two beers. Former and active members of the magnetism group in Munich and at the chair of Geophysics at the LMU are also greatly acknowledged: Jo Wassermann, Michael Winklhofer, Alex Zwing, Jürgen Hauck, Felix Hufenbecher and Christoph Heunemann who turned out to be a great support in discussing my work and taking my mind off things when needed. You're truly invaluable. Further thanks go to my predecessors in the Pangea project, Barbara Huber (formally Emmer) and Elmar Moser for providing samples and data.
I am greatly indebted to Prof. Stuart Gilder as head of the magnetism group and

to Prof. Hans-Peter Bunge as head of the chair of Geophysics at the LMU for providing access to the university laboratories and infrastructure. Dr. Michael Wack is thanked for running the automated lab system in the paleomagnetic lab in Munich and Manuela Weiß is thanked for keeping the lab in Niederlippach running. Prof. Nikolai Petersen is thanked for maintaining the instruments for rockmagnetic measurements in Munich. Special thanks go to the staff in the workshops for doing an indispensable job in maintaining the equipment needed in the field and for paleomagnetic sampling.
Last but not least, I would like to thank my parents, friends and family for their constant support and belief in me. I must have been a real pain at times, thank you all for bearing with me.